HHS Public Access

Author manuscript

Chem Rev. Author manuscript; available in PMC 2018 June 28.

Published in final edited form as:

Chem Rev. 2017 June 28; 117(12): 7878–7909. doi:10.1021/acs.chemrev.7b00083.

Polycyclic Furanobutenolide-Derived Cembranoid and Norcembranoid Natural Products: Biosynthetic Connections and Synthetic Efforts

Robert A. Craig II and **Brian M. Stoltz***

The Warren and Katharine Schlinger Laboratory of Chemistry and Chemical Engineering, California Institute of Technology, Pasadena, CA 91125, USA

Abstract

The polycyclic furanobutenolide-derived cembranoid and norcembranoid natural products are a family of congested, stereochemically complex, and extensively oxygenated polycyclic diterpenes and norditerpenes. Although the elegant architectures and biological activity profiles of these natural products have captured the attention of chemists since the isolation of the first members of the family in the 1990s, the de novo synthesis of only a single polycyclic furanobutenolide-derived cembranoid and norcembranoid has been accomplished. This article will begin with a brief discussion of the proposed biosyntheses and biosynthetic connections among the polycyclic furanobutenolide-derived cembranoids and norcembranoids followed by a comprehensive review of the synthetic efforts toward each member of the natural product family, including biomimetic, semisynthetic, and de novo synthetic strategies. This body of knowledge has been gathered in order to provide insight into the reactivity and constraints of these compact and highly oxygenated polycyclic structures, as well as to offer guidance for future synthetic endeavors.

TOC image

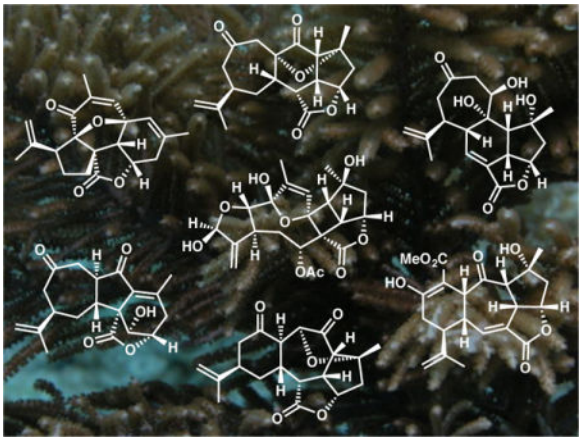

***Corresponding Author:** stoltz@caltech.edu.

Notes

The authors declare no competing financial interests.

1. INTRODUCTION

The cembranoid natural products are a vast family of marine and terrestrial diterpene secondary metabolites found throughout the world. This structurally diverse and highly oxygenated class of metabolites is produced in vast numbers by an array of gorgonian octocorals and soft coral species. Considering the relatively few marine fauna that prey upon gorgonian and soft corals, it has been hypothesized that marine cembranoids serve to defend against competing and/or predatory organisms.[1–3] Indeed, the isolation and investigation of the biological activity of cembranoids has led to the discovery of a vast range of structurally diverse compounds possessing potent cytotoxicity.[4–6]

Among the most biologically active members of the cembranoids is the subclass of macrocyclic furanobutenolides including the C_{20}-cembranoids lophotoxin (**1**), bipinnatin D (**2**), and bipinnatin I (**3**) as well as the C_{19}-norcembranoids sinuleptolide (**4**) and 5-episinuleptolide (**5**, Figure 1). Lophotoxin (**1**) is a potent neurotoxin, functioning as an irreversible antagonist of the nicotinic acetylcholine receptor.[7–9] Alternatively, bipinnatin D (**2**) is active against P-388 murine leukemia in vitro[10] and bipinnatin I (**3**) is strongly cytotoxic (>1 μM GI_{50}) against a variety of cancer cell lines including variants of melanoma and colon cancer.[11] The norcembranoids sinuleptolide (**4**) and 5-episinuleptolide (**5**) also possess antitumor and cytotoxic properties toward human KB oral epidermoid cells, Hepa59T/VGH human liver carcinoma cells, and a panel of squamous cell carcinomas (10–30 μM IC_{50}).[12–15]

Related to this vast family of macrocyclic furanobutenolides are a small subset of highly substituted and extensively oxygenated polycyclic diterpenes and norditerpenes (Figure 2). Examples include bielschowskysin (BSK, **6**), the cytotoxic cyclobutanoid that is highly active against EKVX nonsmall cell lung cancer (GI_{50} < 0.01 μM),[16] as well as the mildly cytotoxic intricarene (**7**)[17] and rameswaralide (**8**).[18–19] The polycyclic norcembranoid diterpenes are exemplified by the antileukemic ineleganolide (**9**)[5,20] and the isomeric sinulochmodin C (**10**),[21] which are both highly compact, cycloheptanone-containing dihydrofuranones. The beauty and complexity of these structures, paired with their pertinent and variable bioactivity, have and continue to entice synthetic chemists to pursue their syntheses and further explore the biological activities of these scarce natural products.

The purpose of this review is not to present a comprehensive catalog of the literature surrounding the cembranoid family of natural products.[22] A tremendous amount of research has been performed previously by Trauner[23] and Pattenden,[1,24] among others,[6,25–26] to compile a series of scholarly works covering the known members of the cembranoid natural products, their biological activity, and the elaborate details of their biosynthetic relationships. Rather, the focus herein will be on the polycyclic furanobutenolide-derived members of the cembranoid natural product family and the array of approaches taken toward their syntheses. We have gathered this body of knowledge, including semisynthetic studies and de novo synthetic efforts, to gain insight into the reactivity and conformational constraints of these compact and highly oxygenated polycyclic structures.

2. POLYCYCLIC FURANOBUTENOLIDE-DERIVED CEMBRANOIDS AND NORCEMBRANOIDS

The polycyclic furanobutenolide-derived natural products can be separated into two categories: cembranoid and norcembranoid (Figure 3). The former is derived from macrocyclic furanobutenolide scaffold **11**, which originates from the linear tetraisoprene geranylgeranyl diphosphate and has retained all 20 carbons.[1] Comparatively, the norcembranoid furanobutenolide-derived natural products are based on macrocyclic lactone precursors related to furan **12**, which contains only 19 carbons. It has been postulated that the loss of C(18) in vivo typically occurs by oxidation and subsequent hydrolysis.[1] The absolute stereochemistry of the polycyclic cembranoids is biosynthetically derived from oxygenated derivatives of scaffolds **11** and **12**, which contain the isopropenyl and butenolide groups in the C(1)-(*R*)-and C(10)-(*S*)-configurations, respectively, as shown.[21,27–30]

There are 10 known polycyclic furanobutenolide-derived cembranoids, including macrocycles BSK (**6**)[16] and verrillin (**13**),[31] polycycles intricarene (**7**),[17] rameswaralide (**8**),[18,19] havellockate (**14**),[32] and the closely related plumarellide (**15**),[1,23,33] plumarellate (**16**),[1,23,33] mandapamate (**17**),[34] isomandapamate (**18**),[35] bishomoisomandapamate (**19**),[36] and confertdiate (**20**, Figure 4).[37] Decorated by a variety of oxygenation states and patterns, these diterpenes display a variety of complex, highly compact, stereochemically dense architectures. In a similar fashion, the related furanobutenolide-derived norcembranoids, including ineleganolide (**9**),[20] horiolide (**21**),[38] kavaranolide (**22**)[39] all possess a central heptacycle (Figure 5). Comparatively, the majority of the remaining members of the polycyclic furanobutenolide-derived norcembranoids including dissectolide (**23**),[40] sinulochmodin C (**10**),[21] scabrolide B (**24**),[15] scabrolide A (**25**),[15] yonarolide (**26**),[41] and 12-hydroxyscabrolide A (**27**)[42] are all constructed around a central 6-membered carbocycle with a cycloheptanone ring decorating the peripheral structure. The final members of this family of polycycles are sinulanorcembranolide A (**28**)[43] and 1-epi-sinulanorcembranolide A (**29**),[44] which also contain a cycloheptanone on the outer reaches of the carbocyclic scaffold, but contrastingly possess a unique polycyclic scaffold containing a transannular cyclopentenone with a flanking, bridged hydroxylactone.

3. BRIEF SUMMARY OF BIOSYNTHETIC CONNECTIONS

Despite the breadth of complexity found within the family of polycyclic furanobutenolide-derived cembranoids and norcembranoids, these natural products are typically co-isolated with (and hypothesized to be derived from) the more simplified furanobutenolide macrocycles. Before discussing synthetic strategies, it is critical to establish a context of the interconnected nature of these polycycles, derived from postulated biosyntheses. While comprehensive reviews of the biosynthesis of the cembranoid and norcembranoid natural products can be found elsewhere,[1,23–25] a brief overview of postulated biosynthetic routes to these molecules is presented before exploring the in vitro approaches toward the same targets.

3.1. Biosyntheses of Polycyclic Furanobutenolide-Derived Cembranoids

Bielschowskysin (BSK, **6**) is a rare cyclobutane-containing cembranoid that demonstrates significant biological activity, showing excellent cytotoxicity against EKVX nonsmall cell lung cancer (GI_{50} < 0.01 μM) and CAKI-1 renal cancer (GI_{50} = 0.51 μM) as well as antiplasmodial activity.[16] The majority of synthetic efforts toward entry into the polycyclic furanobutenolide-derived cembranoids have focused on the synthesis of BSK (**6**), due to its unique carbocyclic scaffold paired with its bioactivity profile (vide supra). Biosynthetically, BSK (**6**) is thought to be derived from bipinnatin J (**30**, Scheme 1).[1,23,45] Oxidation at C(13) and C(16) followed by intramolecular lactolization would provide acetate **31**. Oxidation of the $\Delta_{7,8}$ bond would afford epoxide **32** and subsequent doubly-vinylogous hydration across the furan ring would furnish hydroxyfuran **33**. Butenolide **33** is then positioned to undergo a light-induced [2 + 2] cycloaddition to construct the characteristic cyclobutane ring and complete BSK (**6**).

The furanobutenolide-derived verrillin **(13)**, similarly based around a central ether-bridged macrocycle, is also likely derived from bipinnatin J (**30**, Scheme 2).[1,23,31] Alternative oxidation of butenolide **30** would not only oxidize C(13) and the isopropenyl group, but also set the epimeric stereochemistry at C(8) compared to BSK (**6**) by epoxidation of the $\Delta_{7,8}$ bond from the opposite face. Doubly-vinylogous hydration of the furan ring would provide vinylogous diketone **34** after tautomerization. Intramolecular Michael addition within vinylogous diketone **34** would construct the C(7)–C(11) bond, furnishing polycycle **35** after migration of the acetate group to reveal an oxyanion at C(13). Ultimately, sequential ketalization of diol **35** through the vinylogous diketone system and hydrolysis of the enol acetate moiety would provide verrillin (**13**).

Furthermore, it is likely that bipinnatin J (**30**) serves as the biosynthetic precursor for the contrasting pentacyclic cytotoxic cembranoid intricarene (**7**).[17] This proposal is supported by experimental work performed in both Pattenden[1,46–47] and Trauner[23,48–49] laboratories as well as by computational studies from the Tantillo laboratories.[50] Oxidative cleavage of the furan ring affords homoallylic alcohol **36** (Scheme 3). Equilibration of alcohol **36** through hydroxypyrone **37** would access oxidopyrylium **38.** The charge-separated aromatic ring within macrocycle **38** is proposed to participate in an intramolecular [5 + 2] cycloaddition, forming the furan-bridged cycloheptenone ring and completing the biosynthesis of intricarene (**7**).

Bipinnatin J (**30**), however, is not the progenitor of every polycyclic furanobutenolide-derived cembranoid. Macrocycle **39**, which in comparison to bipinnatin J (**30**) is oxidized at C(18) rather than C(2) and has an extra unit of unsaturation between C(13) and C(14), is the proposed precursor to the hemolytic cembranoids plumarellide (**15**) and plumarellate (**16**, Scheme 4).[1,23,33] Oxidation across the $\Delta_{7,8}$ bond followed by olefin transposition would afford intermediate hemiketal **40.** Diene **40** could proceed through an intramolecular [4 + 2] cycloaddition with the transannular enol moiety to construct the central cyclohexene ring and complete plumarellide (**15**)**.** Ethanolysis of the lactone by ethanol would provide the tetracyclic derivative plumarellate (**16**).

Analogs of the plumarellides, the cembranoid natural products mandapamate (**17**),[34] isomandapamate (**18**),[35] bishomoisomandapamate (**19**),[36] and confertdiate (**20**)[37] are expected to arise from a related biosynthetic route (Scheme 5).[1,23] Each of these three natural products would be formed from a derivative of macrocycle **37**, a C(8) epimeric analog of intermediate **40**, that has been oxidized to the acid oxidation state at C(18), and possesses methyl ketal rather than a hemiketal at the furan ring (i.e., C(3)). Mandapamate (**17**) would be constructed by the intramolecular [4 + 2] cycloaddition for the *E*-enol isomer of **37** (Scheme 5A). Isomandapamate (**18**), bishomoisomandapamate (**19**), and confertdiate (**20**) would be formed in an analogous manner from the Z-enol isomer of ketal **37** (Scheme 5B).

The biosynthetic formation of the remaining two members of the polycyclic cembranoid natural product family remains unclear. Havellockate (**14**) contains a related tricyclic core to the plumarellides and the mandapamates that is flanked by a spirocyclic butyrolactone whose relative stereochemistry was unambiguously established upon initial isolation (Figure 6).[32] Comparatively, the cytotoxic diterpenoid rameswaralide (**8**) is also characterized by a unique cembranoid scaffold, containing a central 4-cycloheptenone.[18–19] Both havellockate (**14**) and rameswaralide (**8**) bear similarities to the plumarellides and the mandapamates, although they are both epimeric at C(8) compared to the former and epimeric at C(7) compared to the latter. Multiple biosynthetic proposals have been described, hypothesizing that havellockate (**14**) and rameswaralide (**8**) may arise either from the cyclization cembranoids related to macrocycles **36** and **37** with the proper C(8) stereochemistry or from rearrangement cascades directly forming the plumarellides and mandapamates.[1,23,51]

3.2. Biosyntheses of Polycyclic Furanobutenolide-Derived Norcembranoids

The polycyclic furanobutenolide-derived norcembranoid natural products are exclusively found in soft corals of the genus *Sinularia*.[1,24] The progenitors of all of these C_{19} natural products are speculated to be the sinuleptolides (**4** and **5**), being epimeric at C(5) and likely in equilibrium via epimerization in vivo (Figure 7).[1–3,21,24] The biosynthetic derivation of macrocyclic cembranoids to the antitumor norcembranoids sinuleptolide (**4**) and 5-episinuleptolide (**5**) has been described in detail elsewhere and will not be discussed here.[1–3,12–15,24]

The biosynthesis of the antileukemic norditerpenoid ineleganolide (**9**)[20] and the related cycloheptanone natural products horiolide (**21**)[38] and kavaranolide (**22**)[39] are proposed to arise from dihydrofuranone **42**, which is formed after an intramolecular Michael addition of 5-episinuleptolide (**5**) and sequential dehydration (Scheme 6).[1,24] Subsequent *5-exo*-trig Michael addition would forge the C(7)–C(19) bond and complete ineleganolide (**9**). Ineleganolide (**9**) could subsequently undergo a retro-oxa-Michael addition, opening the dihydrofuranone ring, followed by a retro-Michael addition to provide methyl ketone intermediate **43**. Considering ketone **43** has yet to be isolated and described from natural sources, it is proposed to rapidly undergo an intramolecular Michael addition to construct the C(5)–C(9) bond and furnish horiolide (**21**). Ultimately, isomerization of horiolide by elimination of the β-acetoxy group would generate the unsaturated methyl ketone found within kavaranolide (**22**).

In a similar fashion, 5-episinuleptolide (**5**) could serve as the biosynthetic progenitor to sinulochmodin C (**10**),[21] scabrolide B (**24**),[15] scabrolide A (**25**),[15] yonarolide (**26**),[41] and 12-hydroxyscabrolide A (**27**, Scheme 7).[42] The biosynthesis would begin with a 7-*exo*-trig intramolecular Michael cyclization to construct the characteristic peripheral cycloheptanone ring of these related norcembranoids and furnish intermediate **44** after dehydration.[1,24] Dihydrofuranone **44** would furnish sinulochmodin C (**10**) after a second Michael addition to construct the bond between C(7) and C(11). Scabrolide B (**24**) could be biosynthetically produced by one of two possible routes. First, scabrolide B could be formed after a retro-oxa-Michel addition from sinulochmodin C (**10**)**.** Alternatively, direct conversion of biosynthetic intermediate **44** to scabrolide B (**24**) could occur by a retro-oxa-Michael addition and subsequent intramolecular Michael addition. From scabrolide B (**24**), olefin isomerization from a trisubstituted vinylogous diketone to a tetrasubstituted enone would furnish scabrolide A (**25**). Sequential dehydration would provide the dienone polycyclic norcembranoid yonarolide (**26**). Alternative advancement of scabrolide A (**25**) by oxidation at C(12) would provide 12-hydroxyscabrolide A (**27**). Although the biosynthetic route for the formation of 12-hydroxyscabrolide A (**27**) has not previously been described, we postulate that C–H oxidation at C(12) of scabrolide A (**25**), being allylic and at the γ-position of the conjugated system, would provide access to the requisite α-hydroxylactone. Oxidation of C(12) on scabrolide B (**24**) is less likely and oxidation at C(12) at an earlier stage prior to polycyclization would require a distinctly different synthetic route enable the construction of 12-hydroxyscabrolide A (**27**) from 5-episinuleptolide (**5**).

The exact biosynthetic process for the construction of the remaining members of the polycyclic furanobutenolide-derived norcembranoid natural product family is less clear. Two plausible biosynthetic routes for the formation of dissectolide A (**23**) have been postulated (Scheme 8)[1–3,24,40] The core [7,6,5,5]-tetracyclic structure bears remarkable similarity to the mandapamate and plumarellide cembranoids (see Scheme 4), perhaps suggesting that intermediate **45**, with the $\Delta_{13,14}$ bond in the *trans* configuration, undergoes a [4 + 2] cycloaddition with the C(6)–C(7) enol tautomer of the dihydrofuranone ring to directly construct the central cyclohexene moiety of tetrahydrofuran **46.** Macrocycle **45** could alternatively proceed to intermediate furan **46** in a stepwise manner through a Michael addition between C(7) and C(11) and subsequent vinylogous aldol cyclization of the resultant enolate to construct the C(14)–C(6) bond. Proposed intermediate **46** would then only need to undergo the hydrolytic opening of the furan ring in an S_N2 fashion to complete the biosynthesis of dissectolide A (**23**).

The final members of the polycyclic furanobutenolide-derived norcembranoid diterpenes discovered to date are sinulanorcembranolide (**28**)[43] and 1-*epi*-sinulanorccmbranolidc (**29**),[44] which contain a novel [7,5,6]-carbocyclic core that is flanked by a bridging lactone. In the most plausible biosynthetic route, sinulanorcembranolide (**28**) is proposed to derive from 5-episinuleptolide (**5**) after a retro-oxa-Michael addition to form enone **47** (Scheme 9A).[52] Tautomerization of enone **47** through conjugated enol **48** could produce zwitterion **49**, enabling an intramolecular dipolar [3 + 2] cycloaddition to construct cyclopentanone **50.** After protonation of enolate **50**, dehydration of the tertiary alcohol would complete sinulanorcembranolide (**28**).

Contrastingly, the biosynthetic formation of 1-*epi*-sinulanorcembranolide (**29**) remains unclear. Although the authors failed to speculate on the biosynthetic pathway at the initial isolation of the natural product, it seems likely 1-*epi*-sinulanorcembranolide (**29**) arises via one of two pathways (Scheme 9B). Firstly, 1-*epi*-sinulanorcembranolide (**29**) could be derived from 5-episinuleptolide (**5**) through a biosynthetic pathway distinct from that invoked for the formation of sinulanorcembranolide (**28**), as the proposed biosynthetic pathway does not offer the opportunity for epimerization at C(1). Alternatively, 1-*epi*-sinulanorcembranolide (**29**) could be derived from the currently unknown natural product 1,5-bisepisinuleptolide (**51**) by an identical biosynthetic pathway invoked for the formation of its epimer (cf. **28**). Since the absolute stereochemistry of 1-*epi*-sinulanorcembranolide (**29**) has not yet been established, it remains a possibility that in fact 1-*epi*-sinulanorcembranolide (**29**) is not epimeric only at C(1), but rather is antipodal to sinulanorcembranolide (**28**) at all chiral centers *except* C(1).

4. SYNTHETIC STUDIES TOWARD POLYCYCLIC FURANOBUTENOLIDE-DERIVED CEMBRANOIDS

A testament to the synthetic challenge of accessing the complex structures of the polycyclic furanobutenolide-derived cembranoid and norcembranoid natural products is the fact that the synthesis of only a single member of this family has been completed. The remainder of this article will explore this success along with the literature concerning the numerous synthetic efforts toward the other members of the polycyclic furanobutenolide-derived cembranoid and norcembranoid natural products. Collating the knowledge surrounding the pursuit of these natural products and the exploration of the limitations around the construction and the synthetic manipulations of their polycyclic scaffolds will help to guide the continued investigation of these stereogenically complex and biologically active natural products.

4.1. Synthetic Efforts Toward Bielschowskysin

Bielschowskysin (BSK, **6**) has been the most studied member of either the polycyclic cembranoid or norcembranoid family of natural products, piquing the interest of the scientific community with its unique cyclobutane scaffold and potent biological activity.[16] Six different research groups have reported synthetic studies toward BSK (**6**), five of them employing a light-induced cyclobutane formation. While the total synthesis of BSK (**6**) has not yet been reported, a tremendous amount of progress toward the functionalization of the BSK (**6**) scaffold has been accomplished. Because this body of literature is extensive, syntheses described herein will be limited to a brief summary of the approaches taken and the limitations that prevented each method from advancement to BSK (**6**).

4.1.1. Photochemical [2 + 2] Cycloaddition Approaches to Bielschowskysin—

The majority of approaches toward the synthesis of BSK (**6**) have hinged on a photo-induced [2 + 2] cycloaddition to construct the characteristic fused cyclobutane moiety. In that sense, there are two directions to retrosynthetically disconnect the central cyclobutane within building block **52** (Scheme 10). The most commonly employed retrosynthetic disconnection of the four-membered carbocycle has been along the axis of the [4,5]-bicycle (Pathway A, green arrow) to furnish retron **53**.

The utility of this synthetic approach was explored by Ghosh and coworkers.[53–54] Early synthetic studies to explore the planned copper-catalyzed [2 + 2] photocycloaddition were performed on a model system (**55**) that was accessible as a single enantiomer after three synthetic transformations from a known derivative of α-D-glucofuranose (Scheme 11). Copper(I) triflate-catalyzed [2 + 2] cycloaddition of 1,6-diene **55** proceeded smoothly to furnish cyclobutane **56** in 75% yield as a single diastereomer. The cycloaddition is hypothesized to proceed exclusively through the copper-coordinated intermediate **57**, accounting for the observed stereoselectivity.

This copper-catalyzed [2 + 2] cycloaddition manifold was then applied to more densely functionalized diene **58**, furnishing cyclobutane **59** in 65% yield (Scheme 12).[53–54] Under these copper-catalyzed conditions, the photocycloaddition proceeded with concomitant transketalization from the acetonide to the acetal of acetaldehyde through photochemical oxidation of the ethereal solvent and expulsion of ethylene, a mechanism that has been explored and developed by Ghosh and coworkers.[55] The resultant mixture of diastereomers proves inconsequential as the ketal is immediately removed under oxidative conditions. Sequential periodate-mediated 1,2-diol cleavage and methylenation of the resultant aldehyde provided olefin **60** in 57% yield. Aldehyde **61** was then available after removal of the remaining acetonide and another oxidative 1,2-diol cleavage, enabling the completion the tricyclic core of BSK (**62**) after global oxidation and chemoselective ketone reduction with in situ intramolecular lactonization.

Recently, Ghosh and coworkers disclosed an alternative synthetic route to the tricyclic core of BSK (**6**) with varied peripheral functionalization.[56] Olefin metathesis of triene **63**, which was available in >99% enantiomeric excess (ee) from D-mannitol, provided 2,5-dihydrofuran **65** in 87% yield as the exclusive product (Scheme 13). Application of the copper-catalyzed [2 + 2] photocycloaddition methodology proved fruitful, enabling access to cyclobutane **66** in 65% yield as a single diastereomer. Oxidation of tetrahydrofuran **66** with ruthenium tetroxide provided lactone **67**, completing the tricyclic core of BSK (**6**).

Attempting to apply the copper-catalyzed photocycloaddition reaction manifold to a functionalized system more closely related to BSK (**6**), Ghosh and coworkers synthesized allylic alcohol **68** (Scheme 14A).[53] Under the same copper-catalyzed light-induced [2 + 2] cycloaddition conditions, cyclobutane **69** was isolated in a comparable 66% yield. Although substrate-control has dictated the stereoselective formation of many of the stereocenters around cyclobutane **69** as desired for BSK (**6**), the configuration at C(8) and C(10) were epimeric to those found in the natural product.

Finding cyclobutane **69** an intractable substrate, Ghosh and coworkers pursued the development of a method for the tandem epimerization of C(8) and C(10) on closely related allylic alcohol **70** (Scheme 14B). Photocycloaddition again under copper(I)-catalyzed conditions produced cyclobutane **71** in 78% yield. A five step redox procedure from *trans*-1,3-cyclopcntancdiol **71** accomplished the inversion of configuration at both C(8) and C(10) by a tandem oxidation-elimination pathway, setting the relative stereochemistry within cyclobutane **72** as required for BSK (**6**). At this stage, any advancement was halted, as the removal of the acetoni de from diol **72** could not be accomplished. To date, protected

trans-1,3-cyclopentanediol **72** represents the most advanced published compound produced by Ghosh and coworkers in their work toward BSK (**6**).

Sulikowski and coworkers also envisioned accessing BSK (**6**) by a similar retrosynthetic strategy (Scheme 15).[57–58] Simplifying BSK to scaffold **73**, they planned to construct the core central cyclobutane through an intramolecular [2 + 2] photocycloaddition of bisbutenolide **74.** Importantly, control over the diastereoselectivity of this cycloaddition depends on both the geometry of the exocyclic olefin as well as the steric encumbrance of the butenolide-substituted olefin cycloaddition partners.

Development of the reaction conditions for the desired photochemical [2 + 2] cycloaddition began with the model butenolide **80** (Scheme 16). Access to this model system began from aldehyde **75**, which was available in stereoselective fashion from (−)-malic acid. Still-Genari olefination of aldehyde **75** with phosphonate **76** followed by Sonogashira coupling employing allylic iodide **77** provide Z-enoate **78** in 53% yield over two steps. After sequential oxidation, carboxylic acid **79** was advanced to bisbutenolide **80** through silver-mediated cycloisomerization and acetal cleavage. Intramolecular cycloaddition of alkylidene butenolide **80** proceeded smoothly, through presumed 1,4-biradical intermediate **81**, furnishing a 5:1 mixture of diastereomeric cyclobutanes in 50% yield. Within this mixture, desired cyclobutane **82** was the major product and mirrors the relative stereochemistry found in BSK (**6**), with the minor product remaining unassigned. UV light was not required in order to induce the desired cycloaddition and the choice of acetone for the solvent was critical for the minimization of impurity formation.

Having succeeded in selectively forming the tetracyclic scaffold of BSK, Sulikowski and coworkers turned their attention to the construction of a more densely functionalized cyclobutane (i.e., methyl ester-substituted butenolide ***Z*-83**) for synthetic advancement toward BSK (**6**, Scheme 17).[59] In contrast to the unsubstituted butenolide substrate (**80**), irradiation of bisbutenolide ***Z*-83** provided no trace of the desired cyclobutane adduct, but rather provided a mixture of olefin isomers. The isomerization was hypothesized to proceed again through a 1,4-biradical intermediate (**84**). The installation of the methyl ester substituent stabilizes biradical **84**, which prevents formation of the cyclobutane product and instead enables cycloreversion to alkylidene butenolide **83**, scrambling the olefin geometry in the process.

In an effort to restore the efficacy of the photocyclization, Sulikowski and coworkers sought to replace the methyl ester substituent with a less stabilizing group. Toward this end, the [2 + 2] cycloaddition of substrate **85** was explored, where the butenolide cycloaddition partner has been functionalized with a side chain derived stereoselectively from D-glyceraldehyde (Scheme 18). Fully-elaborated butenolide **85** underwent a visible light-induced [2 + 2] cycloaddition to provide cyclobutane **87** in 81% yield over two steps after the removal of the benzyl ether by hydrogenolysis. Pleasingly, cycloaddition adduct **86** was produced as a single diastereomer. Spirocycle **87** contains the fully elaborated fused cyclobutane polycyclic portion of BSK (**6**) and represents the most advanced intermediate detailed by the Sulikowski group to date.

Mulzer and coworkers envisioned accomplishing the construction of the cyclobutane moiety from an even more functionalized, late-stage intermediate.[60–61] Access to BSK (**6**) was planned by the late-stage oxidation of exocyclic olefin **88** (Scheme 19). Construction of the central macrocycle would be accomplished by an intramolecular Heck reaction of alkenyl bromide **89.** Olefin **89** would be constructed by employing an intramolecular light-mediated [2 + 2] cycloaddition from aliene **90** to form the characteristic cyclobutane-containing tricycle found within BSK (**6**).

Synthetic advancement toward BSK (**6**) began with propargyl alcohol **91** that, in similar fashion to other synthetic approaches, was available as a single enantiomer from (−)-malic acid (Scheme 20). Crabbé homologation of alkyne **91** smoothly furnished aliene **92** after silyl ether formation en route to selenide **93.** Convergent assembly of the BSK scaffold was then accomplished by intermolecular aldol coupling of aliene **93** and aldehyde **94**, which was available in stereoselective fashion from α-D-ribofuranose. Butenolide **95** was isolated as an inseparable 1:1 mixture of diastereomers after selenoxide elimination and carried forward in order to investigate cyclobutane formation via photo-induced [2 + 2] cycloaddition. Exposure of aliene mixture **95** to UV-C light in cyclohexane provided cyclopentanes **96** and **97** in 67% combined yield as a 1:1 mixture of diastereomers, with isomeric cyclohexenes **98** and **99** as the minor products. Cyclobutane **97**, containing the targeted tricyclic cyclobutane fragment and desired flanking relative stereochemistry, was separated and advanced further toward BSK (**6**).

Primary silyl ether **97** was advanced to alkenyl bromide **100** over 5 steps in order to provide the substrate for the proposed Heck macrocyclization. After exposure of alkenyl bromide **100** to reaction conditions intended to affect the planned Heck cyclization, Mulzer and coworkers were surprised to isolate cyclooctane **101** as the major product (Scheme 21). The desired cyclononene product (**102**) was not observed. The observed cyclization of alkenyl bromide **100** was accompanied by concomitant acetoxylation of the 1,1-disubstituted olefin to provide acetate **101.** Although this work represents the first example of the conversion of a 1,1-disubsitited olefin directly to a neopentyl acetate, no productive advancement of alkenyl bromide **100** toward BSK (**6**) could be achieved.

The observed lack of desired reactivity forced Mulzer and coworkers to pursue a series of alternative macrocyclization strategies in pursuit of the total synthesis of BSK (**6**).[61] The authors sought to form the core macrocycle of BSK (**104**) from propargyl alcohol **103** via transition metal-mediated cycloisomerization (Scheme 22A). Although the exploration of a variety of reaction conditions employing gold(I) or copper(I) sources provided analytical traces of desired macrocycle **104**, the authors were unable to isolate any measurable quantity of the product. In a complementary approach, the authors sought to apply a halolactonization approach to methylenecyclobutane **105** to provide access to BSK macrocyclic scaffold **106** (Scheme 22B). Unfortunately, olefin **105** proved largely unreactive under the reaction conditions, typically resulting in the reisolation of starting material or nonspecific decomposition of the substrate. Without a method to accomplish the planned macrocyclization, the authors prepared homoallylic alcohol **107**, as an inseparable mixture of diastereomers, in order to test the potential to form alkene **110** through ring-closing

metathesis (Scheme 22C). After screening numerous ruthenium catalysts, including the Grubbs–Hoveyda 2nd generation (**108**) and Grubbs 2nd generation (**109**) complexes, the authors were yet again unable to isolate desired macrocycle **110**, most commonly observing the dimerization of alkene **107** as the major product. Unable to successfully accomplish the formation of the BSK macrocycle through derivatives of any densely elaborated methylenecyclobutanes (i.e., **100**, **103**, **105**, or **107**), Mulzer and coworkers completely redesigned their 2nd generation synthetic approach toward BSK (**6**, vide infra).

In contrast to Mulzer's planned late-stage formation of the central macrocycle after construction of the cyclobutane moiety, Nicolaou and coworkers explored the potential to accomplish the formation of the 4-membered carbocycle after completion of the macrocyclic scaffold in a manner reminiscent of the proposed biosynthesis of BSK (**6**, see Scheme 1).[62–63] Retrosynthetically, BSK (**6**) was simplified to a model core scaffold **111**, retaining the required functionalization or providing a functional group handle at C(2), C(3), and C(8) (Scheme 23). Synthesis of polycycle **111** would be accomplished by the transannular photochemical [2 + 2] cycloaddition of alkene **112**.

Enantioselective synthesis of the macrocyclic cycloaddition precursor (**112**) began with the asymmetric reduction of α-ketofuran **113** using the Noyori catalyst (**114**, Scheme 24). Through this reaction manifold, furyl alcohol **115** was produced in 84% yield with 92% ee. Coupling of furyl alcohol **115** and β-ketoester **116** was then accomplished under oxidative conditions. After sequential ring-closing metathesis using Grubbs 1st generation catalyst (**64**), macrocycle **117** was furnished as the major product in 26% yield with a 15:1 ratio favoring the *trans* isomer. Epimeric macrocycle **118** was also produced through this reaction sequence in a comparable 21% yield, although in a reduced 3:1 ratio between the *trans* and *cis* olefin isomers. Although these mixtures of olefin isomers proved inseparable at this stage, both macrocycle **117** (Scheme 24B) and **118** (Scheme 24C) were advanced by reduction of the unsaturated ketone moiety under identical reaction conditions using sodium borohydride. At this stage, each product could be isolated as a single species, providing allylic alcohol **119** from macrocycle **117** in 83% yield and allylic alcohol **120** from macrocycle **118** in 63% yield. Interestingly, the configuration of the ketal moiety within macrocycles **117** and **118** dictated the diastereoselectivity of this reduction, imparting an *anti* relationship between the C(3)-methoxy and newly formed C(8)-hydroxyl moieties.

The potential of both furan macrocycles **119** and **120** to undergo an intramolecular [2 + 2] photocycloaddition was subsequently explored. Furan **119**, when exposed to UV-B light in either benzene or chloroform, produced cyclobutane **121** in high yield as a single diastereomer (Scheme 25A). The new fused carbocycle contained the desired relative stereochemistry, furnishing the spirocyclic furan as found in BSK (**6**). Under identical photocyclization conditions, diastereomeric macrocycle **120** produced carbocycle **122** as the sole product (Scheme 25B). The relative stereochemistry of furan **122** dictated stereoselective formation of the stereocenters on the periphery of the cyclobutane in the opposite and undesirable sense for advancement toward BSK (**6**). Nevertheless, the construction of macrocycle **121** successfully exhibited the utility of this approach toward BSK (**6**). Although cyclobutane **121** contains the proper spirocycle relative to BSK (**6**) and a

series of functional group handles, the Nicolaou group has not disclosed any further studies to date concerning its advancement toward BSK (**6**), including the utility of this light-induced intramolecular [2 + 2] cycloaddition employing more substituted olefins for the installation of the requisite α-quaternary γ-lactone.

Taking a similar approach toward BSK (**6**), Lear and coworkers envisioned late-stage construction of the cyclobutane moiety from a fully elaborated macrocyclic precursor **123** by a tandem [2 + 2]-oxidative [4 + 2] cycloaddition (Scheme 26).[64–65] Aliene **123** would be generated from alkyne **124** after oxidation of the C(8) hydroxyl group and subsequent isomerization. In the forward sense, aliene **123** would proceed toward BSK (**6**) by first undergoing a light-induced [2 + 2] cycloaddition to furnish cyclobutane intermediate **125** (Scheme 27). Diene **125** would then undergo a photochemical [4 + 2] cycloaddition with singlet oxygen to construct peroxide **126.** Homolytic cleavage of the peroxide bond by cobalt(II) would then result in the formation of elaborated BSK scaffold **127.**

Initial exploration of the planned tandem cycloaddition strategy focused on the potential to accomplish the regioselective [2 + 2] cycloaddition of a tethered allene and butenolide system. In order to assess the viability of this strategy, Lear and coworkers constructed allene model system **133** (Scheme 28). Lear and coworkers began with acetal **128**, an analogous substrate to that employed by Sulikowski (**75**, see Scheme 16),[57–58] being available in stereoselective fashion from (−)-malic acid. Acetal **128** was advanced through a series of synthetic manipulations that inspired Mulzer's 1st generation approach toward a BSK (**6**, see Scheme 20).[60–61] Swern oxidation of the primary alcohol and Wittig olefination of the intermediate aldehyde provided enoate **130** as a 4:1 mixture with the undesired olefin isomer. Ketal cleavage of enoate **130** followed by silyl ether formation and Crabbé homologation provided aliene **133** as the substrate for development of the planned photochemical [2 + 2] cycloaddition. Pleasingly, aliene **133** underwent the desired cyclobutane formation after exposure to ultraviolet light in a mixed solvent system, providing methylenecyclobutane **134** as the sole product, which had been formed with both the relative and absolute stereochemistry as required for BSK (**6**). Incorporation of the tertiary carbinol on the aliene arm of butenolide **133** was critical for the observed regioselective cycloaddition. Although this model system failed to test the utility of the allene [2 + 2] cycloaddition with a substituted butenolide as required for BSK (**6**) itself, Lear and coworkers felt confident enough to move forward with their synthetic strategy.

Construction of the fully elaborated macrocycle en route to BSK (**6**) began with alkenyl iodide **135** and alkyne **136**, which were available in stereoselective fashion from diacetone-D-glucose and (−)-malic acid, respectively (Scheme 29). Sonogashira coupling of iodide **135** with alkyne **136**, macrolactonization, and selective silyl ether cleavage provided β-ketoester **137** in 58% yield over 3 steps. Primary alcohol **137** was then advanced to primary chloride **138** through a modified Appel halogenation. Unfortunately, progress toward BSK (**6**) was halted at intermediate **138** because cyclization between the primary chloride and the α-position of the β-ketoester could not be achieved. Without the ability to form the butenolide moiety, the tandem oxidative cycloaddition cascade could not be investigated and any further advancement toward BSK (**6**) was thwarted.

Although these approaches toward BSK (**6**) had provided numerous methods for the synthesis of cyclobutane-centered polycycles, the total synthesis of BSK (**6**) remained elusive. As a result, Mulzer and coworkers developed a 2nd generation retrosynthetic strategy for the construction of the BSK core **52** (Scheme 30, also see ***red*** retrosynthetic disconnection, Scheme 10).[66] Rather than bisecting the cyclobutane along the axis of the [4,5]-bicycle like previous synthetic approaches, the authors envisioned accessing the 4-membered carbocycle by an intramolecular photo-induced [2 + 2] cycloaddition between the α,β-unsaturated ester and cyclopentenyl olefin moieties within cyclopentenol **54.**

Investigation of the proposed synthetic route began with the assessment of a variety of model systems under photo-induced [2 + 2] cycloaddition reaction conditions (Figure 8). Each substrate was available in high enantiomeric excess from diol **(+)-148**, which was accessed through an asymmetric resolution by enzyme-catalyzed acetylation (see Scheme 31). Mulzer and coworkers initially sought to use the [2 + 2] cycloaddition step to directly install the α-quaternary γ-lactone using diesters **140** and **144** as well as α-allenic alcohols **141** and **145**. Despite screening a number of solvents (e.g., Et_2O, pentane, acetone, CH_2Cl_2) and light sources (e.g., sun lamp, UV-A, UV-B), none of the desired cyclobutane products were ever observed. Even when employing the less congested allenes **142** and **146**, ketene **143**, or ketene iminium salt **147**, no productive reactivity could be identified.

Successful light-induced [2 + 2] cycloaddition could only be accomplished on an ether-linked allene-cyclopentenone substrate (Scheme 31). Beginning with enantioenriched 1,3-*cis*-cyclopenetenediol **(+)-148**, etherification with propargyl bromide followed by Crabbé homologation provided allene **150**. Sequential silyl ether cleavage and allylic oxidation then furnished cyclopentenone **151** as the substrate for the planned [2 + 2] cycloaddition. Pleasingly, exposure of cyclopentenone **151** to UV-B light in Et_2O at slightly above ambient temperature provided methylenecyclobutane **152** in 60% yield. Although the desired tricycle was indeed the major product formed by intramolecular cyclization from enone **151**, Mulzer and coworkers did not make any note about the regioselectivity of this cycloaddition. Additionally, the failure to construct the requisite α-quaternary γ-lactone directly through this synthetic approach forced Mulzer and coworkers to reevaluate their approach toward BSK (**6**), leading to the exploration of a 3rd generation synthetic route through which the cyclobutane moiety was purchased from commercial sources (see Section 4.1.2).

4.1.2. Non-Photochemical Approaches to Bielschowskysin—In the face of the challenges encountered in their efforts toward BSK (**6**), Mulzer and coworkers designed a 3rd generation synthetic strategy toward BSK (**6**) hinging on the production of core scaffold **153** from a cyclobutane-containing feedstock (Scheme 32).[66,67–69] Access to tricycle **153** in enantioenriched form was envisioned from cyclobutanol **(+)-154.** Bicycle **(+)-154** would be synthesized from racemic ketone **(±)-155** by a classical resolution, where cyclobutane **(±)-155** is commercially available, being synthesized by the thermal [2 + 2] cycloaddition between cyclopentadiene and dichloroketene.

Advancement of cyclobutanol **(+)-154** toward BSK (**6**) began with silyl ether formation and highly regioselective allylic oxidation (>20:1 dr) to provide enone **156** (Scheme 33). Conjugate addition of an in situ formed methyl cuprate into enone **156** followed by

Saegusa–Ito oxidation furnished bicycle **157.** Luche reduction of α,β-unsaturated ketone **157** and etherification of the resultant secondary alcohol provided the olefinic substrate for a Mukaiyama–Isayama oxidation-reduction-hydration, which completed the 1,3-*trans*-cyclopentanediol (**158**) required for BSK (**6**) with complete regio- and diastereoselectivity.[70] Silyl ether **158** was then smoothly converted to methylenecyclobutane **160** over six steps in excellent yield. At this stage, exposure of cyclobutane **160** to Jones oxidation conditions resulted in cleavage of both primary silyl ethers and their subsequent oxidation. Further oxidation state manipulation ultimately provided aldehyde **161.** Mulzer and coworkers were able to furnish this enantioenriched tricyclic core of BSK (**161**) in 11% overall yield through 16 synthetic steps from cyclobutane **(+)-154.**

Unfortunately, the advancement of aldehyde **161** toward BSK (**6**) was found to be unfeasible. All attempts to functionalize the 1,1-disubstitued olefin with carbon nucleophiles in a productive manner failed. As a result, intermediate **160**, encountered en route to aldehyde **161**, was utilized in order to explore an alternative synthetic route (Scheme 34). In order to continue toward BSK (**6**), the primary silyl ethers within methylenecyclobutane **160** were converted into a spirocyclic ketal, with sequential oxidation of the exocyclic olefin, furnishing epoxide **162**. Nucleophilic epoxide opening with lithium acetylide complex **163** followed by base-mediated alkyne internalization then provided propargyl alcohol **164** in a combined 64% yield over five steps from methylenecyclobutane **160**. Reduction of propargylic alcohol **164** was accomplished in regioselective fashion through a hydroalumination directed by the tertiary alcohol. The metallated intermediate was quenched with elemental iodine to provide (*Z*)-alkenyl iodide **165**. Complementary furan **166**, synthesized in stereoselective fashion from α-D-glucofuranose, was then appended to alkenyl iodide **165** through a Nozaki–Hiyama–Kishi (NHK) coupling, furnishing polycycle **167** in 64% yield and as a 2.4:1 mixture of diastereomers. The relative stereochemistry of the major and minor diastereomers was not assigned as the mixture proved inconsequential as both diastereomers converged on hemiketal **168** as an unassigned mixture of diastereomers in a 5:1 ratio after Swern oxidation, installing the characteristic spirocyclic dihydrofuranol moiety found within BSK (**6**).

Mulzer and coworkers envisioned advancement of ketal **168** to BSK (**6**) by first completing the eastern tricyclic lactone (Scheme 35).[68] The authors planned to accomplish this transformation employing chemistry previously developed in their laboratory for the construction of aldehyde **161** (see Scheme 33). A formal chemoselective isomerization of the monosubstituted olefin would provide sulfone **169** as the substrate for the key base-mediated macrocyclization. With the core structure of BSK formed, completion of the total synthesis of BSK (**6**) from ketone **170** would consist largely of protecting group removal and oxidation state manipulation. Since the initial communication of this work, however, Mulzer and coworkers have provided neither an update on the advancement of dihydrofuranol **168** nor a rationale for why dihydrofuranol **168** proved to be an intractable intermediate en route to BSK (**6**).

Presumably without any success in advancing dihydrofuranol **168** through the key macrocyclization step, Mulzer and coworkers recently revealed yet another reevaluation of

their synthetic strategy focusing on an alternative macrocyclization strategy.[67] Toward this end, alkenyl iodide **165** was first advanced through a palladium-catalyzed carbonylation, which proceeded with concomitant lactonization, furnishing butenolide **171** after ketal cleavage in 99% yield over two steps (Scheme 36). After cleavage of the methoxymethyl ether using TMS bromide, triol **172** could be sequentially oxidized using manganese dioxide in ethyl acetate to provide lactone **173** followed by Swern oxidation completed aldehyde **174.** Addition of a propargyl nucleophile into aldehyde **174** was then accomplished by forming the propargylindium species in situ from indium metal in the presence of enantiopure **(1*R*,2*S*)-175** as the ligand. Careful temperature control provided propargylic alcohol **176** in 56% yield and in 20:1 dr over two steps from butenolide **173.** At this stage, bromination and diimide-mediated partial reduction of alkyne **176** provided alkenyl bromide **177** as the desired macrocyclization substrate. Yet again, however, Mulzer and coworkers found themselves unable to stitch together macrocyclic scaffold **178**, halting any progress toward BSK (**6**). This work represents the most recent update to the storied pursuit of BSK (**6**) in the Mulzer group.

In contrast to Mulzer's 3rd generation approach, Pattenden and coworkers sought to accomplish the synthesis of BSK (**6**) in biomimetic fashion.[71–72] Toward this end, Pattenden and coworkers offered an alternative biosynthetic pathway for the formation of BSK (**6**, Scheme 37). Beginning with the oxidation of rubifolide (**179**) to bisacetate **180**, subsequent olefin isomerization and hydration would provide conjugated enol ether **181.** Formation of the cyclobutane moiety was then proposed to occur immediately from enol ether **181** before ultimate allylic oxidation and formation of methylenetetrahydrofuranol moiety required for BSK (**6**). Synthetically, Pattenden and coworkers planned to accomplish the biomimetic enol ether [2 + 2] cycloaddition through a non-photochemical Lewis acid-catalyzed reaction manifold.[73] The proposal of the formation of the cyclobutane ring prior to the ultimate biosynthetic step contrasts the other proposed BSK (**6**) biosynthetic pathway (see Scheme 1).

Exploration of the alternative BSK (**6**) biosynthetic pathway began by targeting a simplified macrocyclic butenolide model system from bipinnatin J (**30**, Scheme 38), the synthesis of which had previously been concurrently developed by Pattenden[1,46–47] and Trauner.[23,48–49] Deoxygenation of bipinnatin J (**30**) using triethylsilane smoothly furnished minimally functionalized furanobutenolide **182** in excellent yield. Chemoselective oxidation of furan **182** was then accomplished with *m*-CPBA, providing bisenone **183** in 90% yield. At this stage, exposure of bisenone **183** to acidic conditions was expected to induce hydration, cyclization, or ideally concomitant [2 + 2] cycloaddition to provide tertiary alcohol **185**, hemiketal **186**, or cyclobutane **187**, respectively. Unfortunately, progress toward BSK core scaffold **187** was halted at this stage, as exposure of bisenone **183** to acidic conditions provided only allylic alcohol **184.**

Without success on the simplified system, Pattenden and coworkers sought to construct a more highly elaborated furanobutenolide (e.g., **189** and **191**, Scheme 39) in order to test the proposed [2 + 2] cycloaddition. Synthesis of bishydroxyfuranobutenolide **189** was approached using the same NHK macrocyclization strategy employed in the synthesis of

bipinnatin J (**30**, Scheme 39A).[46–49] Unfortunately, only desbromo-**188** was observed under NHK coupling conditions without any trace of diol **189.** In a complementary approach, furanobutenolide **191** was envisioned to arise via macrocyclic ring-closing metathesis (RCM, Scheme 39B). Yet again, however, attempts to accomplish macrocyclization proved unfruitful. Under a series of conditions employing Grubbs 2nd generation catalyst (**109**), only nonproductive reactivity was observed, including dimerization of vinyl furan 190. To date, no further work has been disclosed that has been able to rigorously test the validity of the proposed BSK (**6**) biosynthetic pathways, although Theodorakis and coworkers have established synthetic access to macrocyclic furanobutenolides related to diol **189.**[74]

In a similar fashion to Pattenden's pursuit of BSK (**6**), Stoltz and coworkers envisioned constructing the characteristic fused cyclobutane through non-photochemical method. In fact, Stoltz and coworkers envisioned the synthesis of the cyclobutane-containing tricycle using a cyclopropane fragmentation-Michael addition strategy in place of a [2 + 2] cycloaddition.[75–76] Retrosynthetically, access to BSK (**6**) was envisioned through the highly functionalized cyclobutane-centered polycycle **192** (Scheme 40). Construction of the cyclobutane was planned through an intramolecular Michael addition of enolate **193** into the extended oxocarbenium fragment. Generation of charge-separated intermediate **193** would be achieved by the fragmentation of cyclopropane **194.**

Investigation of the planned cyclopropane fragmentation began with the enantioselective synthesis of furan-substituted cyclopentenediol **195** by palladium-catalyzed aerobic oxidative kinetic resolution (Scheme 41). By this method, diol **195** was accessible in 93% ee. Acetylation of secondary alcohol with sequential silyl ether cleavage provided allylic alcohol **196** in 85% yield over two steps. Esterification of alcohol **196** with α-diazoacid **197**, a reagent specifically developed for this synthetic application,[76] was then accomplished under coupling conditions mediated by dicyclohexylcarbodiimide (DCC) to smoothly furnish α-diazoester **198**. Intramolecular cyclopropanation of α-diazoester **198** proceeded most efficiently when employing catalytic bis(salicylideneaminato-*N*,*O*)copper(II) complex **199**, providing cyclopropane **200** in 56% yield after heating in anhydrous toluene. Unfortunately, advancement of cyclopropane **200** was plagued by nonproductive translactonization after liberation of the free hydroxyl group at C(8) independent of the identity of the Lewis acid catalyst, solvent, and temperature used to remove the protecting group. For example, saponification of acetate **200** results in translactonization, liberating a free hydroxyl at C(10), which underwent oxidation by DMP and, after cyclopropane fragmentation, regenerated the bicyclic lactone scaffold as ketal **201**. Ultimately, like all of the other synthetic methods disclosed to date, Stoltz and coworkers were not successful in the completion of their efforts toward BSK (**6**), as they were unable to develop conditions for the advancement of any cyclopropane scaffold related to **200** to the desired cyclobutane intermediate (cf. **192**). Bicyclic lactone **201**, however, could still be employed as an intermediate toward the total synthesis of verrillin (**13**), although any progress toward verrillin employing these intermediates has not yet been disclosed.

The final strategy for the synthesis of BSK (**6**) presented in the literature remains only a preliminary investigation that focused on the development of a reaction manifold for access

the γ-furyl-γ-butyrolactones in enantio- and diastereoselective fashion.[77] Reiser and coworkers sought to accomplish this goal through the stereoselective coupling of enantioenriched aldehydic cyclopropanes (e.g., **202**, >99% ee)[78] with siloxyfurans (e.g., **203**) using stoichiometric BF_3•OEt_2, followed by a retroaldol-lactonization cascade catalyzed by Otera's catalyst (**205**, Scheme 42). Under these reaction conditions, the desired γ-furyl-γ-butyrolactones could be accessed in high diastereoselectivity, as exemplified by the formation of butenolide **206** in a dr greater than 99:1. Advancement of butenolide **206** toward the BSK scaffold through a reduction-oxidation sequence provided furan **207** in 63% yield over 2 steps. Palladium-catalyzed alkenylation with ethyl methacrylate (**208**) then afforded unsaturated ester **209.** Chemoselective furyl oxidation of ester **209** was accomplished using elemental bromine under an atmosphere of ammonia, providing bisketal **210** as the initial product. However, after purification on silica gel, only elimination product **211** remained. Although unsaturated ester **211** shares a number of important structural features with the BSK (**6**) scaffold, completion of the synthesis of BSK (**6**) from ester **211** remains a challenging feat, requiring the installation of the western methylenetetrahydrofuranol and the eastern fused cyclobutane tricycle. To date, any continued elaboration of ester **211** or any of its analogues have not yet been reported.

4.2. Synthetic Efforts Toward Verrillin

Efforts toward the total synthesis of the closely related macrocycle verrillin (**13**) have only been disclosed by Theodorakis and coworkers (Scheme 43).[79] Retrosynthetically, the authors envisioned completion of verrillin (**13**) by late-stage oxidation of furan **212** to complete the sequential bridging ketals and the second lactone from the isopropenyl side chain. Convergent assembly of furan **212** would be accomplished by the coupling of three components: aldehyde **213**, furan **214** and *cis*-1,3-cyclopentenediol **215.** The relative stereochemistry throughout the synthesis would be derived from the stereochemistry of the 1,3-*cis*-cyclopentenediol building block.

Theodorakis and coworkers pursued the synthesis of racemic verrillin (**13**) beginning with furyl alcohol **216** (Scheme 44). Conversion of furan **216** to racemic alkenyl iodide **215** was accomplished in 21% yield over 4 steps. Eschenmoser–Claisen rearrangement from tertiary alcohol **215** with amide acetal **217**, followed by removal of the TBS ether with concomitant lactonization provided bicycle **218**. Addition of lactone **218** into aldehyde **213** provided alcohol **219** as a 1.7:1 mixture of diastereomers at C(13) in favor the desired diastereomer as shown. After protecting group manipulation, alkenyl iodide **220** was coupled with furyl stannane **214**. Subsequent Appel halogenation provided bromide **221**, which could be cyclized to provide macrocycle **222** in 39% isolated yield, although **222** was produced in a 4:1 ratio of diastereomers in favor of the desired *anti* configuration between C(1) and C(2) as required for verrillin (**13**). The completion of the furyl core of the natural product marked the end of the only reported synthetic studies toward the total synthesis of verrillin (**13**).

4.3. Synthetic Efforts Toward Havellockate

Havellockate (**14**), which contains the same C(8)/C(10) relative stereochemistry found in verrillin (**13**), has been targeted by two laboratories through two distinct synthetic strategies. Mehta and coworkers disclosed the first synthetic studies toward havellockate in 2001.[80]

They envisioned access to havellockate (**14**) could be achieved through tetracycle **223** after addition of the isopropenyl side chain and ultimate oxidation (Scheme 45). Spirocyclic lactone **223** would in turn be derived from the oxidation of spirocyclic tetrahydrofuran **224**.

Targeting core tetracycle **224**, synthetic advancement toward racemic havellockate (**14**) was pursued from ketal **225** (Scheme 46). Synthesis of *cis*-1,3-cyclopentanediol **226** was achieved after eight synthetic transformations, comprised mainly of a series of stereoselective redox manipulations, in 16% overall yield. Baeyer–Villager oxidation of ketone **226** furnished lactone **227** as a single product. Reductive opening of lactone **227** followed by sequential selective silyl ether formation and oxidation furnished enone **228**. Formation of the targeted spirocyclic furan was accomplished after 1,2-addition of a vinyl nucleophile into the enone, allylic alkylation of the resultant tertiary alcohol, and ring-closing metathesis employing the Grubbs 1st generation catalyst (**64**) to provide spirocycle **229** in 49% yield over three steps. Silyl ether cleavage, oxidation, and olefin isomerization supplied aldehyde **230**, which was globally hydrogenated and oxidized, affording tetrahydrofuran **224**, the targeted core polycycle of havellockate (**14**), with the proper stereochemistry installed at each ring junction. Mehta and coworkers did not advance furan **224** any further toward havellockate (**14**).

More recently, in 2010, Barriault and workers disclosed their progress toward the racemic total synthesis of havellockate (**14**).[81] Access to havellockate (**14**) was envisioned through enone **231** after formation of the spirocyclic lactone moiety (Scheme 47). Enone **231** would be available from bicycle **232** after oxidation and functionalization of the cyclohexene. Bicycle **232** would in turn be formed through a Diels-Alder cycloaddition of diene **233**.

In the forward sense, furyl alcohol **216** was advanced to racemic *cis*-1,3-cyclopentenediol **233** over five steps in 10% overall yield (Scheme 48). Hydroxyl-directed Diels-Alder cycloaddition of diene **233** with acrolein in the presence of excess magnesium(II) bromide followed by global reduction, furnished cyclohexanol **234**. Oxidation of polyol **234** furnished silyl ether **235** after concomitant lactonization. Addition of a vinyl nucleophile to ketone **235** followed by the addition of acetic anhydride provided acetate **236** in 42% yield. Ozonolysis, aldol condensation, and ultimate silyl ether cleavage provided spirocycle **237** after in situ translactonization. Tetracycle **237** is the fully elaborated core of havellockate lacking the appropriate oxidation state and the isopropenyl side chain flanking the cyclohexane, as well as the β-hydroxyl group within the spirocyclic lactone.

While direct advancement of tetracycle **237** toward havellockate (**14**) proved unfruitful, cyclohexanone **235** proved amenable to alternative functionalization of the cyclohexanone moiety (Scheme 49). Two-step oxidative desaturation of cyclohexanone **235** furnished enone **238** in 34% yield. Stille coupling of stannane **239**, after formation of the intermediate alkenyl iodide from enone **238**, afforded diene **240**. Installation of the spirocyclic dihydrofuran was accomplished by a method derived from the work of Mehta and coworkers (see Scheme 46) to provide alcohol **241** after PMB ether cleavage in 44% yield over four steps. Vinylation of allylic alcohol **241** followed by Claisen rearrangement furnished aldehyde **242** in 53% yield as a 1:1 mixture of C(1) diastereomers. The successful installation of the isopropenyl side chain produced another late-stage, highly functionalized

intermediate (**242**) that stands as the Barriault laboratory's most advanced intermediate en route to havellockate (**14**).

4.4. Synthetic Efforts Toward Intricarene

The biomimetic asymmetric total synthesis of intricarene (**7**) was accomplished by both the Pattenden[46–47] and Trauner[48–49] laboratories in 2006, representing two of the rare examples of a completed synthesis of a member of the polycyclic furanobutenolide-derived cembranoid and norcembranoid natural family. The biosynthesis of intricarene (**7**) had been proposed from bipinnatin J (**30**, Scheme 50). Oxidative cleavage of the furan moiety followed by isomerization would produce the hypothesized biosynthetic intermediate oxidopyrylium ion **38.** Subsequent dipolar [5 + 2] cycloaddition would then complete the construction of intricarene (**7**). In order to experimentally confirm this speculated biosynthetic pathway, which had been explored computationally,[50] both Pattenden and Trauner sought initially to complete the asymmetric total synthesis of bipinnatin J (**30**).

Both laboratories took similar routes toward the asymmetric total synthesis of bipinnatin J (**30**). Pattenden and coworkers began their stereoselective synthesis with epoxide **243**, which was available five steps from (+)-glycidol (Scheme 51). Coupling of epoxide **243** with selenide **244** provided alkene **245** in 60% yield. Sequential lactonization, selenide oxidation and elimination, and silyl ether cleavage furnished alkenyl iodide **246** in 62% yield over three steps. Alternatively, Trauner and coworkers pursued the enantioselective synthesis of bipinnatin J (**30**) beginning with alkyne **247**, which was available in with 92% ee after the asymmetric 1,2-reduction of the ketone precursor (Scheme 52). Conversion of silyl alkyne **247** into alkynoate **248** was accomplished in four steps in high yield. Butenolide **250** was formed from ester **248** through a ruthenium-catalyzed Alder ene reaction, followed by olefination of the resultant aldehyde. Redox manipulation of ester **250** completed alternative synthetic access to alkenyl iodide **246**.

Advancement of iodide **246** was accomplished by both Pattenden and Trauner in nearly identical fashion (Scheme 53). Stille coupling of iodide **246** and furfural stannane **214** and subsequent Appel halogenation of the primary allylic alcohol produced allylic bromide **251**. NHK coupling mediated by chromium(II) chloride was then employed to join the allylic bromide and furyl aldehyde moieties and complete the asymmetric total synthesis of bipinnatin J (**30**).

With the asymmetric total synthesis of bipinnatin J (**30**), both Pattenden and Trauner turned their attention to the investigation of the biomimetic synthesis of intricarene (**7**, Scheme 54). Pattenden and coworkers proceeded with the vanadium-catalyzed epoxidation of allylic alcohol **30** followed by acetylation of the resultant hemiketal to provide hydroxypyrone **252** in 30% yield. Alternatively, Trauner and coworkers accomplished the oxidation of furan **30** with *m*-CPBA. Acetylation of the intermediate hemiketal furnished enone **252** in an improved 81% yield from bipinnatin J (**30**). Advancement of acetate **252** was accomplished under basic conditions. Pattenden and coworkers found that exposure of hydroxypyrone **252** to DBU in refluxing acetonitrile furnished intricarene (**7**) in 10% yield, proposing the reaction proceeded through oxidopyrylium ion **38** and ultimately [5 + 2] cycloaddition in

analogous fashion to the proposed biosynthesis (see Schemes 3 and 50). Similarly, Trauner and coworkers found that in the presence of TMP in DMSO at 150 °C, acetate **252** was converted to intricarene (**7**) in 26% yield, again invoking the intermediacy of the same speculated biosynthetic precursor (**38**). These studies led the authors to conclude that the biosynthetic speculations surrounding the formation of intricarene (**7**) from a hydroxypyrone precursor are likely correct and the production of intricarene likely happens in vivo directly from bipinnatin J (**30**).

As Trauner and coworkers continued their investigations toward the polycyclic furanobutenolide-derived natural products, they serendipitously encountered and alternative synthetic route that provided intricarene (**7**) from bipinnatin J (**30**) by single electron transfer under photochemical reaction conditions (Scheme 55). Bipinnatin J (**30**) was first converted to 2-*O*-methylbipinnatin J (**253**), another macrocyclic natural product that co-occurs with bipinnatin J in Caribbean soft corals of the genus *Pseudopterogorgia*.[82] Oxidation of 2-*O*-mcthylbipinnatin J (**253**) with singlet oxygen then provided butenolide **254** in 80% yield as the substrate for photochemical investigations. Irradiation of butenolide **254** under aqueous photochemical conditions designed to mimic the UV intensity in the natural environment of *Pseudopterogorgia* was expected to furnish BSK scaffold **255.** Although no trace of BSK scaffold **255** could be detected, to the author's surprise, intricarene (**7**) was produced in 25% yield. Paired with computational investigations,[48] these experimental results cast doubt on the exact biosynthetic pathway through which intricarene is produced. Indeed, whether intricarene is naturally produced in a concerted or step-wise manner, the bio-inspired production of the natural product by two distinct synthetic routes represents an impressive achievement.

4.5. Synthetic Efforts Toward Rameswaralide

Several approaches to the core structure of rameswaralide (**8**) have been described, although the synthesis of rameswaralide itself has not yet been achieved. Mehta and coworkers envisioned access to rameswaralide (**8**) through core tricycle **256** after Diels–Alder cycloaddition (Scheme 56).[83] Cycloheptenone **256** would in turn be synthesized by a ring-closing metathesis from diene **257.** Access to enone **257** would be accomplished by the functionalization of bicyclic lactone **258**, a derivative of the Corey lactone.

The pursuit of (±)-rameswaralide (**8**) was accomplished from bicyclic ketone **(±)-260**, which was available from acetate **259** in 49% yield over six steps (Scheme 57). Baeyer–Villager oxidation of ketone **260** provided lactone **261** as a single product in excellent yield. Silyl ether cleavage and subsequent iodolactonization furnished bicyclic iodide **262.** Global silyl ether formation followed by reduction of the secondary iodide moiety provided lactone **263** in 85% yield over two steps from halide **262.** Advancement of lactone **263** was then accomplish by alkylation with either allyl or propargyl bromide. Sequential selective primary silyl ether cleavage and oxidation of the resultant primary alcohol provided intermediate bicycle **264** as a single diastereomer independent of the identity of the α-lactone substituent. Addition of a vinyl nucleophile to aldehyde **264** followed by oxidation of the intermediate secondary alcohol provided allyl-substituted lactone **265** and propargyl-substituted lactone **266** in 47% and 41% yield, respectively, over five steps from bicycle **263.**

Pleasingly, exposure of allylic bicycle **265** to Grubbs 2nd generation catalyst (**109**) smoothly furnished tricycle **267**, completing the core scaffold of rameswaralide (Scheme 58A). Unfortunately, all attempts to advance dienophile **267** toward rameswaralide (**8**) through a Diels–Alder cycloaddition were unfruitful. In an attempt to alternatively access rameswaralide (**8**), Mehta and coworkers sought to complete the more extensively functionalized core of rameswaralide (**268**) by enyne metathesis from alkyne **266** (Scheme 58B). Unfortunately, this synthetic approach could not be successfully employed for the formation of the characteristic 7-membered ring integral to the carbocyclic scaffold of rameswaralide (**8**).

Comparatively, Srikrishna and coworkers envisioned the use of a ring-closing metathesis to access two different rameswaralide core bicycles **269** and **271** (Scheme 59).[84] The [6,7]-core scaffold **269** would arise directly from olefin **270** by ring-closing metathesis. Alternatively, synthetic access to [5,7]-core scaffold **271** was also envisioned from olefin **270** after ring contraction and subsequent ring-closing metathesis.

The stereoselective synthesis of the [6,7]-bicyclic core of rameswaralide (**269**) began with the alkylation of (*R*)-carvone (**272**) with allyl bromide to provide *anti* product **273** in 12% yield as the minor diastereomer (Scheme 60). Sequential 1,2-addition of butenyl bromide **274** in the presence of lithium metal and oxidative 1,3-allylic transposition of the intermediate tertiary alcohol provided enone **275** in 80% yield over two steps. Ring-closing metathesis of tetraene **275** furnished **269** in 98% yield as the core [6,7]-bicycle of rameswaralide, possessing the proper relative *anti* configuration between the isopropenyl substituent and the fused cycloheptene.

Construction of the complementary [5,7]-bicyclic core of rameswaralide began with the diastereoselective reduction and sequential diastereo- and chemoselective epoxidation to provide alcohol **276** in 62% yield over two steps (Scheme 61). Oxidation of secondary alcohol followed by a Favorskii-type ring contraction produced cyclopentane **277**. Ultimate ring-closing metathesis furnished bicyclic cycloheptene **271** in 95% yield from cyclopentanol **277**. Although the core carbocyclic scaffold of the cycloheptene **271** contains a portion of the core bicyclic structure of rameswaralide (**8**), the substitution and oxidation pattern would need to be greatly altered in order to utilize bicycle **271** in total synthetic efforts toward the natural product. Srikrishna and coworkers have not provided any update concerning the utility of either [6,7]-bicycle **269** or [5,7]-bicycle **271** in further advancement toward rameswaralide (**8**).

A third approach to the core scaffold of rameswaralide (**8**) was disclosed by Trost and coworkers.[85] Synthetic access to core tricycle **278** would be accomplished by an acyl radical cyclization and epoxidation of selenide **279** (Scheme 62). Acylselenide **279** would be produced by the acylation of secondary alcohol **280.** Construction of bicycle **280** could be achieved by the intramolecular [5 + 2] cycloaddition of allylic cyclopropane **281.**

Synthesis of the racemic core tricycle of rameswaralide commenced with known cyclopropane **282** (Scheme 63). Stereoselective 1,2-reduction of enone **282** furnished *syn*-1,3-diol **(±)-283** in a 20:1 diastereomeric ratio in favor of the desired product.

Subsequent ruthenium-catalyzed intramolecular [5 + 2] cycloaddition provided cycloheptadiene **284** in 73% yield.[86] Acylselenide **285** was then formed over two steps from secondary alcohol **284** in high yield. Reductive radical cyclization of acylselenide **285** furnished tricycle **286** in 88% yield. Epoxidation of allylic alcohol **286** provided tetracycle **287**, which was advanced to sulfoxide **288** over two steps. Ultimately, elimination of sulfoxide **288** by heating in toluene at 90 °C provided two isomeric forms of the desired core of rameswaralide, **289** and **290**, although further progress toward the natural product itself has not been disclosed at this stage.

4.6. Synthetic Efforts Toward Rameswaralide, Plumarellides, and Mandapamates

Pattenden and coworkers, in addition to their work toward bielschowskysin (**6**) and intricarene (**7**), developed synthetic access to the core of rameswaralide during their pursuit of a unified biomimetic approach to the mandapamates and plumarellides.[87–93] The plumarellides (**15–16**) and mandapamates (including confertdiate, **17–20**) and share a common carbocyclic scaffold (Figure 9). Although they are varied to a different extent in overall oxidation state and relative configuration at the spirocyclic furan ring juncture, Pattenden and coworkers sought to test their biosynthetic hypotheses for the construction of each of these six natural products (**15–20**) through related mechanisms.

Hypothesizing that each of the plumarellides and mandapamates arises in vivo from the corresponding macrocyclic precursor by an intramolecular [4 + 2] cycloaddition (e.g., macrocycle **40** to plumarellide (**15**, Scheme 64), Pattenden and coworkers designed a series of model substrates (**291–294**) to explore the propensity of related systems to construct the desired carbocyclic scaffold. Enantioenriched acyclic diastereomeric diols **291** and **292** were synthesized through an asymmetric dihydroxylation route while macrocyclic ester **293** and acetate **294** were each constructed in stereoselective fashion from (−)-malic acid.

Exposure of acetonide **292** to TFA resulted in the cleavage of the ketal and subsequent intramolecular rearrangement (Scheme 65). Based on the isolated products, Pattenden and coworkers hypothesize that under the reaction conditions, furan **292** proceeds through intermediate **295** en route to allylic cation **296** after intramolecular cyclization. Cation **296** would then undergo nucleophilic attack from either C(6) or C(5) of the furan ring to furnish cyclohexene **297** or cycloheptene **298**, respectively. Cyclohexene **297**, the minor product, represents the core structure of the mandapamates with the lactone found in plumarellide (**15**) still intact. Pentacycle **297** is epimeric to the plumarellide core, however, at C(8). The unexpected major product, tetracycle **298**, is the core structure of rameswaralide (**8**), containing all of the required relative stereochemistry.

In an effort to construct the plumarellide core, diastereomeric diol **291** was subjected to identical reaction conditions (Scheme 66). Surprisingly, the only observed product was the C(7) and C(8) diastereomer of the rameswaralide core (**301**). This empirical evidence suggests that the configuration at the C(8) stereocenter is critical for the productive formal intramolecular cycloaddition of the nonmacrocyclic substrates **291** and **292**.

Macrocyclic substrates **293** and **294** were then exposed to aqueous TFA and both selectively furnished unexpected tetracycles **304** and **305**, respectively, as the sole product without any

trace of the desired plumarellide scaffold (**306**, Scheme 67). Tetracycles **304** and **305** are proposed to arise from furans **293** and **294** after elimination to form oxocarbenium **302** and subsequent isomerization to provide vinylogous diketone **303.** Formal intramolecular cycloaddition between C(4) and C(5) within the vinylogous diketone moiety and the 1,3-diene found between C(11) and C(14) of macrocycle **303** would then furnish the novel tetracyclic cembranoid scaffolds **304** and **305.** Plumarellide core **306**, the expected product, would have been produced by the proposed biomimetic [4 + 2] cycloaddition between the olefin at C(6) and C(7) of macrocycle **302** with the 1,3-diene moiety before isomerization to vinylogous diketone **303.**

Although these results did not disprove the originally proposed biosynthesis of the plumarellides (**15–16**) and mandapamates (**17–20**), Pattenden and coworkers began exploring alternative biosynthetic pathways for the formation of these two natural product families. Considering the biosynthesis of plumarellide (**15**), oxidation of the olefin between C(7) and C(8) followed by olefin transposition and intramolecular Michael addition would provide intermediate ketal **307** (Scheme 68). Subsequent vinylogous aldol addition would complete plumarellide (**15**). Although the exact biosynthesis of the plumarellides (**15–16**) and mandapamates (**17–20**) remains unknown, the work done by Pattenden and workers has provided a wealth of information about the chemistry of the macrocyclic furanobutenolide cembranoid natural products.

4.7. Synthetic Efforts Toward Plumarellides, Mandapamates, and Dissectolide

The only other work toward the plumarellides (**15–16**) and mandapamates (**17–20**) was carried out by Mehta and coworkers in their pursuit of a unified strategy to the carbocyclic core of both families of polycyclic furanobutenolide-derived cembranoids as well as the furanobutenolide-derived norcembranoid dissectolide (**22**, Scheme 69).[94] Synthetic access to common [7,6,5]-carbocyclic core **308** was envisioned through the intramolecular Diels–Alder cycloaddition of diene **309**. Vinylogous diketone **309** would in turn be synthesized by the oxidative cleavage of furan **310**.

Synthetic advancement began with furfural derivative **311** (Scheme 70). A Negishi coupling of alkyl zinc reagent **312** followed by nucleophilic addition of bromide **313** into the aldehyde moiety of heterocycle **311** provided butenolide **314** in 47% yield over two steps. Sequential reduction, Stille coupling, and ring-closing metathesis yielded macrocycle **315** in 14% yield over three steps. This synthetic route only provides access to the *cis*-macrocyclic product **315** with no trace of the desired *trans*-macrocycle (**310**). Advancement of *cis*-macrocycle **315** by oxidative cleavage of the furan moiety provided *cis*-vinylogous diketone **316** in excellent yield. Diene **316** was then heated in toluene in order to induce an intramolecular Diels–Alder cycloaddition. Under the reaction conditions, the *cis*-dienophile **316** isomerized to *trans*-vinylogous diketone **317**, as evidenced by the resulting *trans*-stereochemistry in tricycle **318**, which was isolated as the sole product from diene **316** in 67% yield after concomitant opening of the lactone.

Unfortunately, core scaffold **318** possesses the improper relative stereochemistry at C(7) in comparison to the plumarellides (**15–16**) and dissectolide (**22**), and at C(11) as required for

plumarellides (**15–16**), mandapamates (**17–20**), and dissectolide (**22**). While the epimerization of configuration at C(7) can easily be envisioned, the correction of the *anti*-relationship between C(11) and C(14) to the desired *syn* configuration would be nontrivial. This *anti*-relationship is dictated by the *cis*-configuration of the $\Delta_{13,14}$ bond formed during the macrocyclization of butenolide **314** by ring-closing metathesis. As such, alternative formation of macrocycle **315** would need to be established in order for this synthetic route to warrant further exploration in pursuit of the polycyclic furanobutenolide-derived natural products. Indeed, tricycle **318** stands as the most advanced intermediate disclosed by Mehta and coworkers to date.

5. SYNTHETIC STUDIES TOWARD POLYCYCLIC FURANOBUTENOLIDE-DERIVED NORCEMBRANOIDS

5.1. Synthetic Efforts Toward Yonarolide

The synthesis of yonarolide (**26**) has only been studied by Ito and coworkers in their development of a strategy for the construction of the tricyclic portion if its core scaffold (**319**, Scheme 71).[95] Cyclopentene **319** would be formed after intramolecular aldol condensation of methyl ketone **320**. Synthesis of bicyclic cyclohexenone **320** would be constructed by the Diels–Alder cycloaddition of bisenol ether **321** and butenolide **322**.

In the forward sense, Ito and coworkers pursued the racemic synthesis of the core structure of yonarolide beginning with butenolide **324**, which was available from β-ketoester **323** in 65% yield over four steps (Scheme 72). Diels–Alder cycloaddition of bisenol ether **325** with butenolide **324** proceeded smoothly in the presence of trimethylaluminum and bis(trifluoromethanesulfonyl)methane. Subsequent ketal cleavage provided methyl ketone **326** in 52% yield over two steps from unsaturated lactone **324**. Although methyl ketone **326** contained the wrong relative stereochemistry at the lactone carbinol, exposure of the substrate to TFA in toluene at elevated temperature resulted in the isomerization of configuration at this stereocenter, likely through a retro-conjugate addition and cyclization pathway, and induced the desired aldol condensation to furnish the yonarolide core (**327**) in 55% yield. No trace of epimeric, undesired core **328** was observed. By this synthetic route, Ito and coworkers showed the viability of their retrosynthetic strategy for accessing the tricyclic core of yonarolide (**327**), however, the employment of this method for further advancement toward yonarolide (**26**) has not yet been disclosed.

5.2. Synthetic Efforts Toward Ineleganolide and Sinulochmodin C

Since the initial isolation and stereochemical assignment of ineleganolide (**9**) in 1999,[20] the elegant, compact, and highly oxygenated polycyclic structure has captivated synthetic chemists. Indeed, many groups have pursued the total synthesis of ineleganolide, including the laboratories of Nicolaou,[96] Frontier,[97–98] and Romo[99–100] with only limited success. In addition, four other groups have disclosed the accounts of their efforts. The first of these was presented by Moeller and coworkers in 2007 and targeted a key electrochemical anodic cyclization to construct the central cycloheptanone of the natural product (**9**) from enol ether **329** (Scheme 73).[101–104] Convergent assembly to cyclization precursor **329** would be

accomplished through the Michael addition of tricycle **331** into (*R*)-desmethylcarvone ((***R***)-330). Tricycle **331** would be synthesized in turn from bicyclic lactone **332**.

At the outset of the research program, Moeller and coworkers sought to test the viability of their planned anodic cyclization on model systems, beginning with dihydrofuran **333** (Scheme 74). Under optimized conditions, using a reticulated vitreous carbon (RVC) anode in tandem with a carbon cathode and lithium perchlorate as the electrolyte, the planned oxidative coupling proceeded furnishing acetals **334** and **335** in a combined 75% yield. Acetal **334** displays a *syn* relationship between the methyl substituent at the newly formed all-carbon quaternary center and the acetal moiety on the convex face of the bicyclic scaffold and was formed under these conditions as the major diastereomer in a 6:1 ratio with diastereomer **335.**

Having this early success in hand, Moeller and coworkers sought to extend this methodology to enable the formation of medium-sized carbocyclic scaffold. Of immediate concern was the potential for this reaction manifold to enable the formation of the central heptacycle found within ineleganolide (**9**)**.** Thus, Moeller and coworkers built model system **336**, where substitution at the β-position of the enol ether was tested to explore how polarization of the enol ether system would affect the oxidative cyclization (Scheme 75). Unfortunately, after screening a variety of electrochemical conditions on a series of substrates, no trace of desired heptacycle **337** was ever detected. As studies on the model system failed to generate even the bicyclic core of ineleganolide, Moeller and coworkers abandoned their pursuit of ineleganolide (**9**).

The second approach toward ineleganolide (**9**) was disclosed in 2011 by Pattenden and coworkers as they set out to explore the biosynthetic speculations for the production of both ineleganolide (**9**) and its constitutional isomer sinulochmodin C (**10**).[105] Previously, Pattenden and coworkers had postulated the biosynthesis of both ineleganolide (**9**) and sinulochmodin C (**10**) occurred from the common macrocyclic precursor 5-episinuleptolide (**5**) through sequential transannular Michael additions (see Schemes 6 and 7).[1,24] In order to explore these biosynthetic hypothesis, Pattenden and coworkers took a portion of 5-episinuleptolide (**5**) isolated from the natural source for exploratory semisynthetic studies, since to date there are no reports of the total synthesis of 5-episinuleptolide (**5**, Scheme 76). Acetylation of 5-episinuleptolide (**5**) was accomplished in 92% yield using acetic anhydride in the presence of triethylamine. Exposure of acetate **338** to LHMDS over an extended reaction time, warming slowly from −78 °C to 0 °C furnished both ineleganolide (**9**) and sinulochmodin C (**10**) in 22% yield and 9% yield, respectively. The production of both natural products from acetate **338** strongly supports the proposed biosyntheses and represents the first laboratory-furnished samples of any polycyclic furanobutenolide-derived norcembranoid diterpene.

Additionally, Pattenden and coworkers sought to accomplish the biomimetic semisynthesis of another norcembranoid diterpene natural product horiolide (**21**), guided by their biosynthetic speculations,[24] from acetate **338** (Scheme 77). Exposure of acetate **338** to strongly basic conditions, now using NaHMDS in place of LHMDS, provided novel

norcembranoid derivative **339** as the major product in 75% yield. Despite their efforts, no trace of either horiolide (**21**)[38] or kavaranolide (**22**)[39] was detected.

The third description of a research program targeting ineleganolide (**9**) came from the Vanderwal laboratory in early 2016 and described their efforts toward the asymmetric total synthesis of the natural product.[106–107] Retrosynthetically, Vanderwal and coworkers proposed access to ineleganolide (**9**) through identical bond disconnections as were made by Moeller and coworkers (see Scheme 73). Rather than constructing the central cycloheptanone of ineleganolide (**9**) using electrochemical oxidation, Vanderwal and coworkers planned the closure of the carbocyclic scaffold through an intramolecular nucleophilic cyclization from enol ether **340** (Scheme 78). Tetracycle **340** would be formed by Michael addition of lactone **341** into (*R*)-desmethylcarvone ((*R*)-**330**). Tricyclic lactone **341** would in turn be constructed through a radical bicyclization from functionalized cyclopentene **342.**

For the purpose of synthetic development, the enantiomer *ent*-ineleganolide (***ent*-9**) was targeted. Toward this end, advancement toward the natural product began with the asymmetric deprotonation and subsequent rearrangement of epoxide **343** to furnish *cis*-1,3-cyclopcntcncdiol **(+)-345** in 79% yield with 89% ee (Scheme 79). Oxidation of allylic alcohol **(+)-345** with PCC provided the cyclopentenone building block **346** in 97% yield. Advancement of enantioenriched cyclopentenone **346** was accomplished with the 1,2-addition of methyl lithium, with sequential alkylation of the resultant tertiary alcohol and cleavage of the silyl ether to afford propargyl ether **347** in 87% yield over three steps. Exposure of secondary alcohol **347** to ethyl vinyl ether (**348**) in the presence of NBS enabled the formation of bromide **349** in 87% yield as a 1:1 mixture of diastereomers. Radical cascade cyclization of cyclopentene **349** initiated by tri(*n*-butyl)tin hydride in the presence of AIBN furnished tricycles **350** and **351** in a 1:1 mixture after sequential ozonolysis in a combined 78% yield over two steps.[108–109]

The mixture of epimers **350** and **351** formed after radical bicyclization was the exposed to *p*-toluenesulfonic acid for an extended period at ambient temperature, enabling the enrichment of the epimeric mixture in favor of acetal **351** and the isolation of pure acetal **351** in 95% yield (Scheme 80). Dihydrofuranone **351** was then smoothly converted to enol triflate **352** in 72% yield. At this stage, it became clear that the thermodynamic favorability of epimer **351** was extraordinarily fortuitous as inflation of epimer **350** was plagued by a lack of regioselectivity. Nevertheless, having established access to triflate **352**, advancement toward *ent*-inclcganolidc (***ent*-9**) continued with the Jones oxidation to form lactone **353**, providing the targeted surrogate to synthon **341.**

The asymmetric synthesis of complementary enone (*S*)-dcsmcthylcarvonc (**(*S*)-330**), as necessary for *ent*-inclcganolidc (***ent*-9**), began with racemic cyclohexanone **(±)-354** (Scheme 81). Diastereoselective reduction of the carbonyl followed by enzymatic acetylation provided both alcohol **(+)-355** and acetate **(+)-356**, each in greater than 95% ee.[110] Advancement of desired diastereomer **(+)-356** was accomplished by saponification and oxidation of the intermediate secondary alcohol. Oxidative desaturation of the resultant

cyclohexanone was accomplished over two steps to provide (*S*)-desmethylcarvone (**(*S*)-330**) in 69% yield from acetate (+)-**356**.

Coupling of fragments **353** and **(*S*)-330** was then accomplished using a Mukaiyama–Michael addition, beginning with formation of the silyl enol ether of lactone **353** (Scheme 82). Subsequent exposure of the intermediate enol ether to enone **(*S*)-330** in the presence of lanthanum(III) triflate induced the planned Mukaiyama–Michael addition, providing silyl enol ether **357** in 91% yield in high diastereoselectivity as the undesired epimer at the α-position of the lactone moiety. Despite screening a variety of conditions, Vanderwal and coworkers were unable to accomplish the epimerization to furnish desired lactone **358.**

Exploring alternative approaches toward *ent*-inclcganolidc (***ent*-9**), enol tritiate **357** was advanced by saponification of the lactone moiety, followed by silylation of the secondary alcohol and alkylation of the carboxylic acid moiety to furnish ketone **359** in 45% yield over three steps (Scheme 83). Bromination of silyl enol ether **359** with NBS furnished α-bromoketone **360** as a mixture of diastereomers. Unfortunately, further advancement toward *ent*-inclcganolidc (***ent*-9**) proved troublesome, as cyclization of bromide **360** to *ent*-inclcganolidc core **261** could not be accomplished under either strongly basic reaction conditions (e.g., LDA, KHMDS) or by exposure to Lewis acids known to effect keto-enol tautomerization (e.g., BF_3•OEt_2, $Sc(OTf)_3$). Additionally, all attempts to induce the intramolecular cyclization of bromide **360** through an α-acyl carbenium ion by abstraction of the secondary halide with a silver(I) salt proved unfruitful. Despite attempting a number of alternative routes, Vanderwal and coworkers were unable to complete the total synthesis of *ent*-inclcganolidc (***ent*-9**).

The final synthetic program directed toward ineleganolide (**9**) was disclosed in 2017 by Stoltz and coworkers and also sought to accomplish the de novo enantioselective total synthesis of the natural product.[111] Access to ineleganolide (**9**) was envisioned from cycloheptadiene **362** after olefin oxidation and ultimately oxa-Michael addition to complete the bridging dihydrofuranone moiety (Scheme 84). Tandem intramolecular cyclopropanation-Cope rearrangement would forge of the tetracyclic core of ineleganolide (i.e., **362)** from α-diazoester **363.**[112–114] Cyclization precursor **363** would be assembled in convergent fashion from carvone-derived carboxylic acid **364** and enantioenriched 1,3-*cis*-cyclopentenediol **365**.

Enantioselective construction of 1,3-*cis*-cyclopentenediol **365** began with the transketalization of tris(hydroxymethyl)aminomethane hydrochloride (**367**) with 1,1-dimethoxycyclohexane (**366**, Scheme 85).[111,115–116] Oxidative cleavage of the resultant amino alcohol product provided ketodioxanone **368** in 94% over 3 steps. Condensation of cyclohexylamine onto ketone **368** prior to deprotonation and alkylation with methyl iodide enabled selective monomethylation. Formation of silyl enol ether **369** was accomplished under typical thermodynamic enolization conditions and was produced in a 9:1 ratio with the kinetic enol ether constitutional isomer. The purification of enol ether **369** was complicated by the presence of this impurity, however, limiting the isolated yield of the desired product (**369**) to 40% over three steps form ketodioxanone **368**. Nevertheless, access to enol ether **369** enabled the development of the first pivotal reaction en route to ineleganolide, a

palladium-catalyzed asymmetric allylic alkylation to from the requisite chiral tetrasubstituted center.[117–119] Under optimized conditions, employing mesylate **370** as the allyl electrophile and (*S*)-*t*-BuPHOX (**(*S*)-371**) as the chiral ligand, ketone **(*S*)-372** was formed in 82% yield with 92% ee. For the purpose of synthetic development, choice of (*S*)-*t*-BuPHOX (**(*S*)-371**) as the most readily available and cost-effective enantiomer of the ligand dictated formation of the antipode necessary for the synthesis of ineleganolide (**9**). From this point continuing toward *ent*-ineleganolide (***ent*-9**), ketone **(*S*)-372** was advanced by oxidation of the chlorovinyl fragment and intramolecular Wittig annulation under optimized conditions using tri(*n*-butyl)phosphine to provide enone **373** in 94% yield. Careful temperature control combined with the use of a bulky hydride source enabled the chemoselective 1,2-reduction of enone **373**, affording allylic alcohol **374** in near quantitative yield as a single diastereomer. Benzoylation of secondary alcohol **374** followed by fumaric acid-mediated ketal cleavage yielded primary alcohol **375**. Subsequent oxidation, methylenation of the intermediate aldehyde, and ultimately saponification to remove the benzoyl protecting group provided 1,3-*cis*-cyclopentenediol ***ent*-365** in fifteen steps and 24% overall yield from triol **367**.

Continuing toward *ent*-ineleganolide (***ent*-9**), construction of the corresponding coupling partner began with the selection of the proper enantiomer of desmethylcarvone (**(*R*)-330**), which was available in six synthetic steps from (*R*)-carvone (Scheme 86).[120–122] Addition of the preformed lithium enolate of ethyl acetate (**376**) into enone **(*R*)-330** in 1,2-fashion with sequential 1,3-oxdiative allylic transposition provided ester **377** in 68% yield over two steps. Saponification of ester **377** followed by coupling of the resultant carboxylic acid with 1,3-*cis*-cyclopentenediol ***ent*-365** and sequential diazotransfer with *p*-ABSA (**378**) afforded α-diazoester ***ent*-363** in 75% yield over three steps. Advancing toward the natural product, initial explorations revealed the propensity of α-diazoester ***ent*-363** to undergo the pivotal tandem intramolecular cyclopropanation-Cope rearrangement cascade under mild conditions. Indeed, under optimized conditions using catalytic dirhodium tetraacetate in CH_2Cl_2 at ambient temperature, the tetracyclic core of *ent*-ineleganolide (***ent*-9**) was isolated as cycloheptadiene **379** in 53% yield. Tetracycle **379** represents the first known de novo synthesis of the complete carbocyclic core of ineleganolide or any member of the polycyclic furanobutenolide-derived norcembranoid diterpene family of natural products.

Cycloheptadiene **379** was subsequently oxidized chemoselectively by a hydroxyl-directed epoxidation to provide *ent*-isoineleganolide A (**380**), so termed due to the fact that pentacycle **380** contains all of the atoms required for ineleganolide in the correct molecular oxidation state (Scheme 87). At this stage, the direct conversion of *ent*-isoineleganolide A (**380**) to *ent*-isoineleganolide B (**383**) was envisioned directly through a *syn*-facial 1,2-hydride migration. Although the desired rearrangement was never successfully induced, alternative advancement of *ent*-isoineleganolide A (**380**) began with nucleophilic opening of the epoxide moiety with $MgBr_2$, which proceed with concomitant transannular oxa-Michael addition. Kornblum oxidation of the intermediate secondary bromide provided ketopyran **381** in 96% yield over two steps. Chemoselective reduction of α-alkoxyketone **381** was then accomplished using SmI_2 in combination with LiCl as an additive, which provided a mixture of reduced products in 85% yield. The relative configuration of the major product, hemiketal

382, could be established by single crystal X-ray diffraction, confirming protonation of the intermediate samarium enolate from the α-face at C(7) as required for *ent*-ineleganolide (***ent*-9**). Exposure of the resultant mixture of reduction products, including hemiketal **382**, to an acidic resin in CH_2Cl_2 facilitated the formation of *ent*-isoineleganolide B (**383**) in 63% yield with concomitant epimerization of the configuration at C(7).

At this stage, completion of *ent*-ineleganolide (***ent*-9**) was planned by epimerization of configuration at C(7) paired with isomerization of enone **383** into the isomeric vinylogous diketone, at which point an intramolecular oxa-Michael addition would complete the natural product. Unfortunately, neither could the olefin isomerization be induced nor could any method be developed for the advancement of *ent*-isoineleganolide B (**383**) to *ent*-ineleganolide (***ent*-9**). Retreating several steps, Stoltz and coworkers developed an alternative late-stage synthetic strategy beginning with cycloheptadiene **379** (Scheme 88). Conjugate reduction of cycloheptadiene **379** with SmI_2 using water as an additive, paired with careful temperature control, provided ketone **384** as a single diastereomer, installing the desired configuration across the [6,7]-ring junction. Hydroxyl-directed epoxidation of allylic alcohol **384** then afforded epoxide **385** in 94% yield, which proved unable to undergo the previously developed two-step Kornblum oxidation sequence. Epoxide **385** was instead opened reductively using titanocene monochloride, with zinc metal as the terminal reductant, resulting in protonation of the intermediate anion from the α-face as desired for *ent*-ineleganolide (***ent*-9**). Ultimately, oxidation of the intermediate 1,3-diol with Dess–Martin periodinane provided 2*H*-*ent*-ineleganolide (**386**). Yet again, completion of *ent*-ineleganolide (***ent*-9**) from 2*H*-*ent*-ineleganolide (**386**) by oxidative formation of the dihydrofuranone and installation of the final requisite bond could not be accomplished despite extensive investigation. The synthesis of 2*H*-*ent*-ineleganolide (**386**), however, represents a significant accomplishment, as this advanced intermediate is only a single C–O bond removed from *ent*-ineleganolide (***ent*-9**).

In an effort to thoroughly understand why the final late-stage synthetic manipulations of these ineleganolide-like intermediates continuously proved recalcitrant and untenable, Stoltz and coworkers examined the three-dimensional conformations of 2*H*-*ent*-ineleganolide (**386**, established by single crystal X-ray diffraction)[111] in comparison to ineleganolide (**9**, established by single crystal X-ray diffraction, Figure 10).[20] This comparison clearly established that although the conformation of 2*H*-*ent*-ineleganolide (**386**) is closely related to the natural product, the central cycloheptanone is creased, bisecting the molecular scaffold, and leaving the apical methylene a great distance from the hydroxyl group (purple) required for the dihydrofuranone. Thus, 2*H*-*ent*-ineleganolide (**386**) would have to undergo a significant conformational isomerization in order to position the free hydroxyl in close enough proximity to the apical methylene in order to be able to forge the final bond need to complete *ent*-ineleganolide (***ent*-9**). Currently, Stoltz and coworkers are continuing to computationally evaluate the energy landscape around the completion of the natural product from 2*H*-*ent*-ineleganolide (**386**) and other advanced intermediates.

6. CONCLUDING REMARKS

The synthetic efforts toward ineleganolide (**9**) are a tremendous representation of the pattern of successes and failures around the synthetic studies of the polycyclic furanobutenolide-derived cembranoid and norcembranoid natural products. The extremely limited examples of completed syntheses of members of this natural product family have been exclusively biomimetic synthetic (i.e., intricarene (**7**) by Pattenden[46–47] and Trauner[48–49]) or semisynthetic (i.e., ineleganolide (**9**) and sinulochmodin C (**10**) by Pattenden[105]). *The de novo synthesis of only a single member* of the polycyclic furanobutenolide-derived cembranoid and norcembranoid family has been completed to date (intricarene (**7**), Pattenden[46–47] and Trauner[48–49]). Aside from this success, only three other synthetic efforts have even managed to successfully complete the carbocyclic core of another member of the polycyclic furanobutenolide-derived cembranoid and norcembranoid, namely the efforts toward the cembranoids verrillin (**13**) by Theodorakis[79] and havellockate (**14**) by Barriault[81] as well as the construction of core of the norcembranoid ineleganolide (**9**) by Stoltz and coworkers.[111]

A number of studies toward the synthesis of cembranoid and norcembranoid carbocyclic scaffolds have been disclosed, revealing valuable information about the chemistry of these core structures. The fact that only a single one of these synthetic efforts has yielded the targeted natural product, however, highlights the need for further investigations. The continued pursuit of these elegant, biologically active, stereogenically complex, and highly oxygenated family of natural products will require the development of new synthetic methods for the synthetic manipulations of compact and highly oxidized polycycles. Success in this area and completion of the syntheses of the polycyclic furanobutenolide-derived cembranoids and norcembranoids will benefit not only other areas of synthetic chemistry through methodological development, but also medicinal chemistry and chemical biology, providing access to these scarce bioactive compounds for complete biological evaluation.

Acknowledgments

The authors wish to thank the NIH-NIGMS (R01GM080269), Amgen, the Gordon and Betty Moore Foundation, and Caltech for financial support. R. A. C. gratefully acknowledges the support of this work provided by a fellowship from the National Cancer Institute of the National Institutes of Health (NIH) under Award Number F31A17435. Dr. Corey Reeves (Caltech), Dr. Aaron Bedell (Stanford), and Mr. James B. C. Mack (Stanford) for editorial assistance. Additionally, the authors wish to thank all the collaborators and coworkers who have contributed to the synthetic efforts toward ineleganolide and the polycyclic furanobutenolide-derived norcembranoids at Caltech for thoughtful insights and helpful discussions including Prof. Jennifer L. Roizen, Dr. Russell C. Smith, Prof. Amanda C. Jones, Dr. Scott C. Virgil, Mr. Beau P. Pritchett, Mr. Benzi I. Estipona, Dr. Seo-Jung Han, Prof. Amanda Silberstein, Mr. Chris Reimann, and Dr. David Romney.

Biographies

Robert A. Craig II was raised near Philadelphia, Pennsylvania, and received his B.S. degree in 2010 from Davidson College. He subsequently joined the labs of Professor Brian M. Stoltz as a graduate student at the California Institute of Technology, where he completed his Ph.D. in 2015. As an NIH predoctoral fellow, his graduate research focused on total synthetic efforts toward the ineleganolide and the related polycyclic furanobutenolide-derived norcembranoid diterpene natural products. Robert is currently an NIH Postdoctoral

Fellow in the lab of Professor Justin Du Bois at Stanford University and will begin his career as a medicinal chemist focusing on neurodegenerative disease at Denali Therapeutics in July 2017.

Brian M. Stoltz was born in Philadelphia, PA in 1970 and obtained his B.S. degree from the Indiana University of Pennsylvania in Indiana, PA. After graduate work at Yale University in the labs of John L. Wood and an NIH postdoctoral fellowship at Harvard in the Corey labs he took a position at the California Institute of Technology. A member of the Caltech faculty since 2000, he currently is a Professor of Chemistry. His research interests lie in the development of new methods for general applications in synthetic chemistry.

ABBREVIATIONS

Ac	acetyl
AIBN	azobisisobutyronitrile
Bz	benzoyl
CAN	ceric ammonium nitrate
Cp	cyclopentadienyl
CSA	camphorsulfonic acid
Cy	cyclohexyl
DBU	1,8-diazabicyclo[5.4.0]undec-7-ene
DCC	dicyclohexylcarbodiimide
DDQ	2,3-dichloro-5,6-dicyanobenzoquinone
DIBAL	diisobutyl aluminum hydride
DMAP	4-dimethylaminopyridine
DMF	*N*,*N*-dimethylformamide
DMP	Dess–Martin periodinane
DMS	dimethyl sulfide
DMSO	dimethyl sulfoxide
EDC•HCl	*N*-(3-dimethylaminopropyl)-*N*′-ethylcarbodiimide hydrochloride
Et	ethyl
HMDS	hexamethyldisilamide or hexamethyldisilazide
IBX	2-iodoxybenzoic acid
KHMDS	potassium bis(trimethylsilyl)amide

LDA	lithium diisopropylamide
LHMDS	lithium bis(trimethylsilyl)amide
LTMP	lithium 2,2,6,6-tetramethylpiperidide
***m*-CPBA**	*meta*-chloroperbenzoic acid
Me	methyl
MOM	methoxymethyl
MPO	4-methoxypyridine *N*-oxide
Ms	methanesulfonyl
NaHMDS	sodium bis(trimethylsilyl)amide
NBS	*N*-bromosuccinimide
NIS	*N*-iodosuccinimide
NMO	*N*-methylmorpholine *N*-oxide
NMP	*N*-methyl-2-pyrrolidone
***p*-ABSA**	*para*-acetamidobenzenesulfonyl azide
PCC	pyridinium chlorochromate
PDC	pyridinium dichromate
Ph	phenyl
pmdba	4,4′-methoxydibenzylideneacetone
PPTS	pyridinium *para*-toluenesulfonate
***p*-TsOH**	*para*-toluenesulfonic acid
TBAF	tetra-*n*-butylammonium fluoride
TBAT	tetra-*n*-butylammonium difluorotriphenylsilicate
TBHP	*tert*-butyl hydroperoxide
TBS	*tert*-butyldimethylsilyl
TEMPO	(2,2,6,6-tetramethylpiperidin-1-yl)oxidanyl
TEMPO•BF_4	(2,2,6,6-tetramethylpiperidin-1-yl)oxoammonium tetrafluoroborate
TES	triethylsilyl
Tf	trifluoromethanesulfonyl
TFA	trifluoroacetic acid

THF	tetrahydrofuran
TIPS	triisopropylsilyl
TMP	2,2,6,6-tetramethylpiperidine
TMS	trimethylsilyl
TPAP	tetrapropylammonium perruthenate

References

1. Li Y, Pattenden G. Perspectives on the Structural and Biosynthetic Interrelationships Between Oxygenated Furanocembranoids and Their Polycyclic Congeners Found in Corals. Nat Prod Rep. 2011; 28:1269–1310. [PubMed: 21637894]
2. Marrero, J., Rodríguez, II., Rodríguez, AD. The Natural Products Chemistry of the Gorgonian Genus *Pseudopterogorgia* (Octocorallia: Gorgoniidae). In: Mander, L., Liu, H-W., editors. Comprehensive Natural Products II, Chemistry and Biology. Vol. 2. Elsevier; Oxford: 2010. p. 363-428.
3. Weinheimer AJ, Chang CWJ, Matson JA. Naturally Occurring Cembranes. Fortschr Chem Org Naturst. 1979; 36:285–387.
4. Montaser R, Luesch H. Marine Natural Products: A New Wave of Drugs? Future Med Chem. 2011; 3:1475–1489. [PubMed: 21882941]
5. Berrue F, Kerr RG. Diterpenes from Gorgonian Corals. Nat Prod Rep. 2009; 26:681–710. [PubMed: 19387501]
6. Kamel HN, Slattery M. Terpenoids of *Sinularia*: Chemistry and Biomedical Applications. Pharm Biol. 2005; 43:253–269.
7. Abramson SN, Trischman JA, Tapiolas DM, Harold EE, Fenical W, Taylor P. Structure/Activity and Molecular Modeling Studies of the Lophotoxin Family of Irreversible Nicotinic Receptor Antagonists. J Med Chem. 1991; 34:1798–1804. [PubMed: 1676426]
8. Fenical W, Okuda RK, Bandurraga MM, Culver P, Jacobs RS. Lophotoxin: A Novel Neuromuscular Toxin from Pacific Sea Whips of the Genus *Lophogorgia*. Science. 1981; 212:1512–1514. [PubMed: 6112796]
9. Culver P, Jacobs RS. Lophotoxin: A Neuromuscular Acting Toxin from the Sea Whip (*Lophogorgia rigida*). Toxicon. 1981; 19:825–830. [PubMed: 6121394]
10. Wright AE, Burres NS, Schulte GK. Cytotoxic Cembranoids from the Gorgonian *Pseudopterogorgia bipinnata*. Tetrahedron Lett. 1989; 30:3491–3494.
11. Rodríguez AD, Shi J-G, Huang SD. Highly Oxygenated Pseudopterane and Cembranolide Diterpenes from the Caribbean Sea Feather *Pseudopterogorgia bipinnata*. J Nat Prod. 1999; 62:1228–1237. [PubMed: 10514303]
12. Liang C-H, Wang G-H, Chou T-H, Wang S-H, Lin R-J, Chan L-P, So EC, Sheu J-H. 5-*epi*-Sinuleptolide Induces Cell Cycle Arrest and Apoptosis through Tumor Necrosis Factor/Mitochondria-Mediated Caspase Signaling Pathway in Human Skin Cancer Cells. Biochim Biophys Acta. 2012; 1820:1149–1157. [PubMed: 22348919]
13. Yang B, Zhou X-F, Lin X-P, Liu J, Peng Y, Yang X-W, Liu Y. Cembrane Diterpenes Chemistry and Biological Properties. Curr Org Chem. 2012; 16:1512–1539.
14. Ahmed AF, Shiue R-T, Wang G-H, Dai C-F, Kuo Y-H, Sheu J-H. Five Novel Norcembranoids from *Sinularia leptoclados* and *S parva*. Tetrahedron. 2003; 59:7337–7344.
15. Sheu J-H, Ahmed AF, Shiue R-T, Dai C-F, Kuo Y-H. Scabrolides A–D, Four New Norditerpenoids Isolated from the Soft Coral *Sinularia scabra*. J Nat Prod. 2002; 65:1904–1908. [PubMed: 12502336]
16. Marrero J, Rodríguez AD, Baran P, Raptis RG, Sánchez JA, Ortega-Barria E, Capson TL. Bielschowskysin, a Gorgonian-Derived Biologically Active Diterpene with an Unprecedented Carbon Skeleton. Org Lett. 2004; 6:1661–1664. [PubMed: 15128261]

17. Marrero J, Rodríguez AD, Barnes CL. Intricarene, an Unprecedented Trispiropentacyclic Diterpene from the Carribean Sea Plume *Pseudopterogorgia kallos*. Org Lett. 2005; 7:1877–1880. [PubMed: 15844929]

18. Faulkner, DJ., Venkateswarlu, Y., Raghavan, KV., Yadav, JS. Rameswaralide and Rameswaralide Derivatives. U.S. Patent 6300371. Oct 9. 2001

19. Ramesh P, Reddy NS, Venkateswarlu Y, Reddy MVR, Faulkner DJ. Rameswaralide, a Novel Diterpenoid from the Soft Coral *Sinularia dissecta*. Tetrahedron Lett. 1998; 39:8217–8220.

20. Duh C-Y, Wang S-K, Chia M-C, Chiang MY. A Novel Cytotoxic Norditerpenoid from the Formosan Soft Coral *Sinularia inelegans*. Tetrahedron Lett. 1999; 40:6033–6035.

21. Tseng Y-J, Ahmed AF, Dai C-F, Chiang MY, Sheu J-H. Sinulochmodins A–C, Three Novel Terpenoids from the Soft Coral *Sinularia lochmodes*. Org Lett. 2005; 7:3813–3816. [PubMed: 16092882]

22. For general reviews on marine natural products, see:Blunt JW, Copp BR, Keyzers RA, Munro MHG, Prinsep MR. Marine Natural Products. Nat Prod Rep. 2015; 32:116–211. and all preceding reviews in this annual series from *Nat. Prod. Rep.* [PubMed: 25620233]

23. Roethle PA, Trauner D. The Chemistry of Marine Furanocembranoids, Pseudopteranes, Gersolanes, and Related Natural Products. Nat Prod Rep. 2008; 25:298–317. [PubMed: 18389139]

24. Li Y, Pattenden G. Novel Macrocyclic and Polycyclic Norcembranoid Diterpenes from *Sinularia* Species of Soft Coral: Structural Relationships and Biosynthetic Speculations. Nat Prod Rep. 2011; 28:429–440. [PubMed: 21212904]

25. Rodríguez AD. The Natural Products Chemistry of West Indian Gorgonian Octocorals. Tetrahedron. 1995; 51:4571–4618.

26. Tius MA. Synthesis of Cembranes and Cembranolides. Chem Rev. 1988; 88:719–732.

27. The initial studies to determine the absolute stereochemistry of the cembranoid diterpenes were performed on rubifolide (**11**, R = CH_3) and confirmed by subsequent studies on other members of the family.

28. Dorta E, Diaz-Marrero AR, Brito I, Cueto M, D'Croz L, Darias J. The Oxidation Profile at C-18 of Furanocembranolides May Provide a Taxonomical Marker for Several Genera of Octocorals. Tetrahedron. 2007; 63:9057–9062.

29. Gutierrez M, Capson TL, Guzman HM, Gonzalez J, Ortega-Barria E, Quinoa E, Riguera R. Leptolide, a New Furanocembranolide Diterpene from *Leptogorgia alba*. J Nat Prod. 2005; 68:614–616. [PubMed: 15844963]

30. Marshall JA, Sehon CA. Total Synthesis of the Enantiomer of the Furanocembrane Rubifolide. J Org Chem. 1997; 62:4313–4320. [PubMed: 11671752]

31. Rodríguez AD, Shi Y-P. Verrillin: A Highly Oxygenated Marine Diterpene Based on the Novel Verrillane Carbon Skeleton. J Org Chem. 2000; 65:5839–5842. [PubMed: 10970333]

32. Anjaneyulu AS, Venugopal MJ, Sarada P, Clardy J, Lobkovsky E. Havellockate, a Novel Seco and Spiro Lactone Diterpenoid from the Indian Ocean Soft Coral *Sinularia granosa*. Tetrahedron Lett. 1998; 39:139–142.

33. Stonik VA, Kapustina II, Kalinovsky AI, Dmitrenok PS, Grebnev BB. New Diterpenoids from the Far-Eastern Gorgonian Coral *Plumarella* sp. Tetrahedron Lett. 2002; 43:315–317.

34. Venkateswarlu Y, Biabani MF, Reddy MVR, Rao TP, Kunwar AC, Faulkner DJ. Mandapamate, a Diterpenoid from the Soft Coral *Sinularia dissecta*. Tetrahedron Lett. 1994; 35:2249–2252.

35. Anjaneyulu ASR, Sagar KS, Venugopal MJRV. Terpenoid and Steroid Constituents of the Indian Ocean Soft Coral *Sinularia maxima*. Tetrahedron. 1995; 51:10997–11010.

36. Anjaneyulu ASR, Sarada P. Bishomoisomandapamate, a New Tetracyclic Diterpenoid from a New Species of the *Sinularia* Genus of the Indian Ocean. J Chem Res (S). 1999:600–601.

37. Su J-Y, Kuang Y-Y, Zeng L-M, Li H. New Tetracyclic Diterpenoid and New Ceramides from the Soft Coral *Sinularia conferta*. J Asian Nat Prod Res. 2005; 7:107–113. [PubMed: 15621611]

38. Radhika P, Subba Rao PV, Anjaneyulu V, Asolkar RN, Laatsch H. Horiolide, a Novel Norditerpenoid from Indian Ocean Soft Coral of the Genus *Sinularia*. J Nat Prod. 2002; 65:737–739. [PubMed: 12027754]

39. Lillsunde K-E, Festa C, Adel H, de Marino S, Lombardi V, Tilvi S, Nawrot D, Zampella A, D'Souza L, D'Auria M; et al. Bioactive Cembrane Derivatives from the Indian Ocean Soft Coral, *Sinularia kavarattiensis*. Marine Drugs. 2014; 12:4045–4068. [PubMed: 25056629]
40. Kobayashi M, Appa Rao KMC, Krishna MM, Anjaneyulu V. Marine Terpenes and Terpenoids. Part 19. Structure of a Tetracyclic Norcembranolide Derivative Isolated from the Soft Coral *Sinularia dissecta*. J Chem Res (S). 1995:188–189.
41. Iguchi K, Kajiyama K, Yamada Y. Yonarolide: A New Marine Norditerpenoid Possessing a Novel Tricyclic Skeleton, from the Okinawan Soft Coral of the Genus, *Sinularia*. Tetrahedron Lett. 1995; 36:8807–8808.
42. Thao NP, Nam NH, Cuong NX, Quang TH, Tung PT, Dat LD, Chae D, Kim S, Koh Y-S, Kiem PV, et al. Anti-Inflammatory Norditerpenoids from the Soft Coral *Sinularia maxima*. Bioorg Med Chem Lett. 2013; 23:228–231. [PubMed: 23200246]
43. Yen W-H, Su Y-D, Chang Y-C, Chen Y-H, Chen Y-H, Dai C-F, Wen Z-H, Su J-H, Sung P-J. Sinulanorcembranolide A, a Novel Norcembranoidal Diterpene from the Octocoral *Sinularia gaweli*. Tetrahedron Lett. 2013; 54:2267–2270.
44. Hu L-C, Yen W-H, Su J-H, Chiang MY-N, Wen Z-H, Chen W-F, Lu T-J, Chang Y-W, Chen Y-H, Wang W-H, et al. Cembrane Derivatives from the Soft Corals, *Sinularia gaweli* and *Sinularia flexibilis*. Marine Drugs. 2013; 11:2154–2167. [PubMed: 23774887]
45. Tang B, Simion R, Paton RS. Thermal and Photochemical Mechanisms for Cyclobutane Formation in Bielschowskysin Biosynthesis. Synlett. 2015; 26:501–507.
46. Tang B, Bray CD, Pattenden G. Total Synthesis of (+)-Intricarene Using a Biogenetically Patterned Pathway from (–)-Bipinnatin J, Involving a Novel Transannular [5 + 2] (1,3-Dipolar) Cycloaddition. Org Biomol Chem. 2009; 7:4448–4457. [PubMed: 19830294]
47. Tang B, Bray CD, Pattenden G. A Biomimetic Total Synthesis of (+)-Intricarene. Tetrahedron Lett. 2006; 47:6401–6404.
48. Stichnoth D, Kölle P, Kimbrough TJ, Riedle E, de Vivie-Riedle R, Trauner D. Photochemical Formation of Intricarene. Nat Commun. 2014; 5:5597. [PubMed: 25470600]
49. Roethle PA, Hernandez PT, Trauner D. Exploring Biosynthetic Relationships Among Furanocembranoids: Synthesis of (−)-Bipinnatin J, (+)-Intricarene, (+)-Rubifolide, and (+)-Isoepilophodione B. Org Lett. 2006; 8:5901–5904. [PubMed: 17134301]
50. Wang SC, Tantillo DJ. Theoretical Studies on Synthetic and Biosynthetic Oxidopyrylium-Alkene Cycloadditions: Pericyclic Pathways to Intricarene. J Org Chem. 2008; 73:1516–1523. [PubMed: 18205383]
51. Pattenden G, Winne JM. An Intramolecular [4 + 3]-Cycloaddition Approach to Rameswaralide Inspired by Biosynthesis Speculation. Tetrahedron Lett. 2009; 50:7310–7313.
52. Palframan MJ, Pattenden G. Searching for Radical Intermediates and Pathways Implied in the Biosynthesis of Some Polycyclic Cembranoids. A New Plausible Mechanism for the Origin of Sinulanocembranolide A in the Coral *Sinularia gyrosa*. Tetrahedron Lett. 2013; 54:6822–6825.
53. Jana A, Mondal S, Ghosh S. Studies Towards the Synthesis of Bielschowskysin. Construction of the Highly Functionalized Bicyclo-[3.2.0]heptane Segment. Org Biomol Chem. 2015; 13:1846–1859. [PubMed: 25502963]
54. Jana A, Mondal S, Hossain MF, Ghosh S. Stereocontrolled Approach to the Highly Functionalized Bicyclo[3.2.0]heptane Core of Bielschowskysin through Intramolecular Cu(I)-Catalyzed [2 + 2] Photocycloaddition. Tetrahedron Lett. 2012; 53:6830–6833.
55. Mondal S, Yadav RN, Ghosh S. Unprecedented Copper(I)-Catalyzed Photochemical Reaction of Diethyl Ether with Vicinal Diols and Ketals. Tetrahedron Lett. 2010; 51:4452–4454.
56. Datta R, Sumalatha M, Ghosh S. A Simple Approach to the Construction of the Core Structure Present in Bielschowskysin and Hippolachnin A. J Chem Sci. 2016; 128:1019–1023.
57. Collins, NR. M.S. dissertation. Vanderbilt University; Nashville, Tennessee: 2013. Efforts Toward the Total Synthesis of Bielschowskysin.
58. Doroh B, Sulikowski GA. Progress Toward the Total Synthesis of Bielschowskysin: A Stereoselective [2 + 2] Photocycloaddition. Org Lett. 2006; 8:903–906. [PubMed: 16494470]
59. Townsend SD, Sulikowski GA. Progress Toward the Total Synthesis of Bielschowskysin. Org Lett. 2013; 15:5096–5098. [PubMed: 24067163]

60. Himmelbauer M, Farcet J-B, Gagnepain J, Mulzer J. A Palladium-Catalyzed Carbo-oxygenation: The Bielschowskysin Case. Org Lett. 2013; 15:3098–3101. [PubMed: 23724910]
61. Himmelbauer M, Farcet J-B, Gagnepain J, Mulzer J. An Approach to the Carbon Backbone of Bielschowskysin, Part 1: Photocyclization Strategy. Eur J Org Chem. 2013:8214–8244.
62. Nicolaou KC, Hale CRH, Ebner C, Nilewski C, Ahles CF, Rhoades D. Synthesis of Macroheterocycles through Intramolecular Oxidative Coupling of Furanoid β-Ketoesters. Angew Chem Int Ed. 2012; 51:4726–4730.
63. Nicolaou KC, Adsool VA, Hale CRH. An Expedient Synthesis of a Functionalized Core Structure of Bielschowskysin. Angew Chem Int Ed. 2011; 50:5149–5152.
64. Yang EG, Sekar K, Lear MJ. A Macrolactonisation Approach to the Cembrane Carbocycle of Bielschowskysin. Tetrahedron Lett. 2013; 54:4406–4408.
65. Miao R, Gramani SG, Lear MJ. Stereocontrolled Entry to the Tricyclo[3.3.0]oxoheptane Core of Bielschowskysin by a [2 + 2] Cycloaddition of an Allene-Butenolide. Tetrahedron Lett. 2009; 50:1731–1733.
66. Farcet J-B, Himmelbauer M, Mulzer J. Photochemical and Thermal [2 + 2] Cycloaddition to Generate the Bicyclo[3.2.0]heptane Core of Bielschowskysin. Eur J Org Chem. 2013:4379–4398.
67. Farcet J-B, Mulzer J, Himmelbauer M. An Approach Toward the Bridged 14-Membered Carbon Macrocycle of Bielschowskysin. Eur J Org Chem. 2016:2793–2801.
68. Farcet J-B, Himmelbauer M, Mulzer J. An Approach to the Carbon Backbone of Bielschowskysin, Part 2: Non-Photochemical Strategy. Eur J Org Chem. 2013:8245–8252.
69. Farcet J-B, Himmelbauer M, Mulzer J. A Non-Photochemical Approach to the Bicyclo[3.2.0]heptane Core of Bielschowskysin. Org Lett. 2012; 14:2195–2197. [PubMed: 22506798]
70. Isayama S, Mukaiyama T. A New Method for Preparation of Alcohols from Olefins with Molecular Oxygen and Phenylsilane by the Use of Bis(acetylacetonato)cobalt(II). Chem Lett. 1989; 18:1071–1074.
71. Li Y, Pattenden G, Rogers J. Synthesis of *exo* Enol Ether-Cyclic Ketal Isomers of Substituted Furanmethanol Structures Related to Marine Furanocembranoids. Tetrahedron Lett. 2010; 51:1280–1283.
72. Rogers, JN. Ph.D. dissertation. University of Nottingham; Nottingham, United Kingdom: 2009. Biomimetic Studies Towards the Polycyclic Diterpene Bielschowskysin.
73. Takasu K, Ueno M, Inanaga K, Ihara M. Catalytic (2 + 2)-Cycloaddition Reactions of Silyl Enol Ethers. A Convenient and Stereoselective Method for Cyclobutane Ring Formation. J Org Chem. 2004; 69:517–521. [PubMed: 14725468]
74. Saitman A, Sullivan SDE, Theodorakis EA. A Strategy Toward the Synthesis of C_{13}-Oxidized Cembrenolides. Tetrahedron Lett. 2013; 54:1612–1615. [PubMed: 23626379]
75. Meyer ME, Phillips JH, Ferreira EM, Stoltz BM. Use of a Palladium(II)-Catalyzed Oxidative Kinetic Resolution in Synthetic Efforts Toward Bielschowskysin. Tetrahedron. 2013; 69:7627–7635. [PubMed: 23913988]
76. Meyer ME, Ferreira EM, Stoltz BM. 2-Diazoacetoacetic Acid, an Efficient and Convenient Reagent for the Synthesis of α-Diazo-β-Ketoesters. Chem Commun. 2006:1316–1318.
77. Macabeo APG, Lehmann CW, Reiser O. Diastereoselective Synthesis of Enantiopure γ-Butenolide-Butyrolactones Towards *Pseudopterogorgia* Lactone Furanocembranoid Substructures. Synlett. 2012; 23:2909–2912.
78. Böhm C, Schinnerl M, Bubert C, Zabel M, Labahn T, Parisini E, Reiser O. A New Strategy for the Stereoselective Synthesis of 1,2,3-Trisubstituted Cyclopropanes. Eur J Org Chem. 2000:2955–2965.
79. Saitman A, Theodorakis EA. Synthesis of a Highly Functionalized Core of Verrillin. Org Lett. 2013; 15:2410–2413. [PubMed: 23627293]
80. Mehta G, Kumaran RS. Studies Towards the Total Synthesis of Novel Marine Diterpene Havellockate. Construction of the Tetracyclic Core. Tetrahedron Lett. 2001; 42:8097–8100.
81. Beingessner RL, Farand JA, Barriault L. Progress Toward the Total Synthesis of (±)-Havellockate. J Org Chem. 2010; 75:6337–6346. [PubMed: 20815361]

82. Rodríguez AD, Shi J-G, Shi Y-P. Isolation, Structural Characterization, and Synthesis of a Naturally Occurring Bisfuranopseudopterane Ether: Biskallolide A. Evidence for a Carbocation Intermediate during the Facile Conversion of Kallolide A and Isokallolide A into Various Solvolysis Products. J Org Chem. 2000; 65:3192–3199. [PubMed: 10814214]

83. Mehta G, Lakshminath S. Synthetic Studies Towards the Novel Diterpenoid Rameswaralide: RCM Mediated Acquisition of the Tricyclic Core. Tetrahedron Lett. 2006; 47:327–330.

84. Srikrishna A, Dethe DH. Synthetic Approaches to Guanacastepenes. Enantiospecific Syntheses of BC and AB Ring Systems of Guanacastepenes and Rameswaralide. Org Lett. 2004; 6:165–168. [PubMed: 14723519]

85. Trost BM, Nguyen HM, Koradin C. Synthesis of a Tricyclic Core of Rameswaralide. Tetrahedron Lett. 2010; 51:6232–6235.

86. Trost BM, Shen HC. Constructing Tricyclic Compounds Containing a Seven-Membered Ring by Ruthenium-Catalyzed Intramolecular [5 + 2] Cycloaddition. Angew Chem Int Ed. 2001; 40:2313–2316.

87. Li Y, Palframan MJ, Pattenden G, Winne JM. A Strategy Towards the Synthesis of Plumarellide Based on Biosynthesis Speculation, Featuring a Transannular 4 + 2 Type Cyclisation from a Cembranoid Furanoxonium Ion Intermediate. Tetrahedron. 2014; 70:7229–7240.

88. Lygo B, Palframan MJ, Pattenden G. Investigation of Transannular Cycloaddition Reactions Involving Furanoxonium Ions Using DFT Calculations. Implications for the Origin of Plumarellide and Rameswaralide and Related Polycyclic Metabolites Isolated from Corals. Org Biomol Chem. 2014; 12:7270–7278. [PubMed: 25105757]

89. Palframan MJ, Pattenden G. Elaboration of the Carbocyclic Ring Systems in Plumarellide and Rameswaralide Using a Coordinated Intramolecular Cycloaddition Approach, Based on a Common Biosynthesis Model. Tetrahedron Lett. 2013; 54:324–328.

90. Palframan MJ, Pattenden G. Indirect Support for a Stepwise Carbonium Ion Pathway Operating in (4 + 3)-Cycloaddition Reactions between Furanoxonium Ions and 1,3-Dienes. Synlett. 2013; 24:2720–2722.

91. Li Y, Pattenden G. Exploration of a Proposed Biomimetic Synthetic Route to Plumarellide. Development of a Facile Transannular Diels–Alder Reaction from a Macrocyclic Enedione Leading to a New 5,6,7-Tricyclic Ring System. Tetrahedron Lett. 2011; 52:2088–2092.

92. Pattenden G, Winne JM. Synthetic Studies Towards Oxygenated and Unsaturated Furanocembranoid Macrocycles. Precursors to Plumarellide, Rameswaralide and Mandapamates. Tetrahedron Lett. 2010; 51:5044–5047.

93. Pattenden G, Winne JM. An Intramolecular [4 + 3]-Cycloaddition Approach to Rameswaralide Inspired by Biosynthesis Speculation. Tetrahedron Lett. 2009; 50:7310–7313.

94. Vasamsetty L, Khan FA, Mehta G. A Model Approach Towards the Polycyclic Framework Present in Cembranoid Natural Products Dissectolide A, Plumarellide and Mandapamate. Tetrahedron Lett. 2014; 55:7068–7071.

95. Ueda Y, Abe H, Iguchi K, Ito H. Synthetic Study of Yonarolide: Stereoselective Construction of the Tricyclic Core. Tetrahedron Lett. 2011; 52:3379–3381.

96. Pratt, BA. Ph.D. dissertation. Scripps Research Institute; La Jolla, California: 2008. The Design and Synthesis of Highly Potent Epothilone B Analogues And Progress Toward the Total Synthesis of *Sinularia* Natural Products.

97. O'Connell, CE. Ph.D. dissertation. Queen's University of Belfast; Belfast, Northern Ireland, U.K.: 2006. Synthetic Approaches to the Marine Natural Products Eleutherobin (and Analogues) and Norcembranolide I.

98. O'Connell, CE., Frontier, AJ. Efforts Towards the Total Synthesis of Norcembranolide I. Abstracts of Papers, 32nd Northeast Regional Meeting of the American Chemical Society; Rochester, NY. Oct. 31–Nov. 3, 2004; American Chemical Society; 2004. GEN-088

99. Liu, G. Ph.D. dissertation. Texas A&M University; College Station, Texas: 2011. Beta-Lactones as Synthetic Vehicles in Natural Product Synthesis: Total Syntheses of Schulzeines B & C and Omphadiol, and Studies Toward the Total Syntheses of Scabrolide A & B and Sinulochmodin C.

100. Liu, G., Romo, D. Unified Synthetic Strategy Toward Scabrolides, Sinulochmodin, and Ineleganolide via Transannular C–H Insertions and Aldol Condensations. Abstracts of Papers,

237th American Chemical Society National Meeting; Salt Lake City, UT. Mar. 22–26, 2009; American Chemical Society; 2009. ORGN-083

101. Tang F, Moeller KD. Anodic Oxidations and Polarity: Exploring the Chemistry of Olefinic Radical Cations. Tetrahedron. 2009; 65:10863–10875.
102. Moeller KD. Intramolecular Anodic Olefin Coupling Reactions: Using Radical Cation Intermediates to Trigger New Umpolung Reactions. Synlett. 2009:1208–1218.
103. Tang, F. Ph.D. dissertation. Washington University; St. Louis, Missouri: 2009. Intramolecular Anodic Olefin Coupling Reactions: Probing the Effect of the Radical Cation Polarization on Carbon–Carbon Bond Formation. An Approach to the Total Synthesis of Ineleganolide.
104. Tang F, Moeller KD. Intramolecular Anodic Olefin Coupling Reactions: The Effect of Polarization on Carbon-Carbon Bond Formation. J Am Chem Soc. 2007; 129:12414–12415. [PubMed: 17894501]
105. Li Y, Pattenden G. Biomimetic Syntheses of Ineleganolide and Sinulochmodin C from 5-Episinuleptolide via Sequences of Transannular Michael Reactions. Tetrahedron. 2011; 67:10045–10052.
106. Horn EJ, Silverston JS, Vanderwal CD. A Failed Late-Stage Epimerization Thwarts an Approach to Ineleganolide. J Org Chem. 2016; 81:1819–1838. [PubMed: 26863401]
107. Horn, EJ. Ph.D. dissertation. University of California at Irvine; Irvine, CA: 2014. Studies Toward the Synthesis of Ineleganolide.
108. Jasperse CP, Curran DP, Fevig TL. Radical Reactions in Natural Product Synthesis. Chem Rev. 1991; 91:1237–1286.
109. Curran DP, Rakiewicz DM. Tandem Radical Approach to Linear Condensed Cyclopentanoids. Total Synthesis of (±)-Hirsutene. J Am Chem Soc. 1985; 107:1448–1449.
110. Sarakinos G, Corey EJ. Simple and Practical Routes to Enantiomerically Pure 5-(Trialkylsilyl)-2-cyclohexenones. Org Lett. 1999; 1:811–814. [PubMed: 10823209]
111. Craig RA II, Roizen JL, Smith RC, Jones AC, Virgil SC, Stoltz BM. Enantioselective, Convergent Synthesis of the Ineleganolide Core by a Tandem Annulation Cascade. Chem Sci. 2017; 8:507–514. [PubMed: 28239443]
112. Krüger S, Gaich T. Recent Applications of The Divinylcyclopropane–Cycloheptadiene Rearrangement in Organic Synthesis. Beilstein J Org Chem. 2014; 10:163–193. [PubMed: 24605138]
113. Davies HML. Tandem Cyclopropanation/Cope Rearrangement: A General Method for The Construction of Seven-Membered Rings. Tetrahedron. 1993; 49:5203–5223.
114. Vogel E. Valence Isomerizations in Compounds with Strained Rings. Angew Chem Int Ed. 1963; 2:1–52.
115. Craig RA II, Smith RC, Pritchett BP, Estipona BI, Stoltz BM. Preparation of 1,5-Dioxaspiro[5.5]undecan-3-one. Org Synth. 2016; 93:210–227.
116. Craig RA II, Roizen JL, Smith RC, Jones AC, Stoltz BM. Enantioselective Synthesis of a Hydroxymethyl-*cis*-1,3-Cyclopentenediol Building Block. Org Lett. 2012; 14:5716–5719. [PubMed: 23101616]
117. Craig RA II, Stoltz BM. Synthesis and Exploration of Electronically Modified (*R*)-5,5-dimethyl-(*p*-CF_3)$_3$-*i*-PrPHOX in Palladium-Catalyzed Enantio- and Diastereoselective Allylic Alkylation: A Practical Alternative to (*R*)-(*p*-CF_3)$_3$-*t*-BuPHOX. Tetrahedron Lett. 2015; 56:4670–4673. [PubMed: 26257445]
118. Seto M, Roizen JL, Stoltz BM. Catalytic Enantioselective Alkylation of Substituted Dioxanone Enol Ethers: Ready Access to C(α)-Tetrasubstituted Hydroxyketones, Acids, and Esters. Angew Chem Int Ed. 2008; 47:6873–6876.
119. Behenna DC, Stoltz BM. The Enantioselective Tsuji Allylation. J Am Chem Soc. 2004; 126:15044–15045. [PubMed: 15547998]
120. González MA, Ghosh S, Rivas F, Fischer D, Theodorakis EA. Synthesis of (+)- and (–)-Isocarvone. Tetrahedron Lett. 2004; 45:5039–5041.
121. Chen J, Marx JN. A Stereoselective Total Synthesis of (–)-Rishitin. Tetrahedron Lett. 1997; 38:1889–1892.

122. Lavallée J-F, Spino C, Ruel R, Hogan KT, Deslongchamps P. Stereoselective Synthesis of *cis*-Decalins via Diels–Alder and Double Michael Addition of Substituted Nazarov Reagents. Can J Chem. 1991; 70:1406–1426.

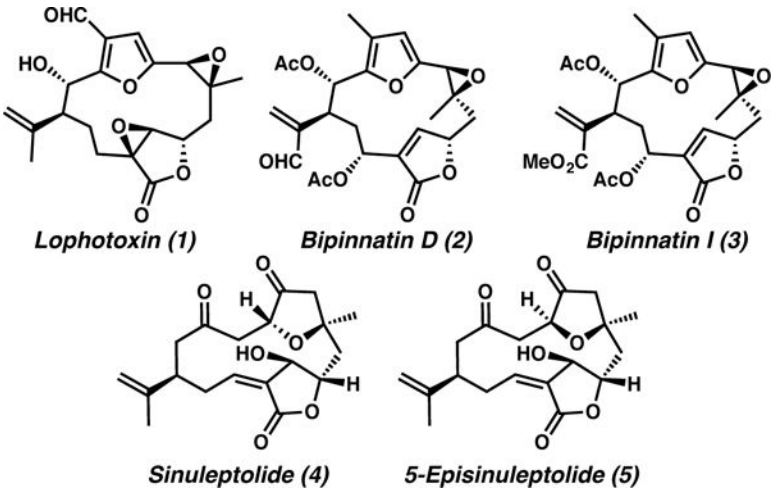

Figure 1.
Characteristic Macrocyclic Furanobutenolide Cembranoids and Norcembranoids

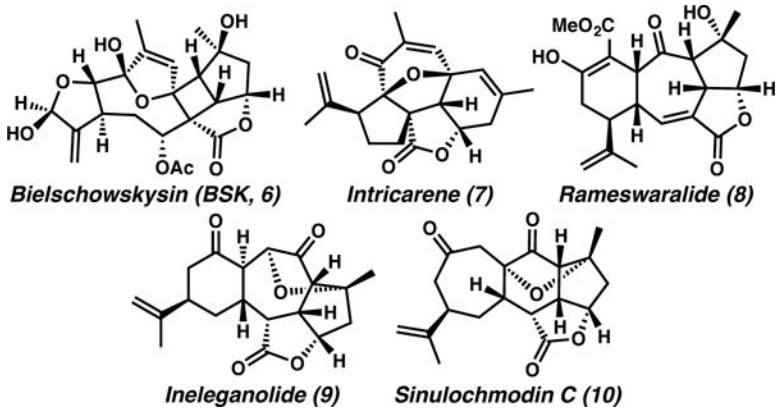

Figure 2.
Characteristic Polycyclic Furanobutenolide-Derived Cembranoids and Norcembranoids

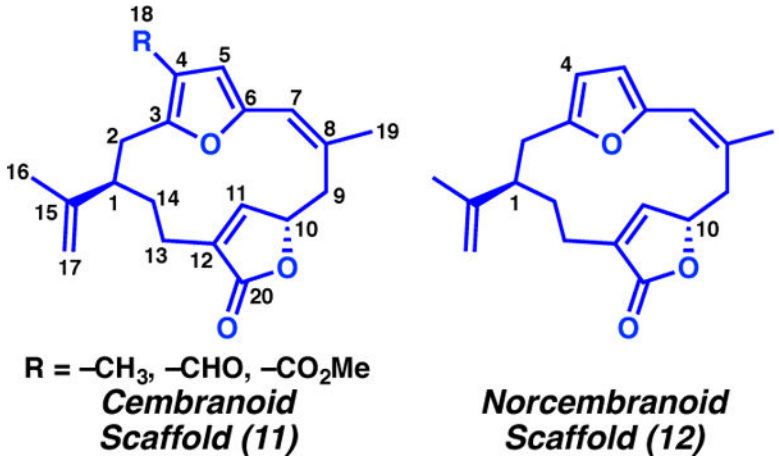

Figure 3.
Cembranoid and Norcembranoid Furanobutenolide Scaffolds

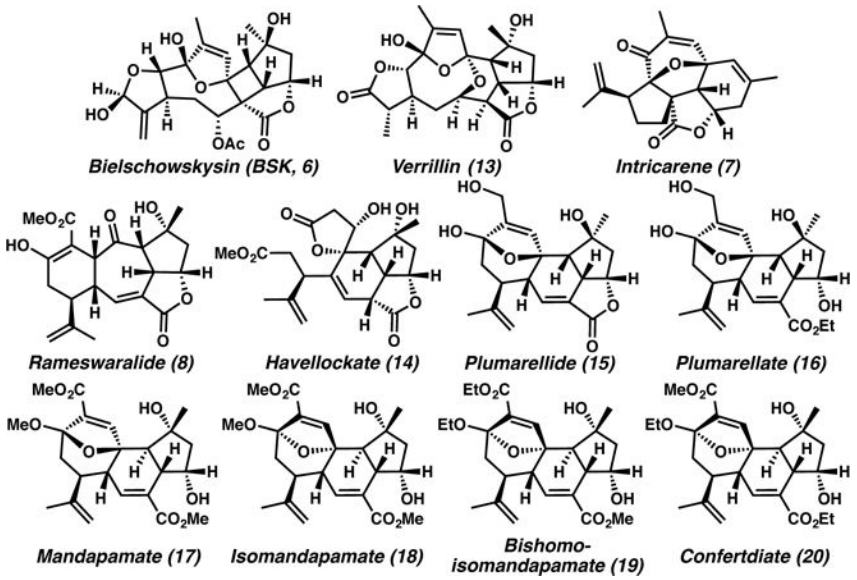

Figure 4.
Polycyclic Furanobutenolide-Derived Cembranoid Natural Products

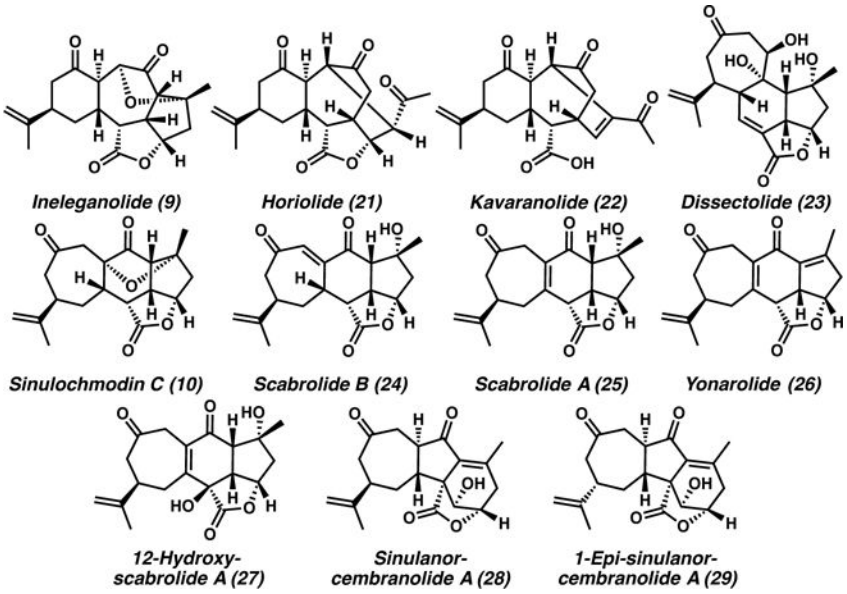

Figure 5.
Polycyclic Furanobutenolide-Derived Norcembranoid Natural Products

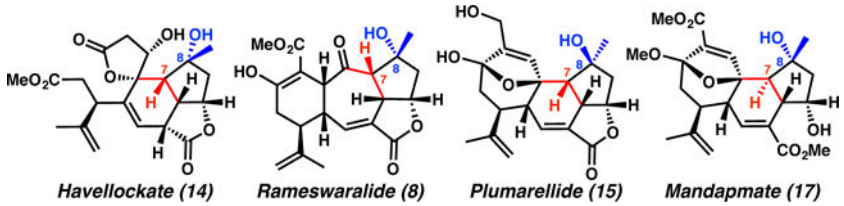

Figure 6.

Structural Comparison of Havellockate (**14**) and Rameswaralide (**8**) to Plumarellide (**15**) and Mandapamate (**17**)

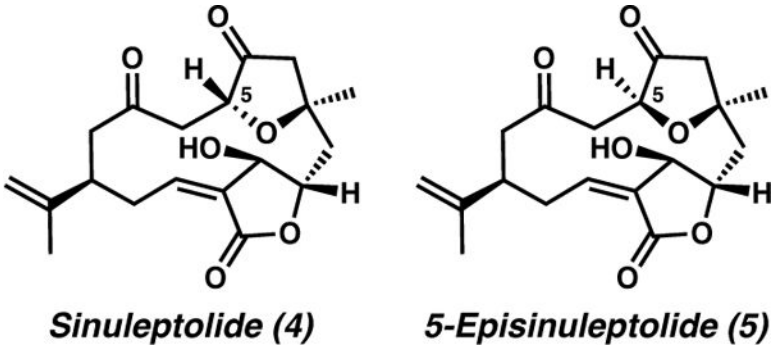

Figure 7.
Sinuleptolide (**4**) and 5-Episinuleptolide (**5**)

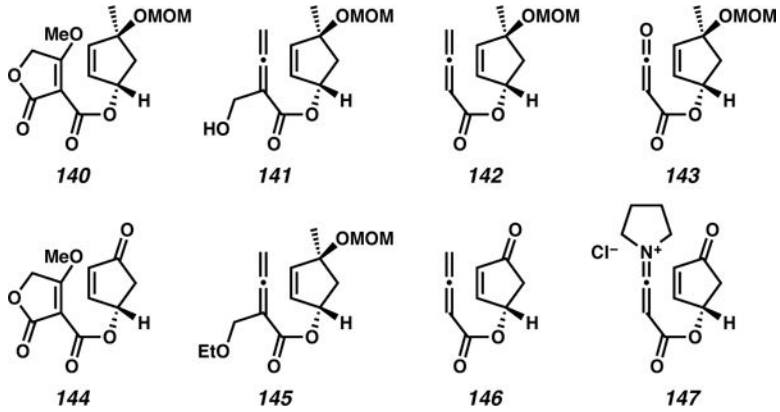

Figure 8.
Unsuccessful Model Substrates for Light-Induced [2 + 2] Cycloaddition (Mulzer)

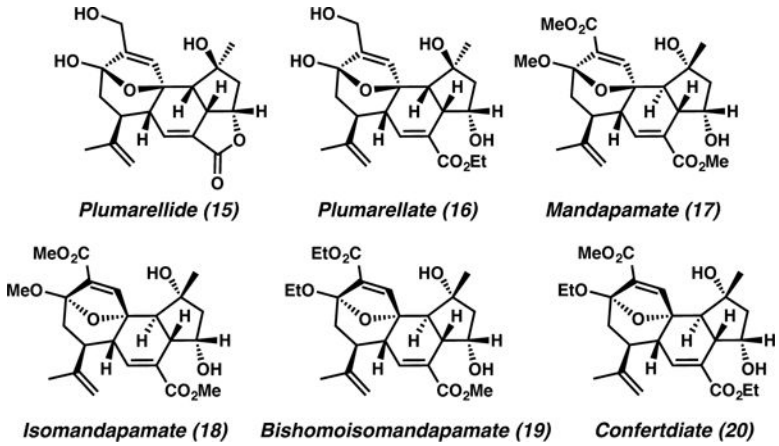

Figure 9.
Plumarellide (**15–16**) and Mandapamate (**17–20**) Natural Products

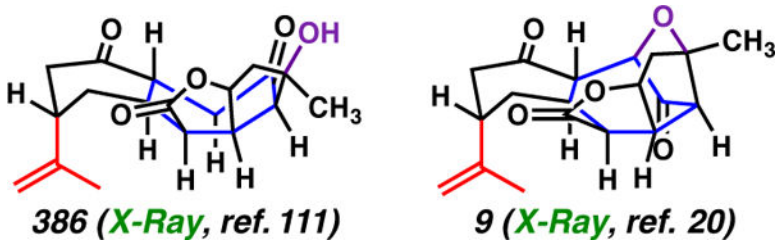

Figure 10.
Conformational Comparison of Synthetic Intermediate **386** to Ineleganolide (**9**, Stoltz)

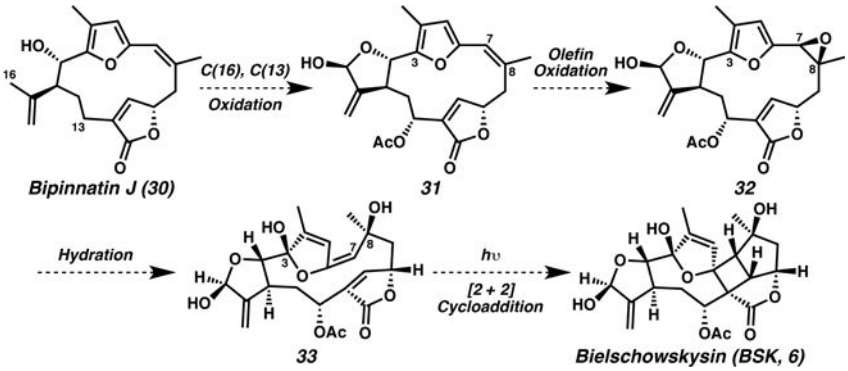

Scheme 1.

Biosynthetic Proposal for the Construction of Bielschowskysin (BSK, **6**)

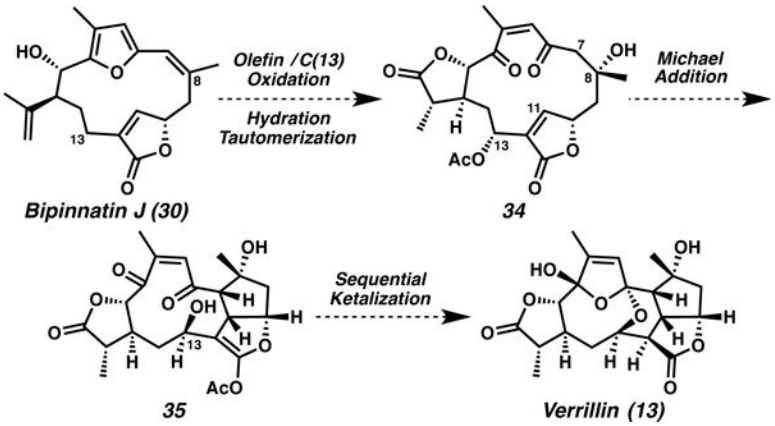

Scheme 2.

Proposed Biosynthesis of Verrillin (**13**)

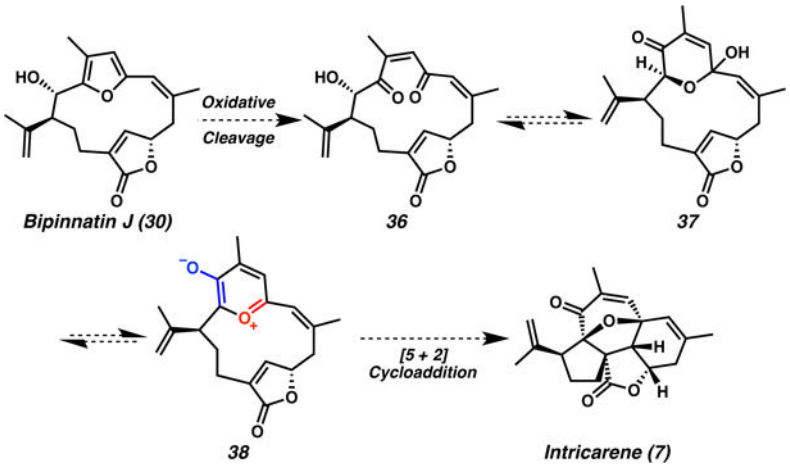

Scheme 3.
Biosynthetic Speculation Concerning the Formation of Intricarene (**7**)

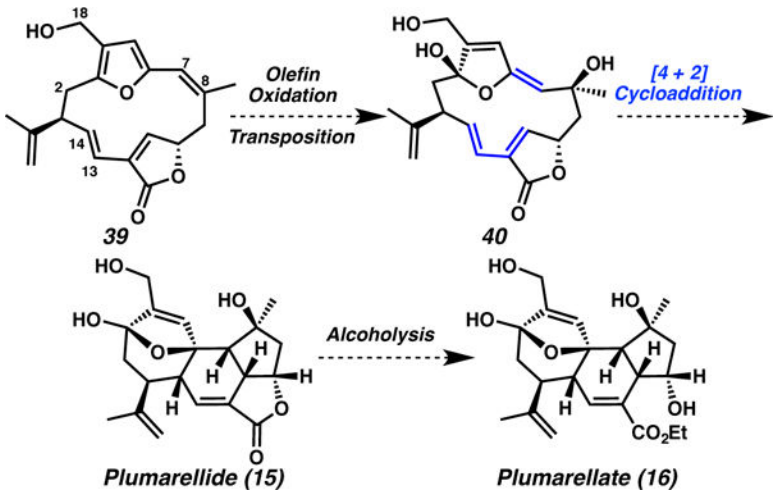

Scheme 4.

Proposed Biosynthetic Construction of the Plumarellides

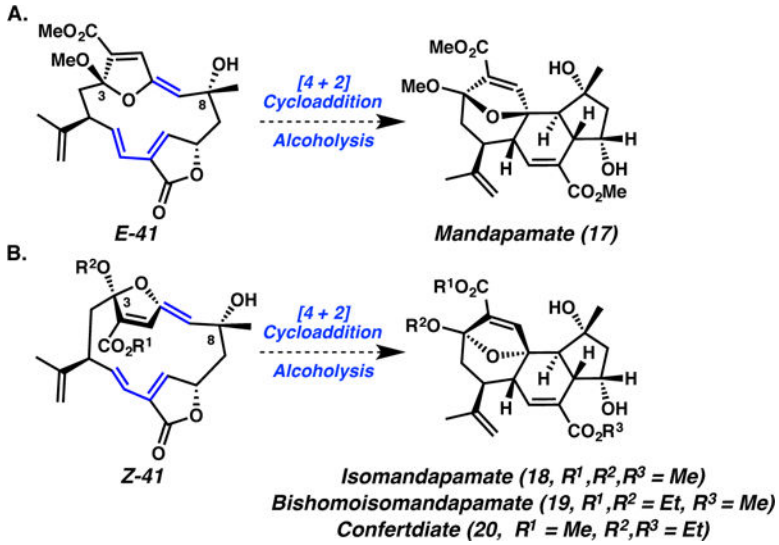

Scheme 5.

Biosynthetic Proposal for the Formation of the Mandapamates (**17–19**) and Confertdiate (**20**)

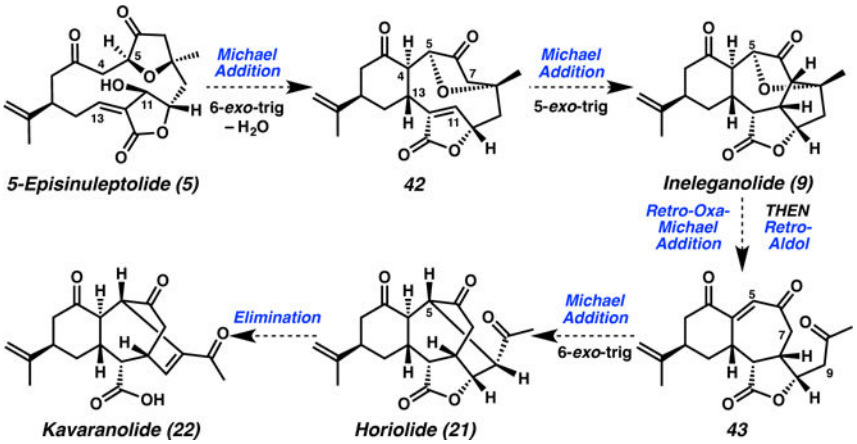

Scheme 6.

Biosynthesis of Ineleganolide (**9**), Horiolide (**21**), and Kavaranolide (**22**)

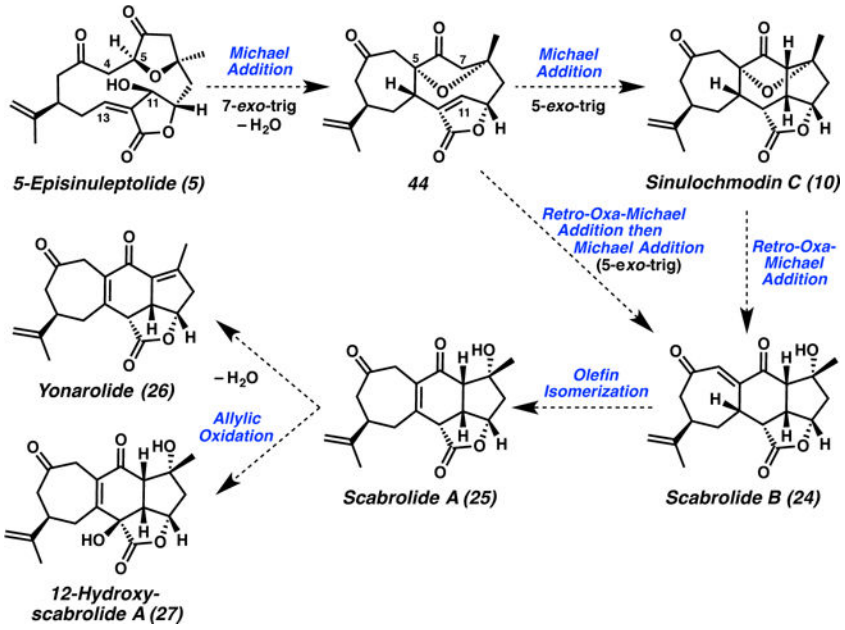

Scheme 7.

Biosynthetic Formation of Sinulochmodin C (**10**), Scabrolide B (**24**), Scabrolide A (**25**), Yonarolide (**26**), and 12-Hydroxyscabrolide A (**27**)

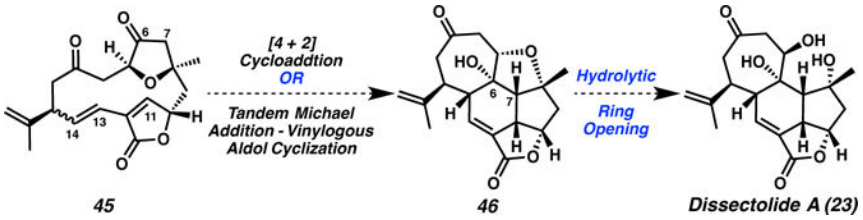

Scheme 8.

Biosynthetic Conjectures for the Formation of Dissectolide A (**23**)

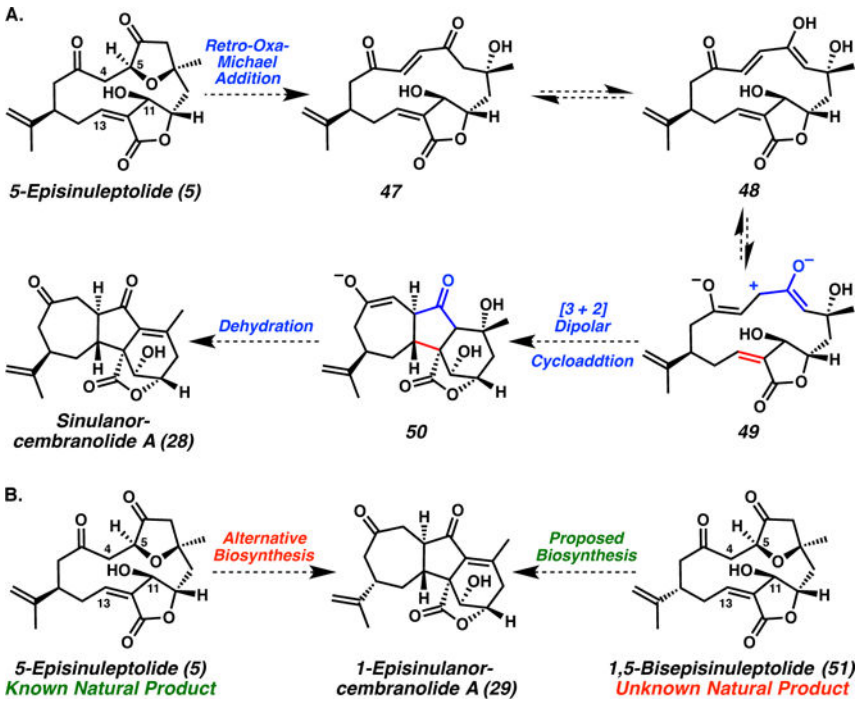

Scheme 9.

Biosynthetic Hypotheses for the Formation of Sinulanorcembranolide (**28**) and 1-*epi*-Sinulanorcembranolide (**29**)

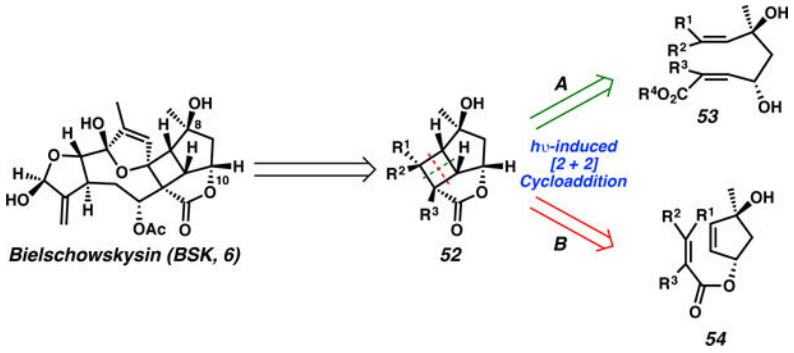

Scheme 10.

Retrosynthetic Analysis of BSK (**6**) Employing Light-Induced [2 + 2]

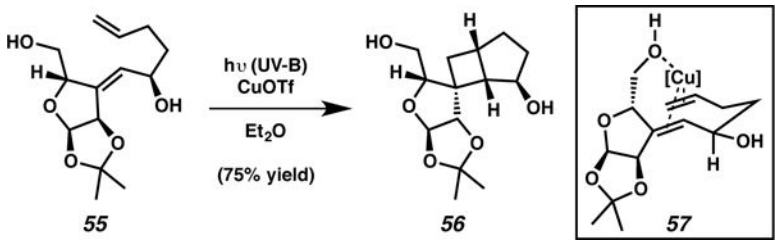

Scheme 11.
Copper-Catalyzed Light-Induced [2 + 2] Cycloaddition (Ghosh)

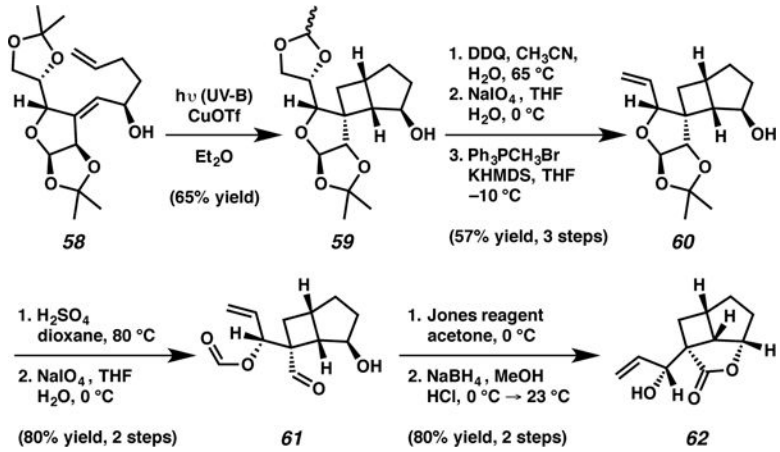

Scheme 12.

Construction of BSK Tricyclic Core **62** from Cyclobutane **59** (Ghosh)

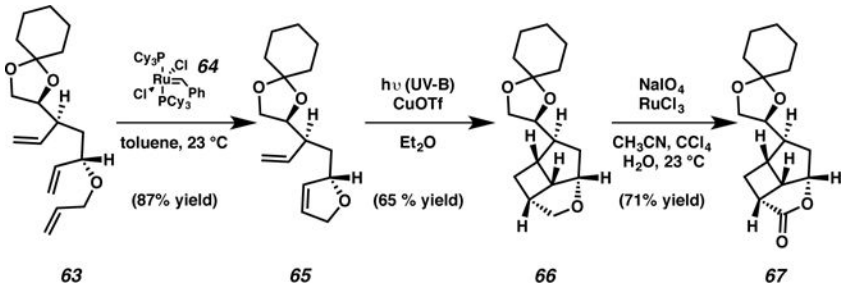

Scheme 13.
Alternative Synthesis of the BSK Tricyclic Core (Ghosh)

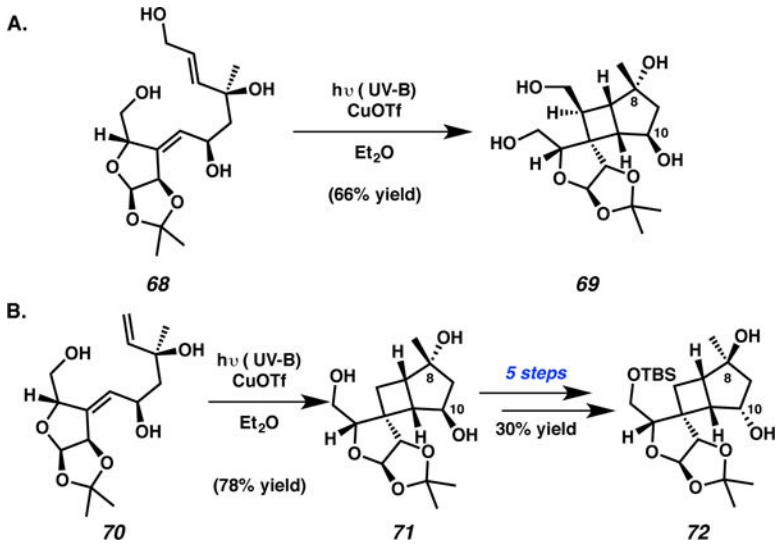

Scheme 14.

Functionalized Dienes **68** and **70** in Copper-Catalyzed [2 + 2] Photocycloaddition (Ghosh)

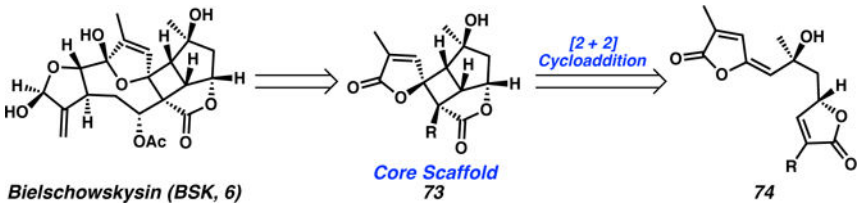

Scheme 15.
Retrosynthetic Strategy Employed by Sulikowski Toward BSK (**6**)

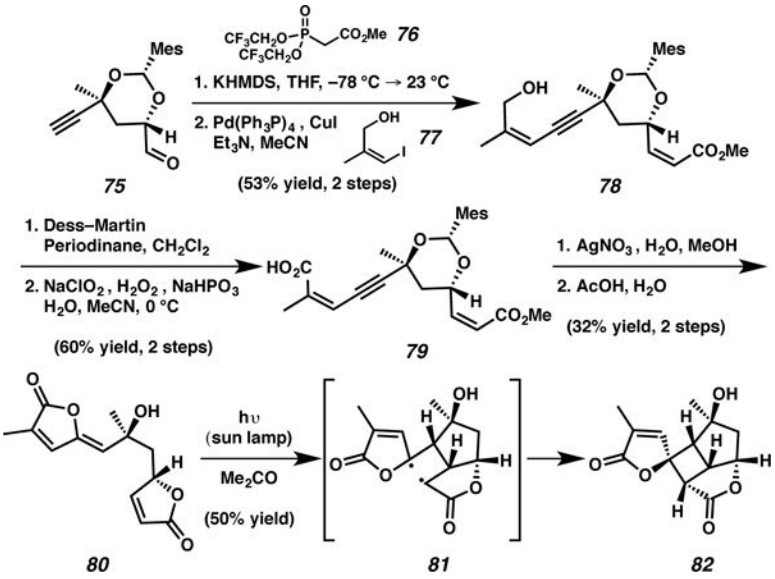

Scheme 16.

Model System for Intramolecular Butenolide [2 + 2] Cycloaddition (Sulikowski)

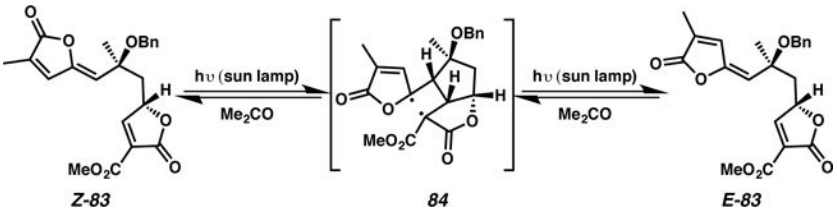

Scheme 17.
Intramolecular [2 + 2] Cycloaddition with Elaborated Butenolide (Sulikowski)

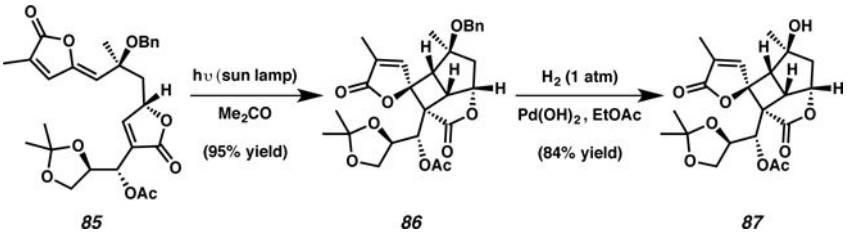

Scheme 18.
Intramolecular [2 + 2] Cycloaddition with Elaborated Butenolide (Sulikowski)

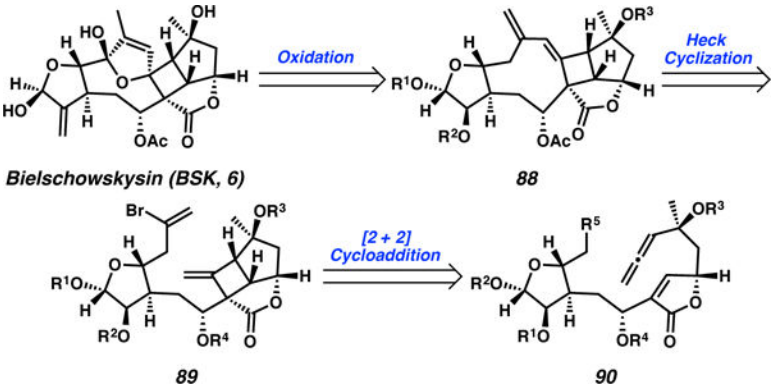

Scheme 19.

Mulzer's Retrosynthesis of BSK (**6**) Employing an Aliene [2 + 2] Cycloaddition

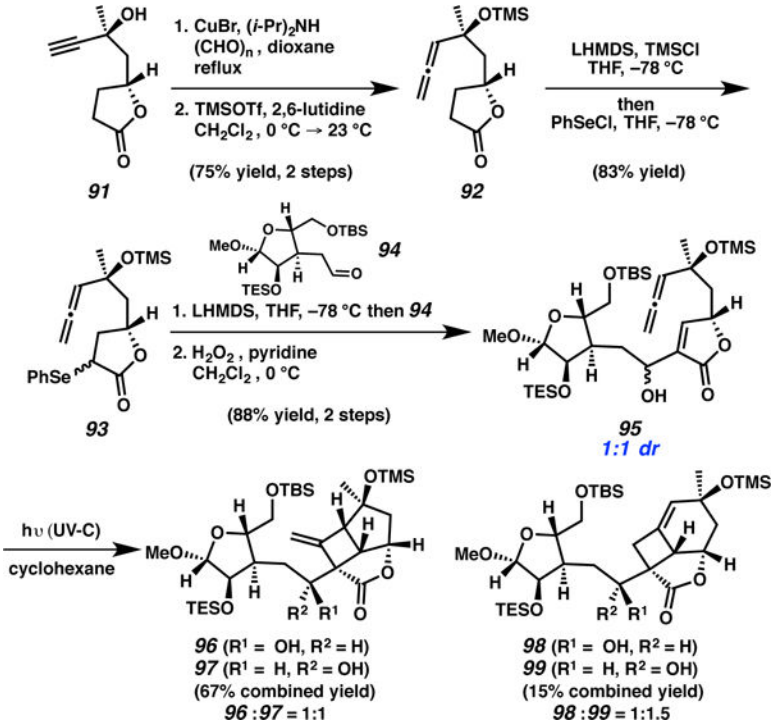

Scheme 20.
Aliene [2 + 2] Cycloaddition (Mulzer)

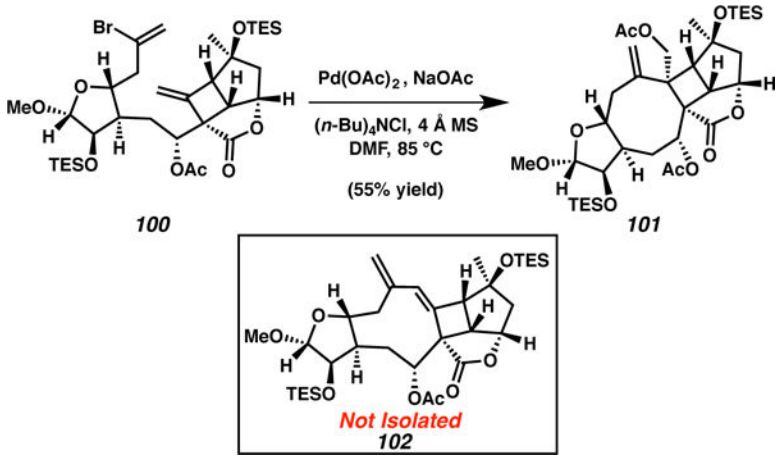

Scheme 21.
Unexpected Cyclooctane Product Formation (Mulzer)

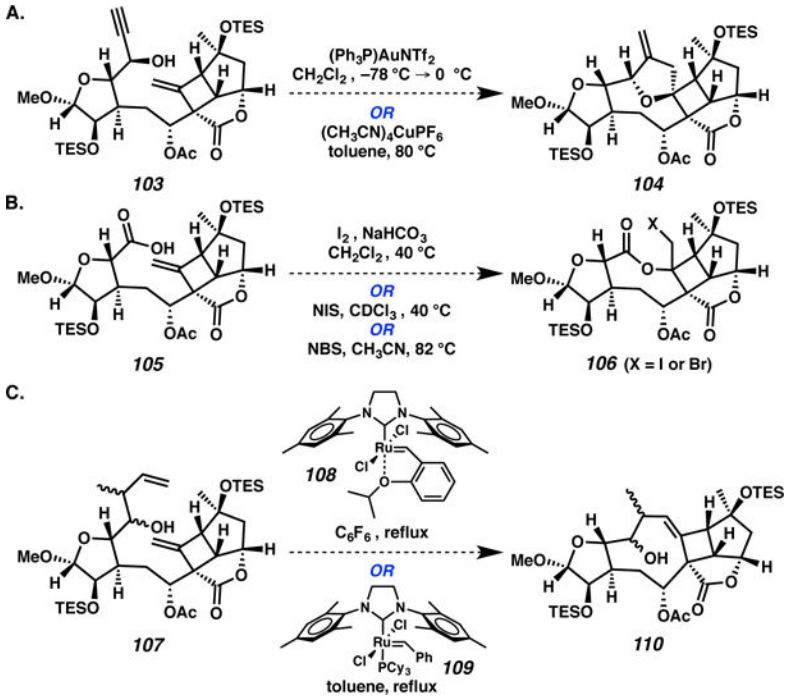

Scheme 22.
Unsuccessful Alterative Macrocyclization Approaches (Mulzer)

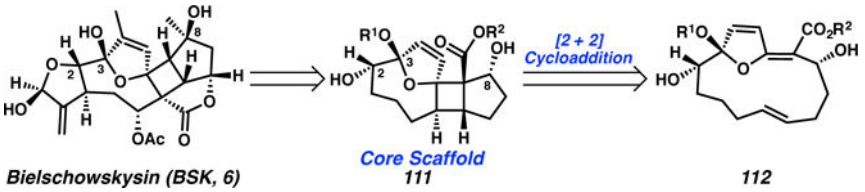

Scheme 23.
Nicolaou's Macrocyclic [2 + 2] Cycloaddition Strategy

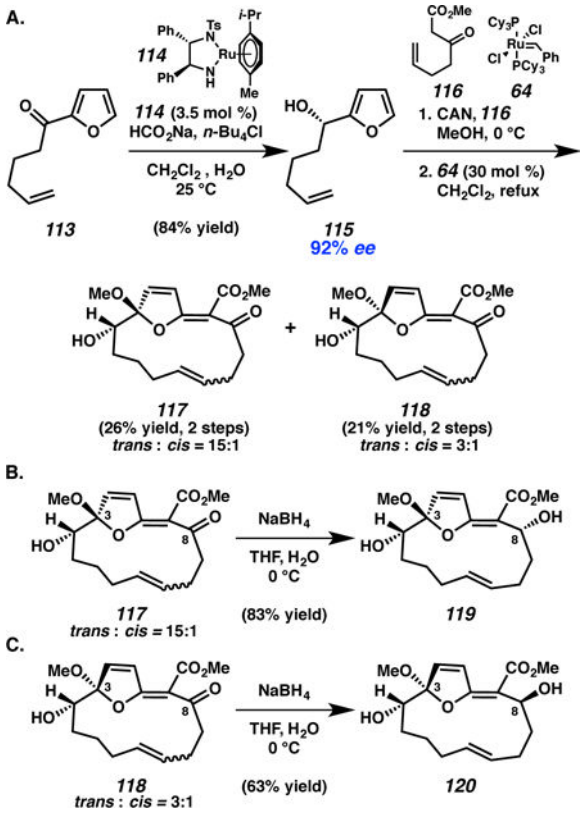

Scheme 24.
Model Macrocycle Synthesis (Nicolaou)

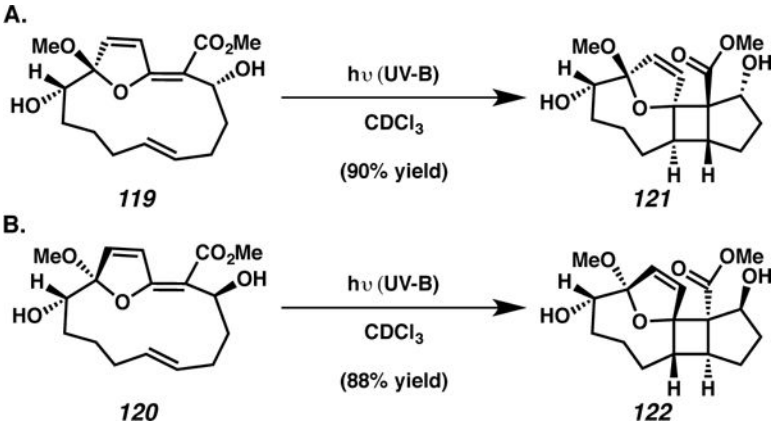

Scheme 25.

Stereochemical Outcome of Macrocyclic [2 + 2] Cycloaddition (Nicolaou)

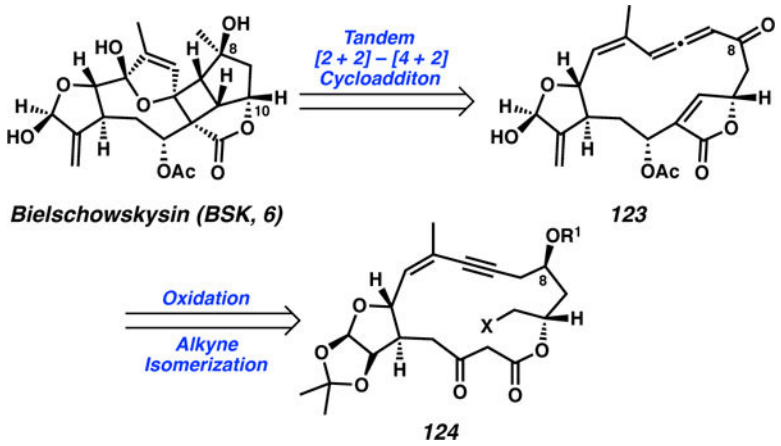

Scheme 26.

Lear's Macrocyclic Tandem [2 + 2] and [4 + 2] Cycloaddition Strategy

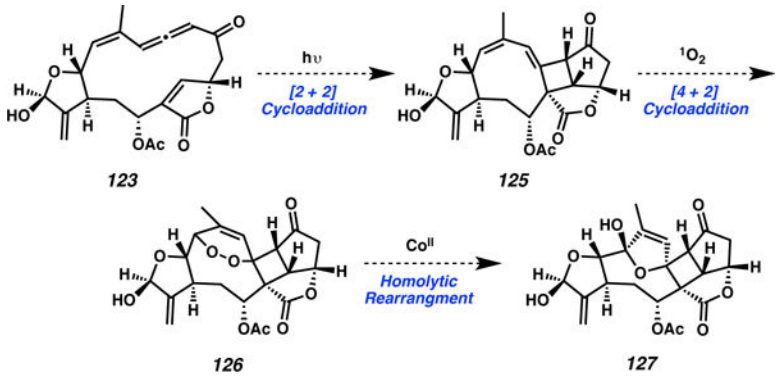

Scheme 27.

Planned Tandem [2 + 2] and [4 + 2] Cycloaddition in the Forward Sense (Lear)

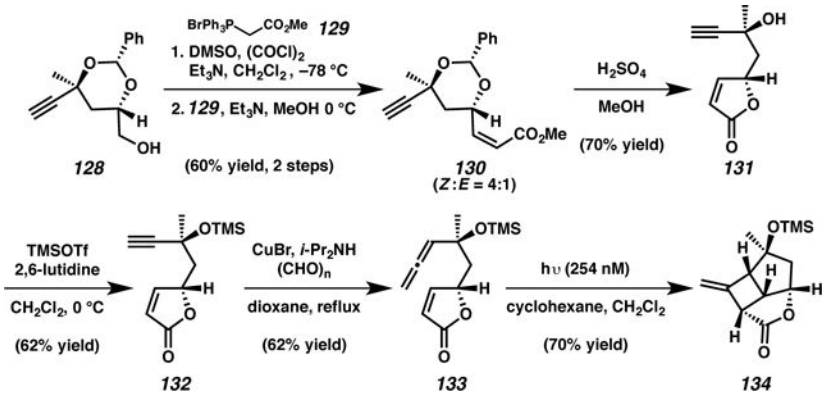

Scheme 28.

Model System Studies on Allene Cycloaddition with a Butenolide (Lear)

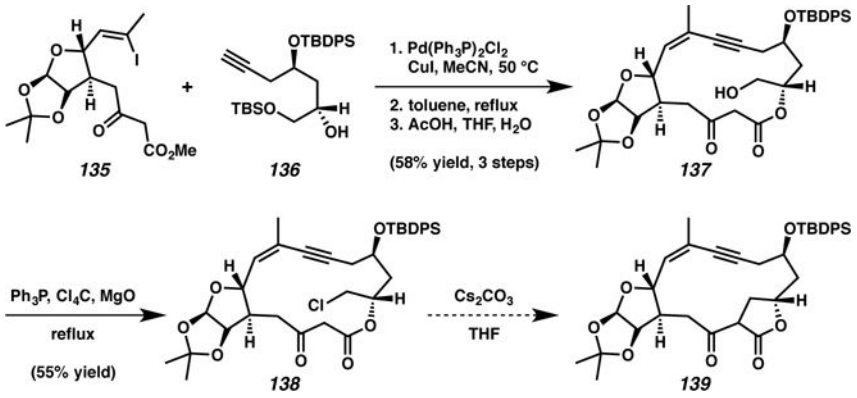

Scheme 29.
Synthetic Advancement Toward BSK (**6**, Lear)

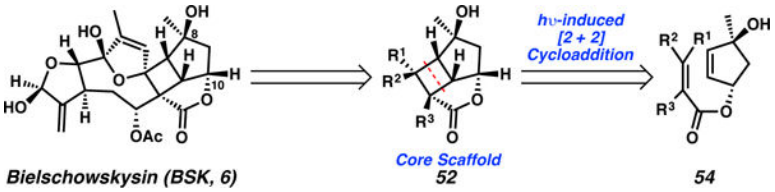

Scheme 30.

Alternative Retrosynthetic Analysis of Cyclobutane Moiety of BSK (**6**, Mulzer)

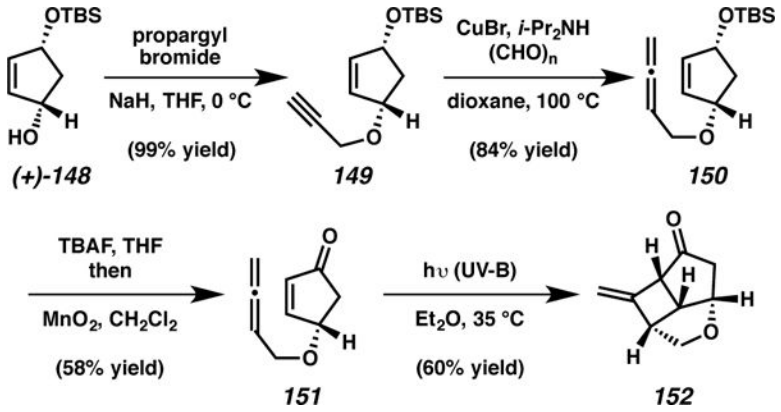

Scheme 31.

Successful Construction of the Cyclobutane-Containing Tricyclic Core of BSK (Mulzer)

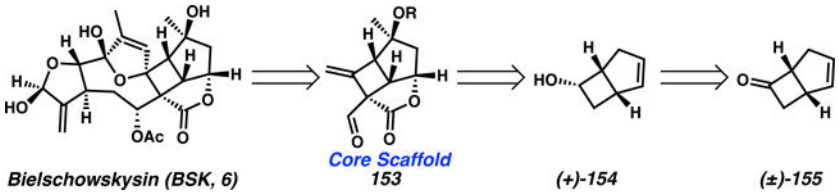

Scheme 32.
Mulzer's 3rd Generation Retrosynthetic Analysis of BSK (**6**)

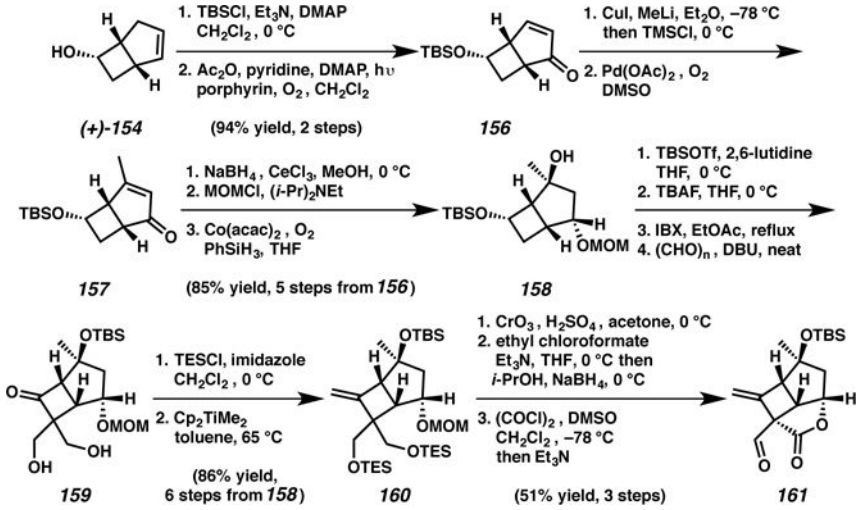

Scheme 33.

Advancement of Enantioenriched Cyclobutanol **(+)-154** Toward BSK (**6**, Mulzer)

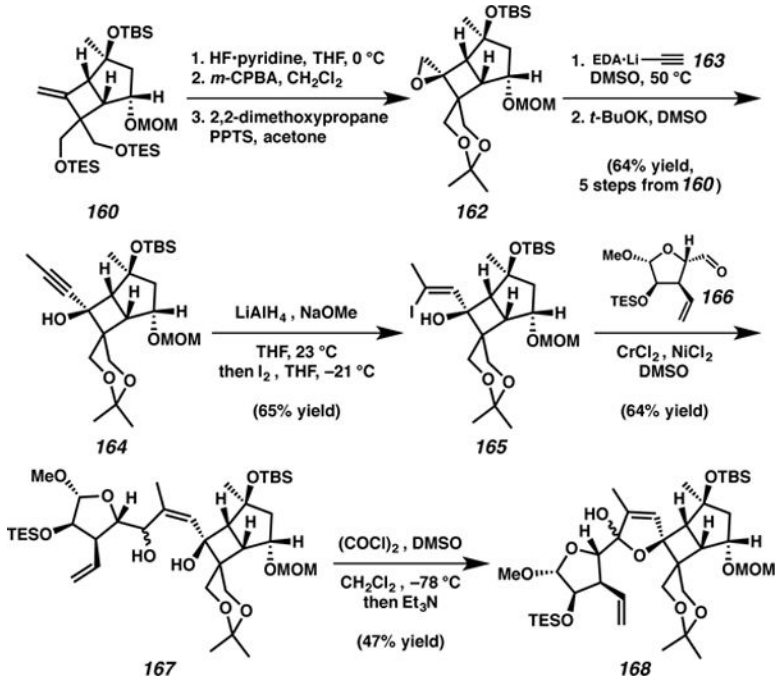

Scheme 34.

Alternative Advancement of Methylenecyclobutane **160** Toward BSK (**6**, Mulzer)

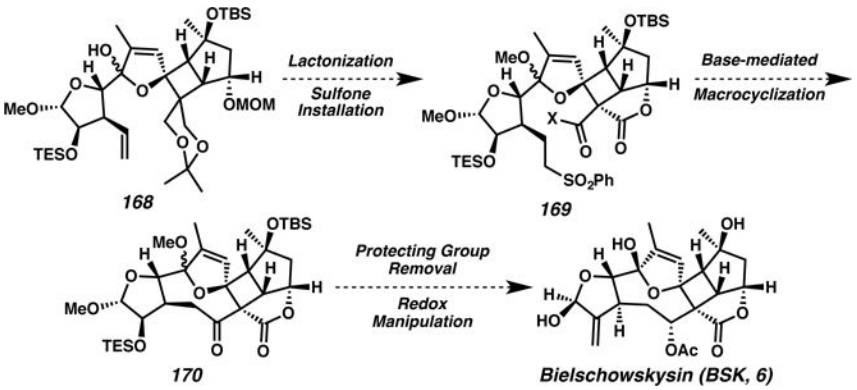

Scheme 35.

Intended Completion of BSK (**6**) from Dihydrofuranol **168** (Mulzer)

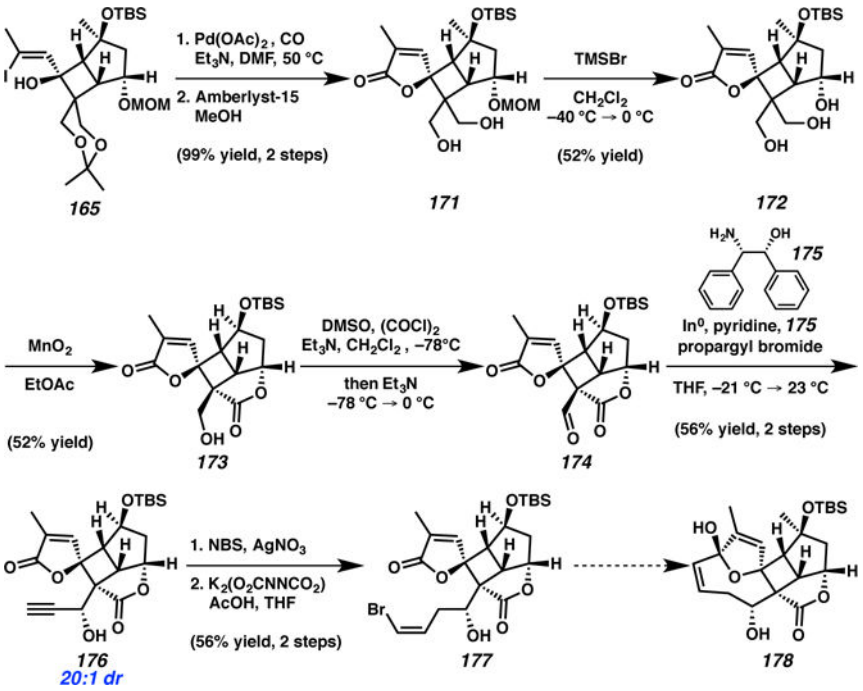

Scheme 36.

Alterative Macrocyclization Strategy from Alkenyl Iodide **165** (Mulzer)

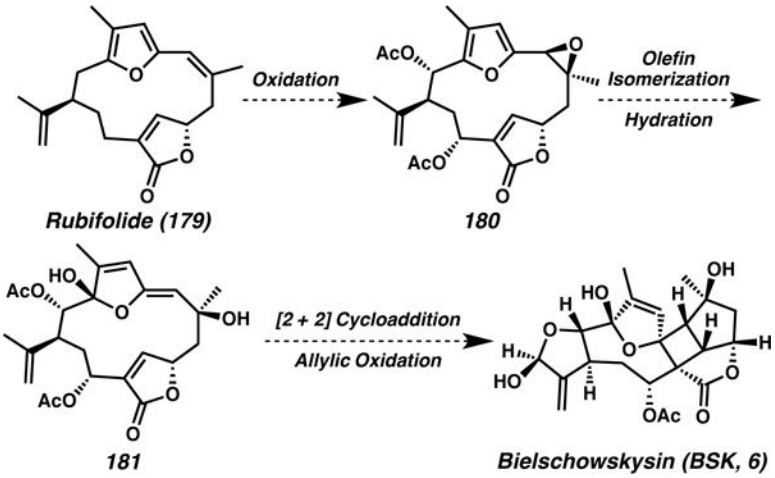

Scheme 37.

Pattenden's Proposed Alternative Biosynthetic Proposal for the Construction of Bielschowskysin (BSK, **6**)

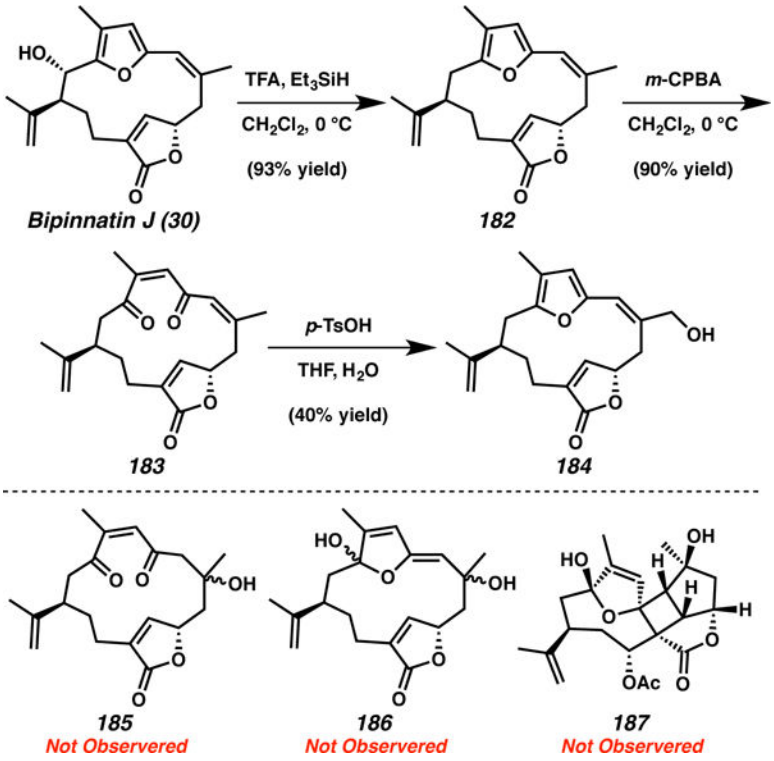

Scheme 38.

Exploration of Biosynthetic Proposal for the Construction of Bielschowskysin (BSK, **6**, Pattenden)

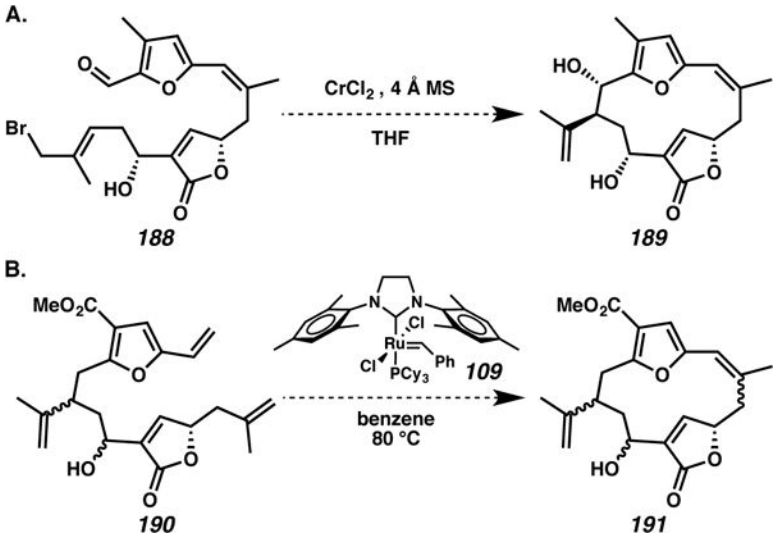

Scheme 39.

Unsuccessful Formation of BSK Model Systems via Macrocyclization (Pattenden)

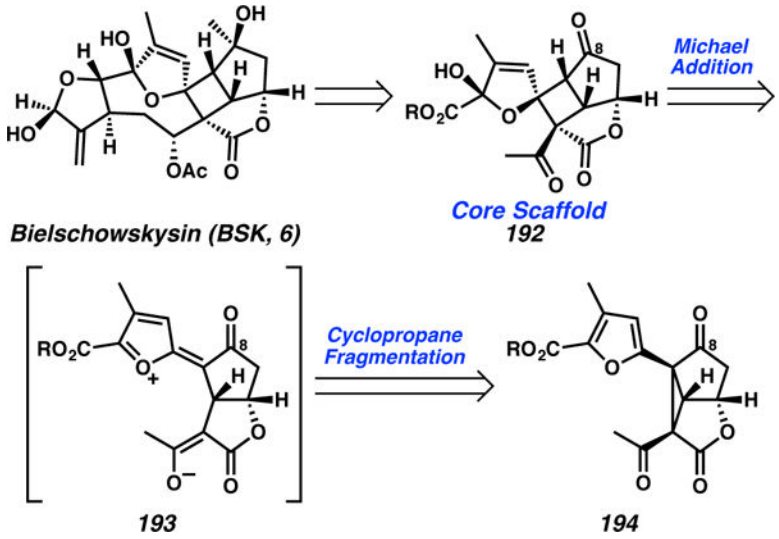

Scheme 40.

Retrosynthetic Analysis of BSK Core Scaffold **192** (Stoltz)

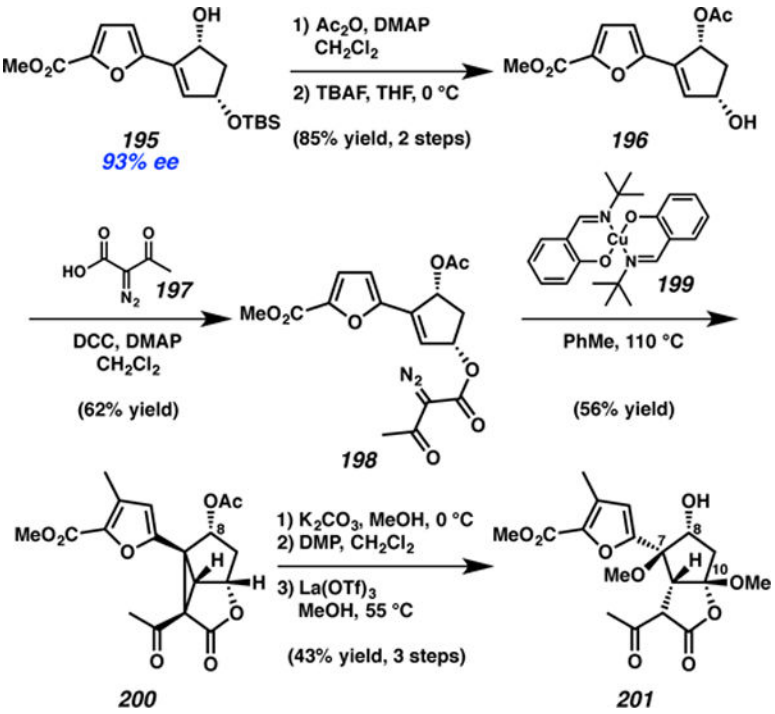

Scheme 41.

Synthesis and Exploration of Reactivity of Cyclopropane Intermediate **200** (Stoltz)

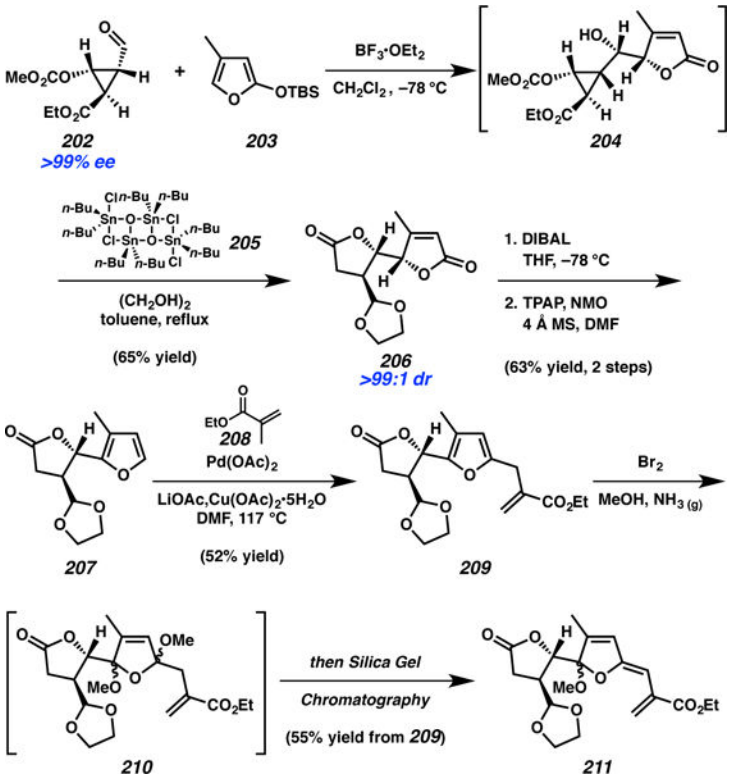

Scheme 42.

Stereoselective Access to γ-Furyl-γ-butyrolactones (Reiser)

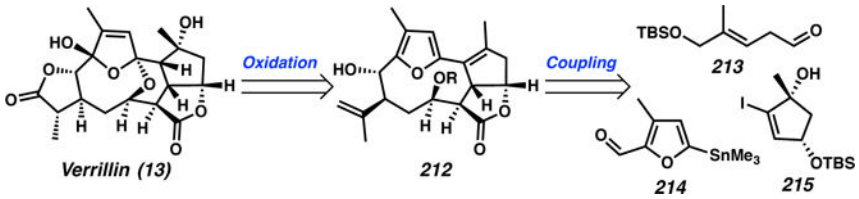

Scheme 43.
Retrosynthetic Analysis of Verrillin (Theodorakis)

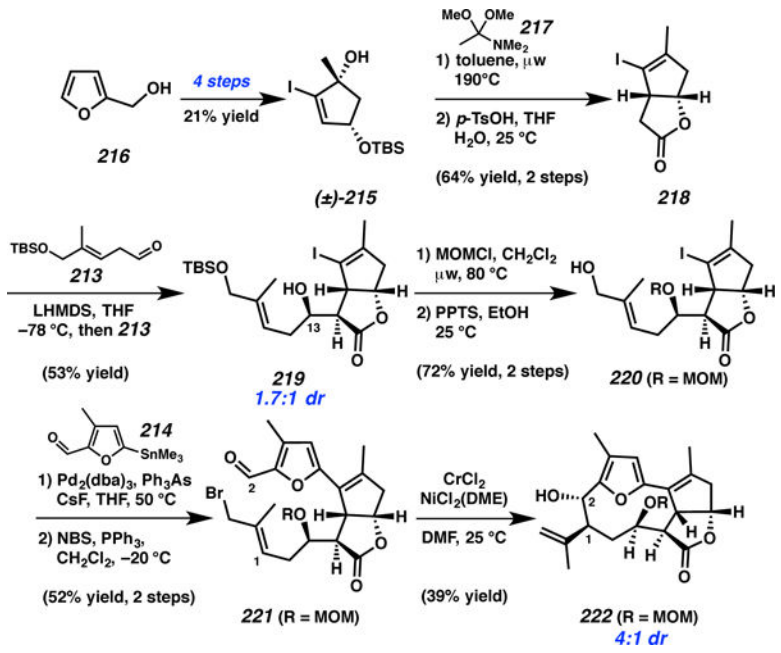

Scheme 44.

Theodorakis' Synthetic Approach Toward Verrillin (**13**)

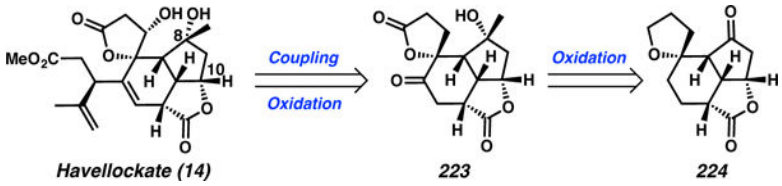

Scheme 45.
Mehta's Retrosynthetic Analysis of Havellockate (**14**)

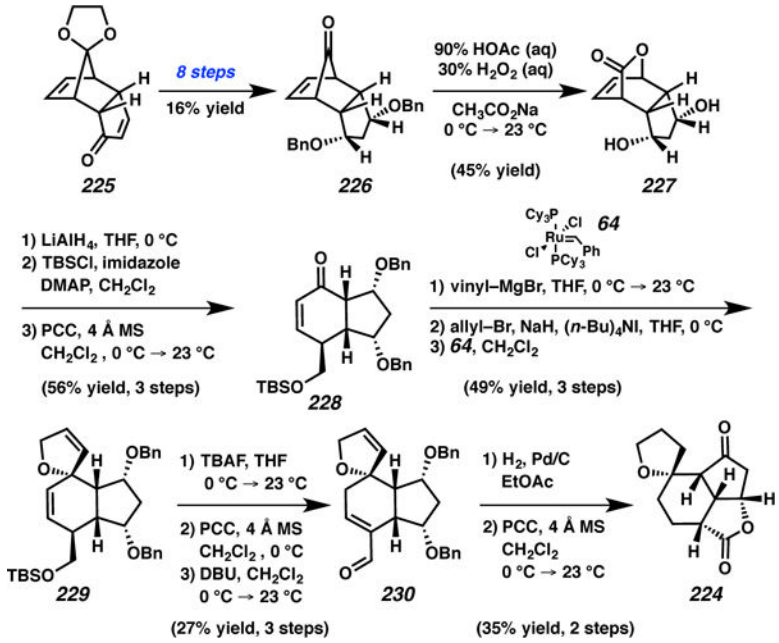

Scheme 46.
Construction of the Havellockate Core (Mehta)

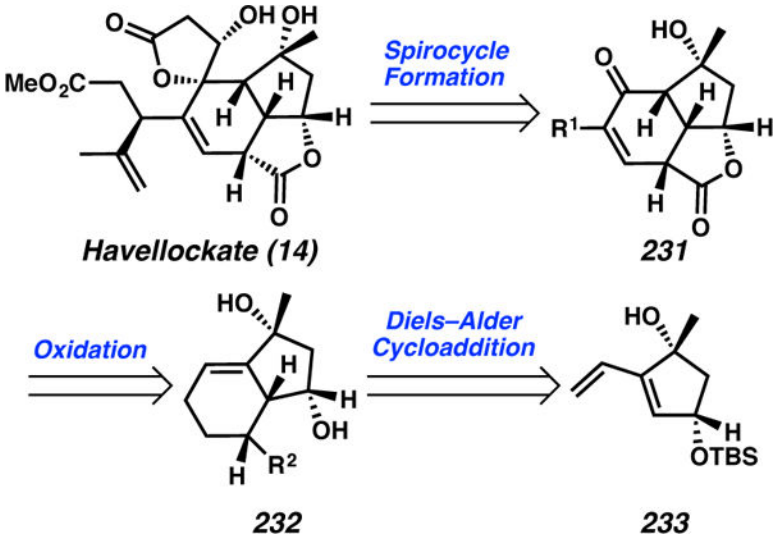

Scheme 47.
Barriault's Retrosynthesis of Havellockate (**14**)

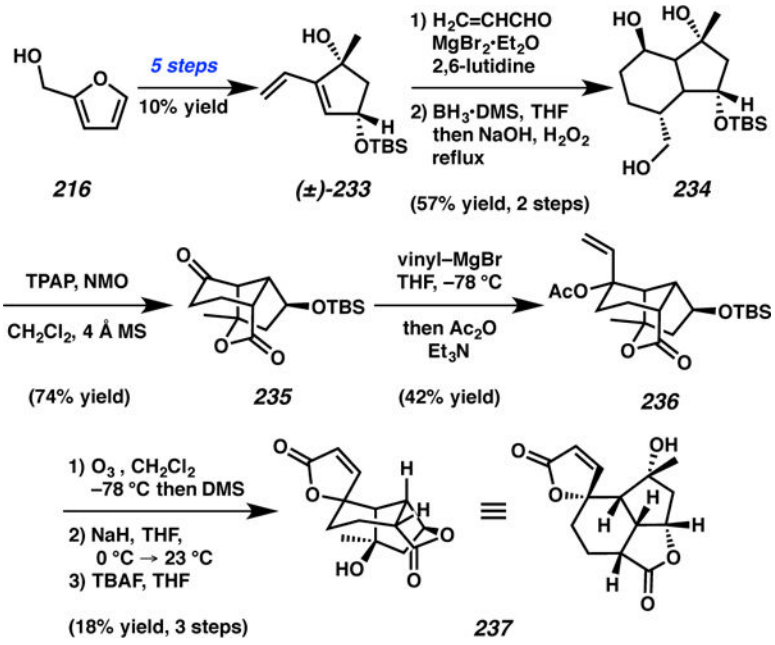

Scheme 48.

Synthesis of Elaborated Core Tetracycle of Havellockate (**14**, Barriault)

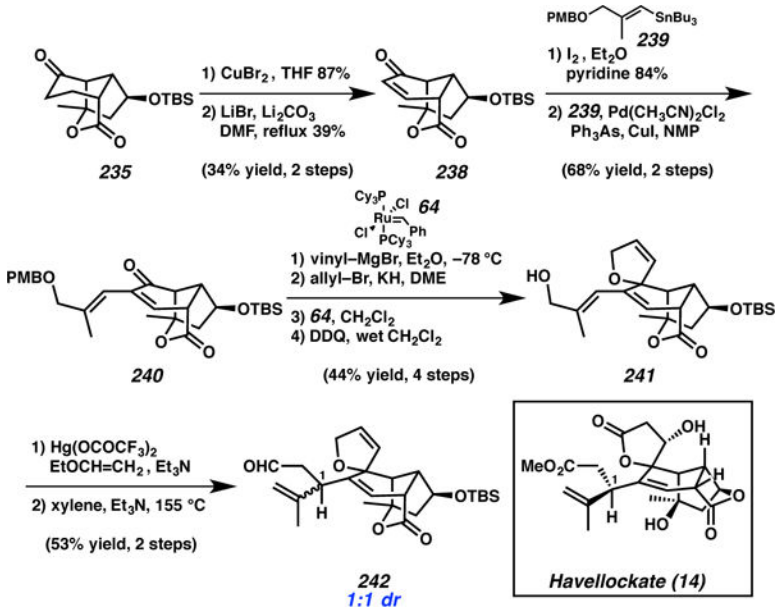

Scheme 49.

Alternative Synthetic Approach Toward Havellockate (**14**, Barriault)

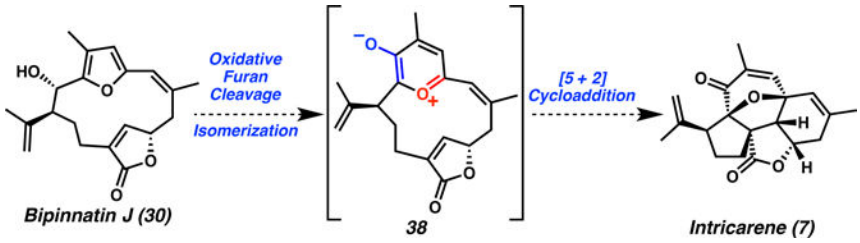

Scheme 50.
Proposed Biosynthesis of Intricarene (**7**)

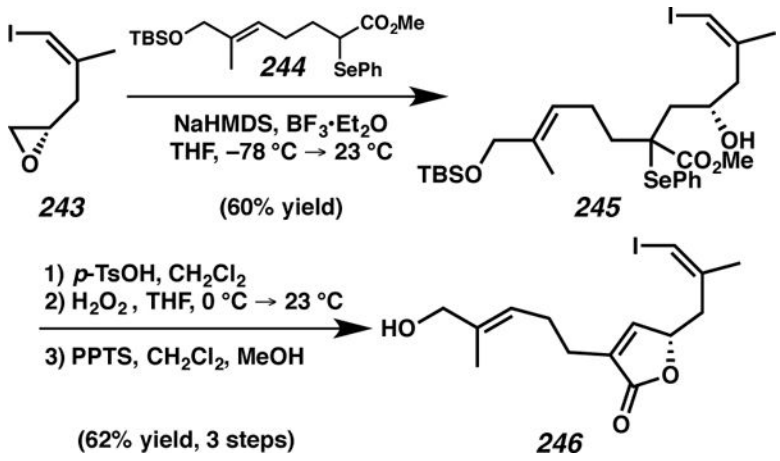

Scheme 51.

Synthesis of Alkenyl Iodide **246** (Pattenden)

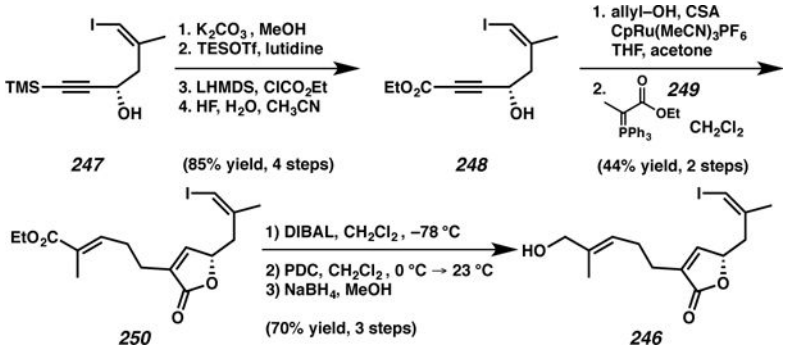

Scheme 52.

Alternative Synthesis of Common Intermediate Alkenyl Iodide **246** (Trauner)

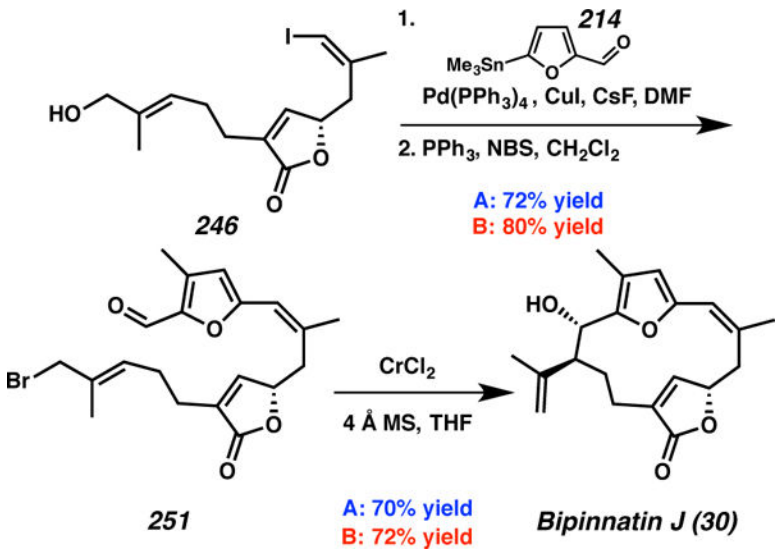

Scheme 53.

Completion of Asymmetric Total Synthesis of Bipinnatin J (**30**, A: Pattenden and B: Trauner)

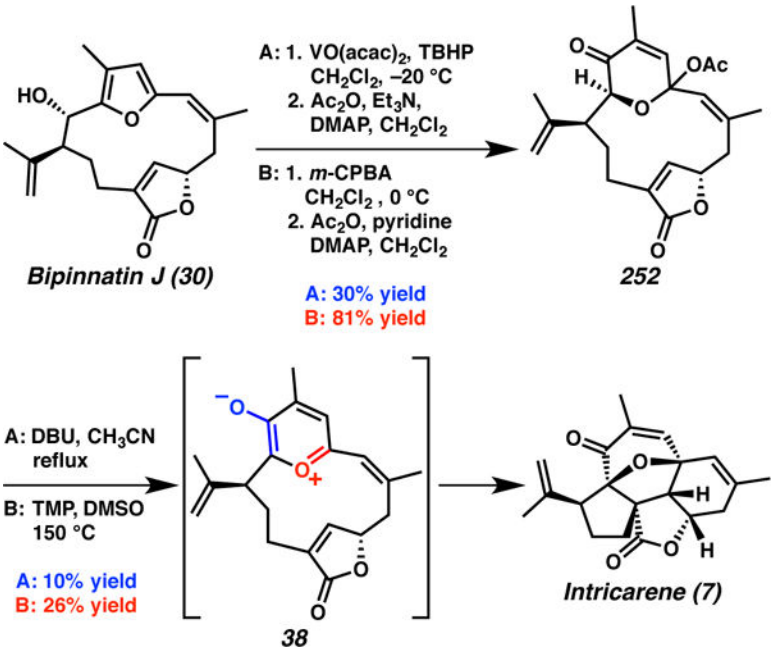

Scheme 54.

Biomimetic Syntheses of Intricarene (**7**) from Bipinnatin J (**30**, A: Pattenden and B: Trauner)

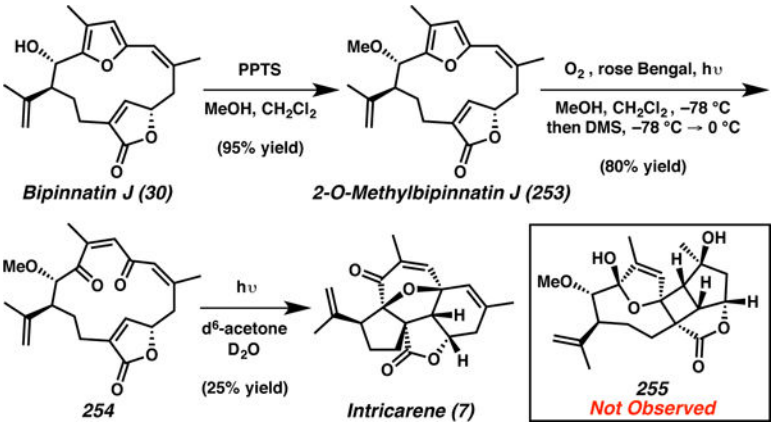

Scheme 55.
Unanticipated Photochemical Synthesis of Intricarene (**7**, Trauner)

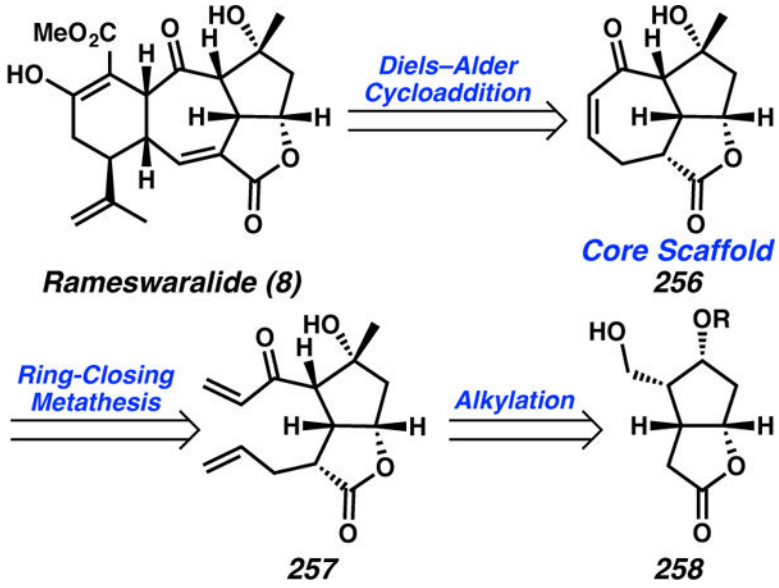

Scheme 56.

Mehta's Retrosynthetic Analysis of Rameswaralide (**8**)

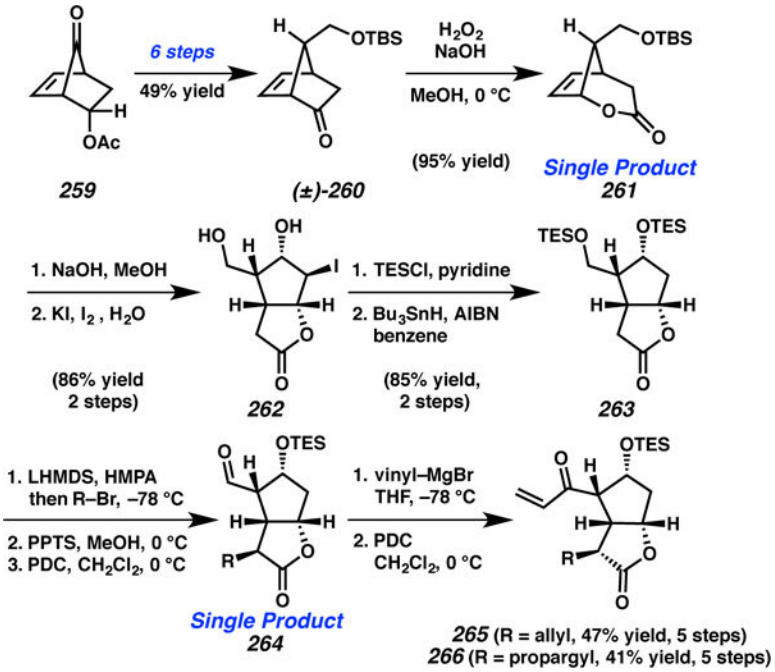

Scheme 57.

Synthesis of Bicyclic Metathesis Substrates **265** and **266** (Mehta)

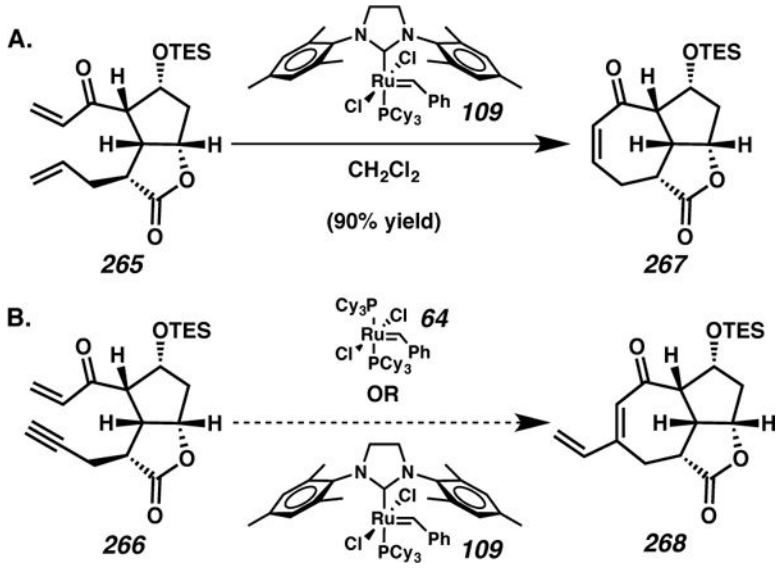

Scheme 58.
Construction of the Rameswaralide Tricyclic Core (Mehta)

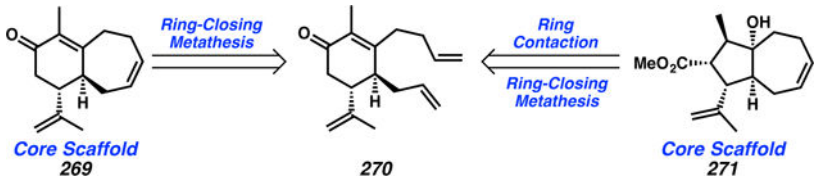

Scheme 59.

Srikrishna's Proposed Construction of Two Rameswaralide Cores from Common Intermediate **271**

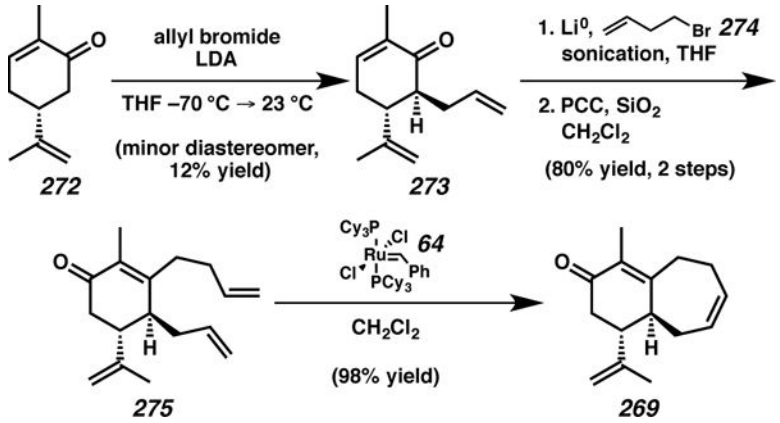

Scheme 60.

Synthesis of the [6,7]-Bicyclic Core of Rameswaralide (Srikrishna)

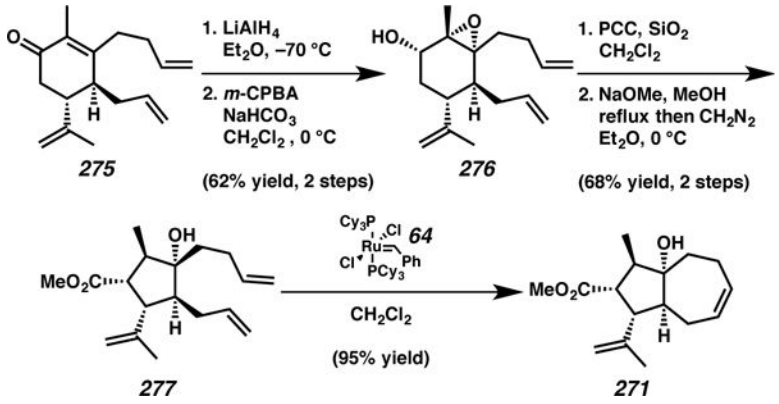

Scheme 61.

Formation of the [5,7]-Bicyclic Core of Rameswaralide **(271**, Srikrishna)

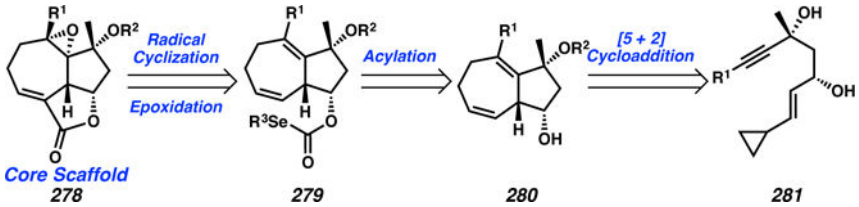

Scheme 62.

Trost's Retrosynthetic Approach Toward Rameswaralide Core **278**

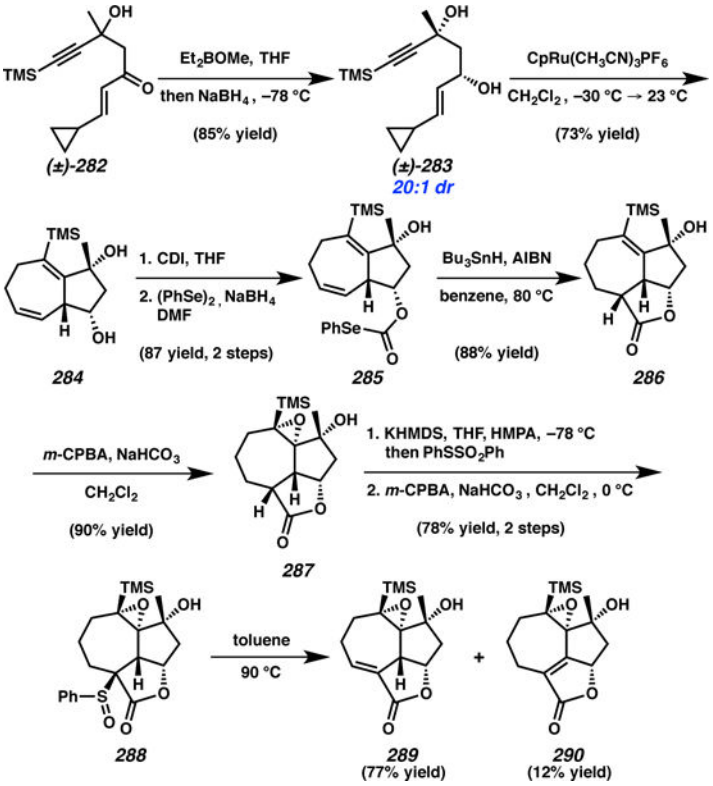

Scheme 63.

Trost's Construction of the Rameswaralide Tricyclic Scaffold

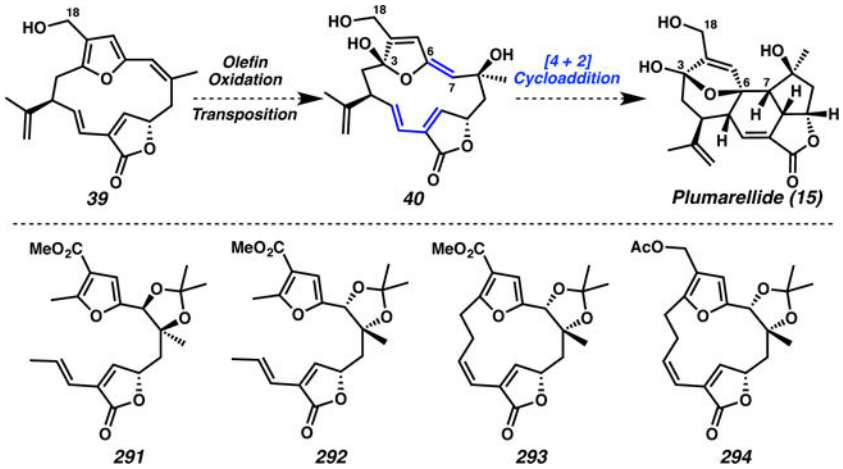

Scheme 64.
Substrates for Exploration of Proposed Biosynthesis (Pattenden)

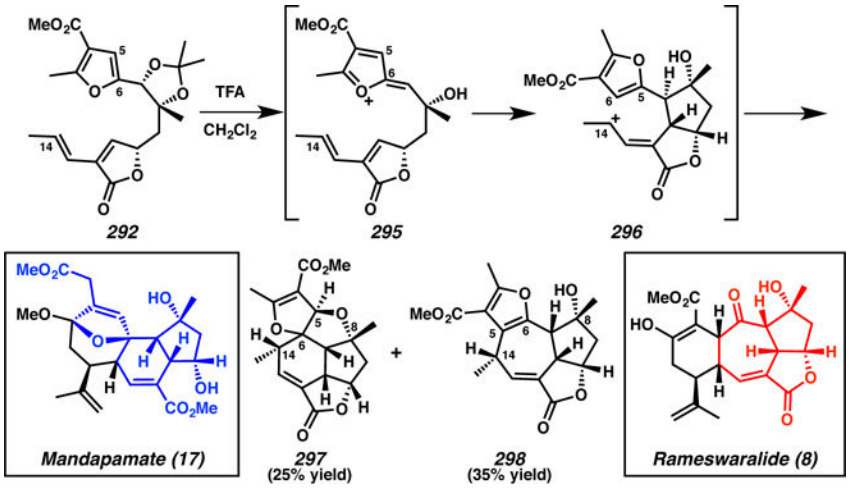

Scheme 65.

Synthesis of the Mandapamate and Rameswaralide Core Scaffolds (Pattenden)

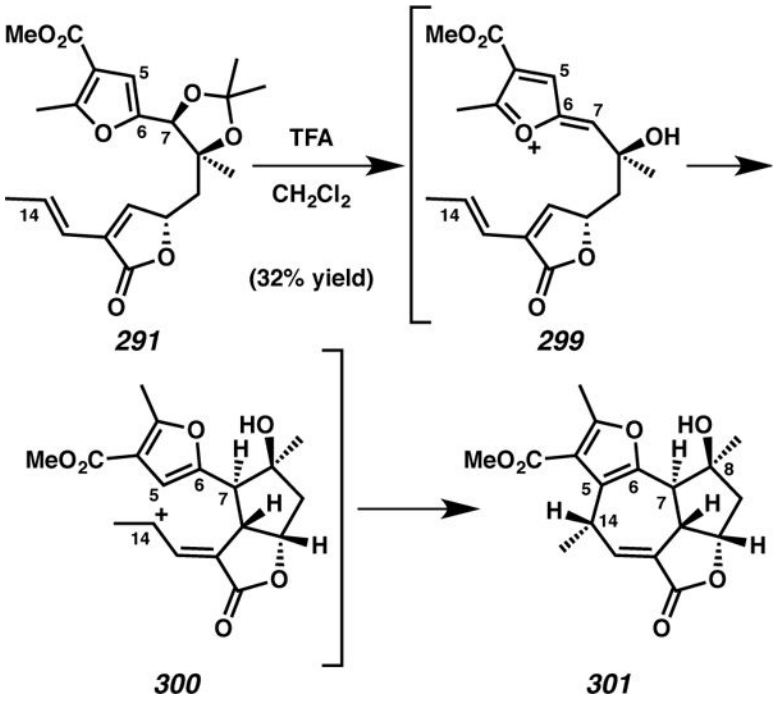

Scheme 66.

Formation of Rameswaralide Core from Diol **291** (Pattenden)

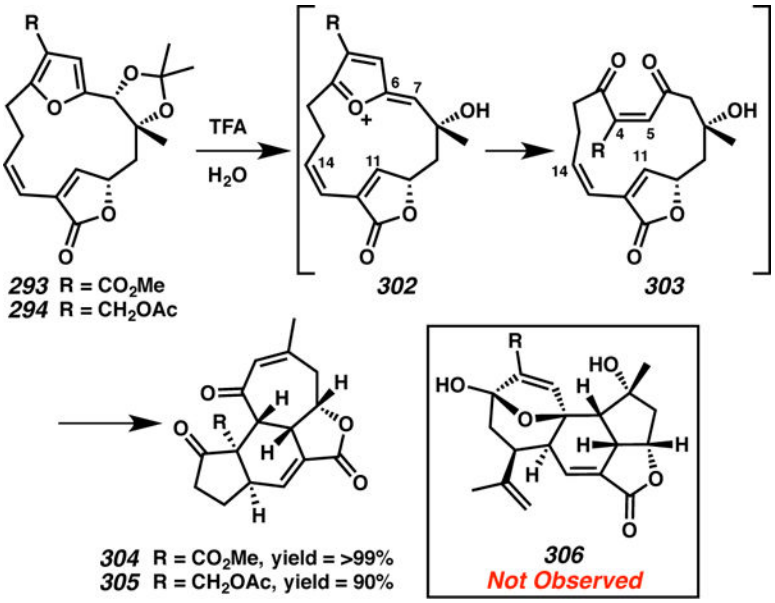

Scheme 67.

Synthesis of Unexpected Novel Cembranoid Cores **304** and **305** (Pattenden)

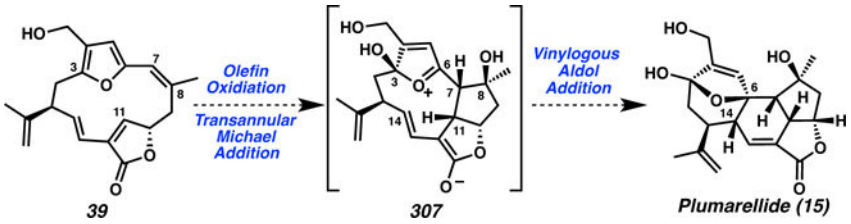

Scheme 68.

Pattenden's Alternative Proposal for the Biosynthesis of Plumarellides (**15–16**) and Mandapamates (**17–20**)

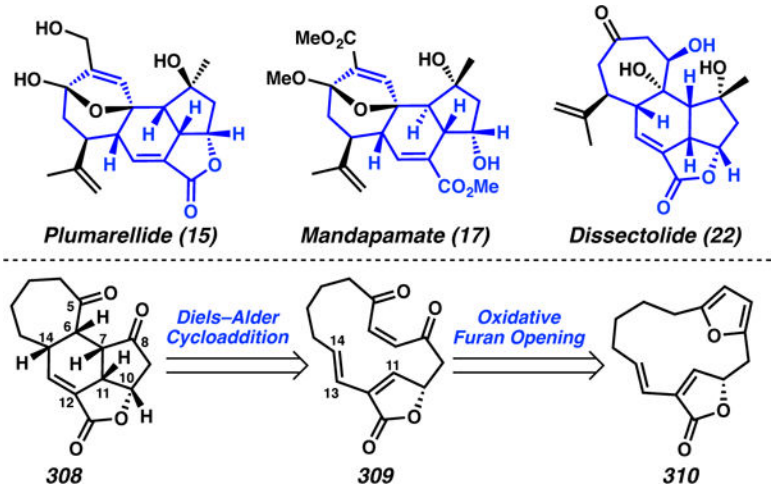

Scheme 69.
Retrosynthesis of Common Carbocyclic Core (Mehta)

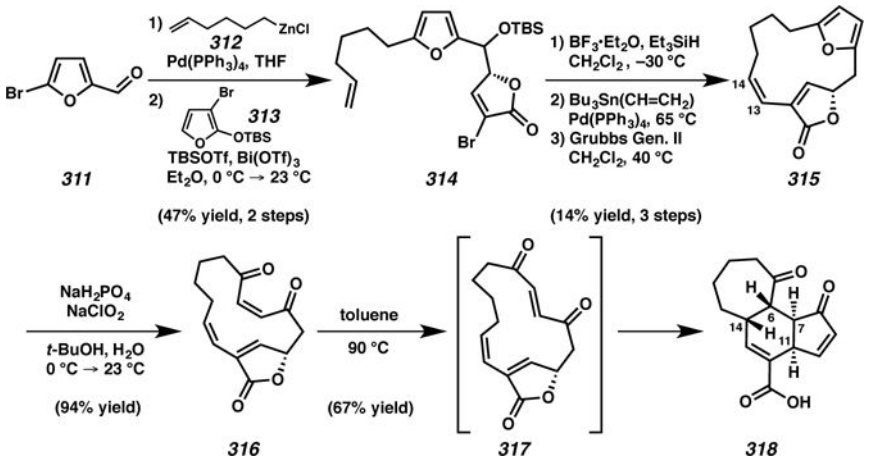

Scheme 70.

Construction of Tricycle **318** by Diels–Alder Cycloaddition (Mehta)

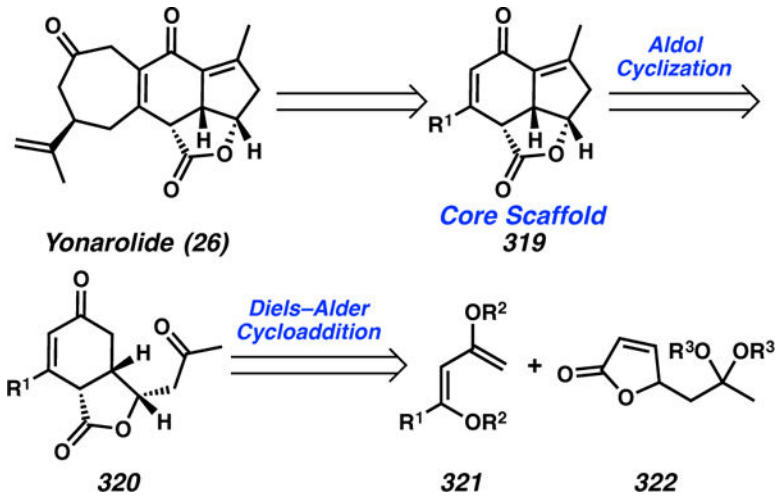

Scheme 71.
Retrosynthetic Analysis of Yonarolide (**26**, Ito)

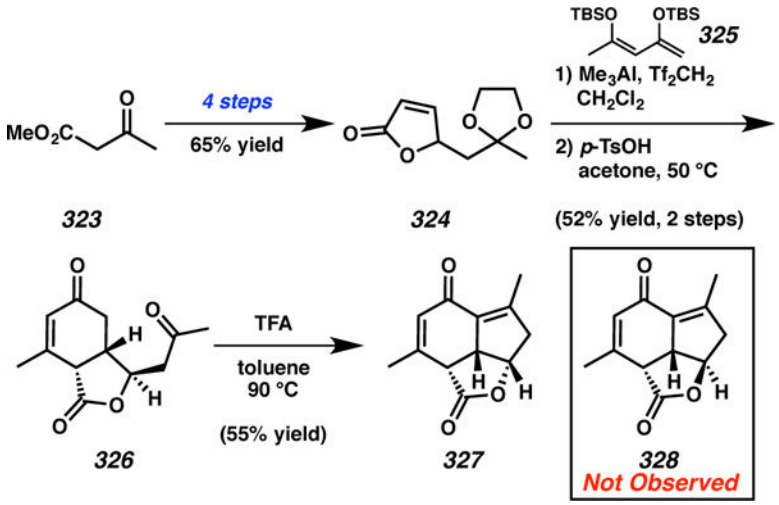

Scheme 72.

Synthesis of the Yonarolide Core by Tandem Isomerization-Aldol Cyclization (Ito)

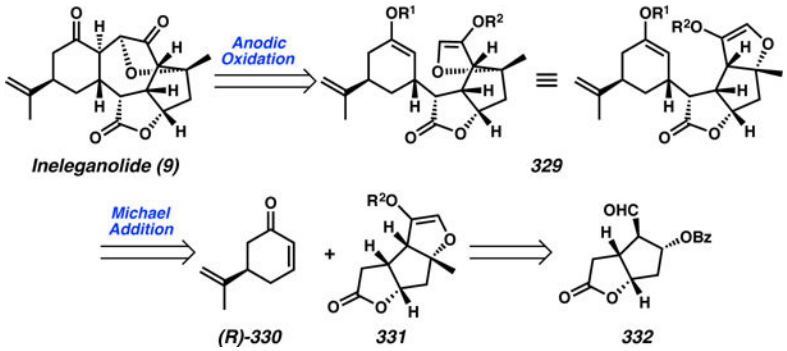

Scheme 73.

Moeller's Retrosynthetic Analysis of Ineleganolide (**9**)

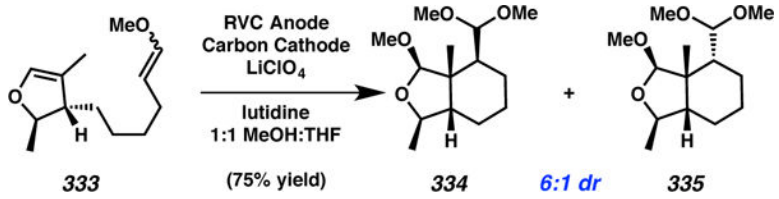

Scheme 74.

Initial Development of Anodic Oxidation for the Formation of Fused Carbocycles (Moeller)

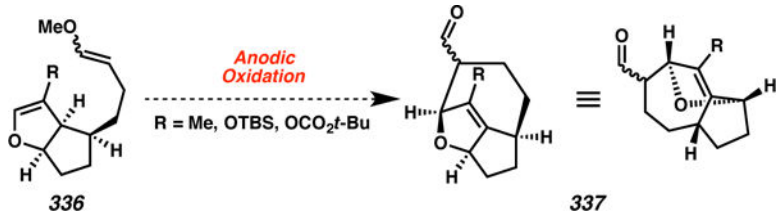

Scheme 75.
Failed Construction of Cycloheptene **337** by Anodic Oxidation (Moeller)

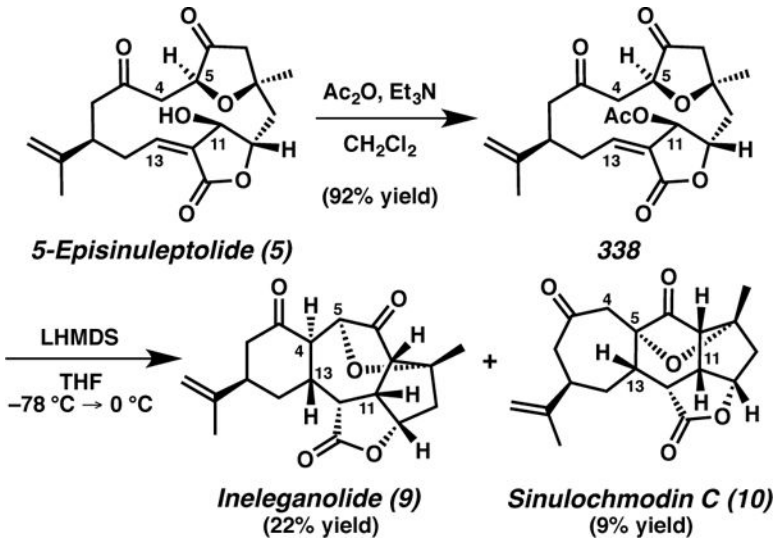

Scheme 76.

Biomimetic Semisynthesis of Ineleganolide (**9**) and Sinulochmodin C (**10**, Pattenden)

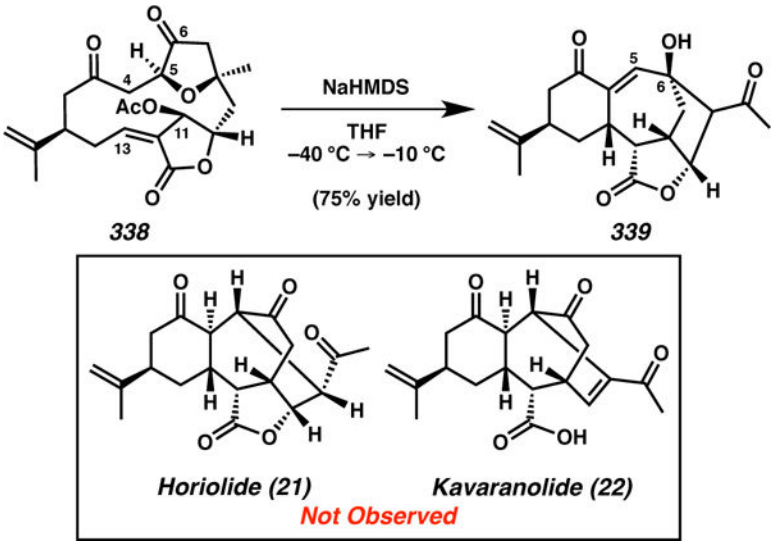

Scheme 77.

Attempted Biomimetic Semisynthesis of Additional Norcembranoids Horiolide (**21**) and Kavaranolide (**22**, Pattenden)

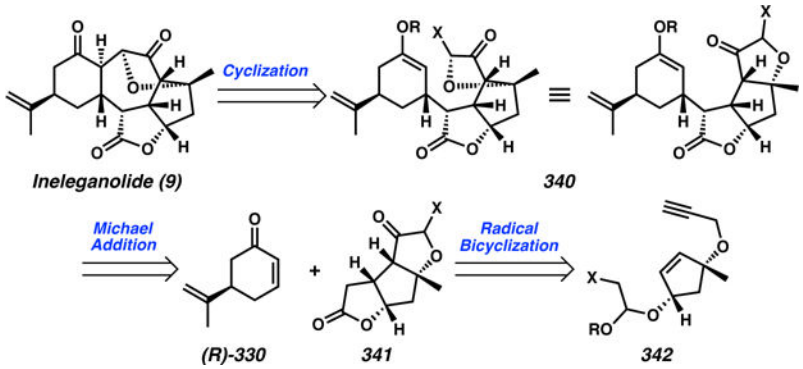

Scheme 78.
Vanderwal's Retrosynthesis of Ineleganolide (**9**)

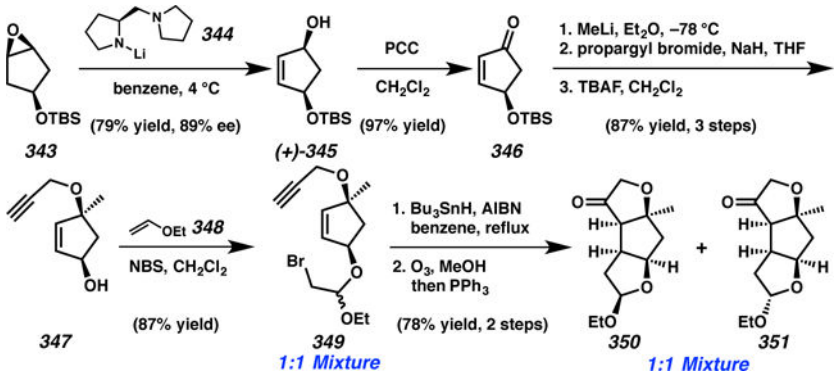

Scheme 79.

Enantioselective Construction of Dihydrofuranones **350** and **351** Through Radical Bicyclization (Vanderwal)

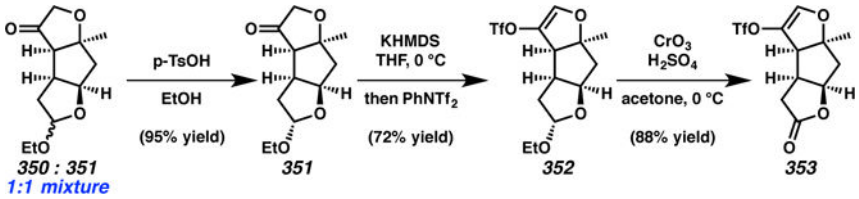

Scheme 80.
Completion of Tricyclic Coupling Partner (Vanderwal)

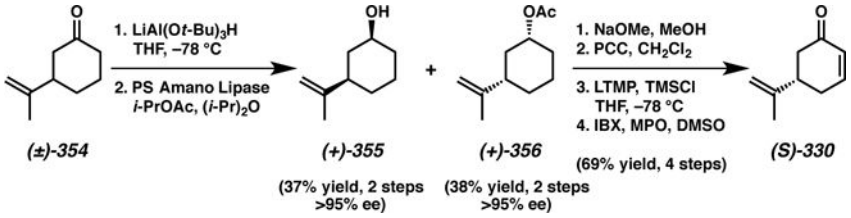

Scheme 81.

Asymmetric Synthesis of Complementary Cyclohexenone (***S***)-**330** (Vanderwal)

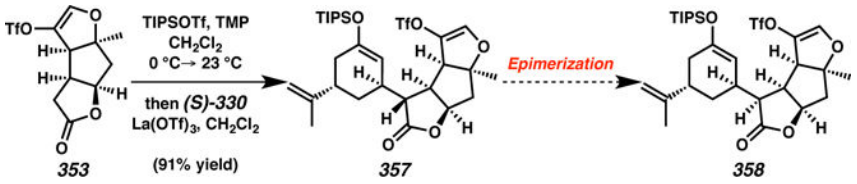

Scheme 82.

Coupling of Fragments **353** and **(*S*)-330** Toward *ent*-Inclcganolidc (***ent*-9**, Vanderwal)

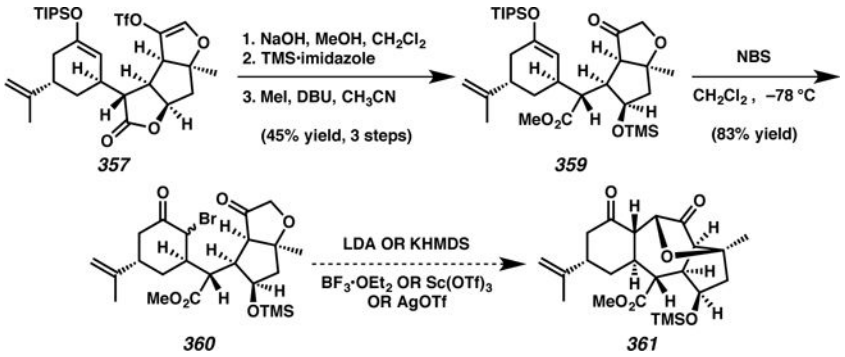

Scheme 83.
Alternative Advancement Toward *ent*-Ineleganolide (Vanderwal)

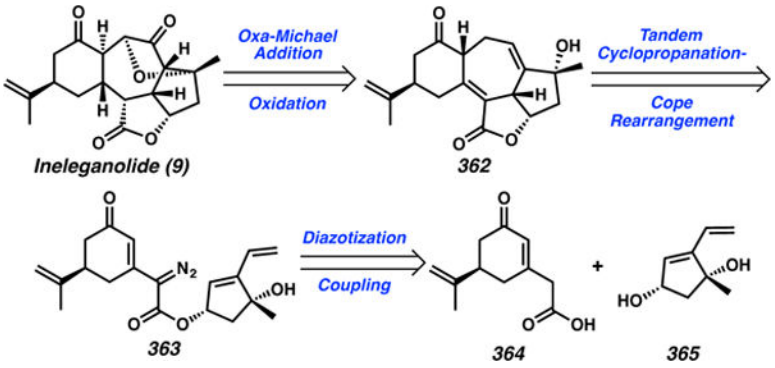

Scheme 84.
Stoltz's Retrosynthetic Analysis of Ineleganolide (**9**)

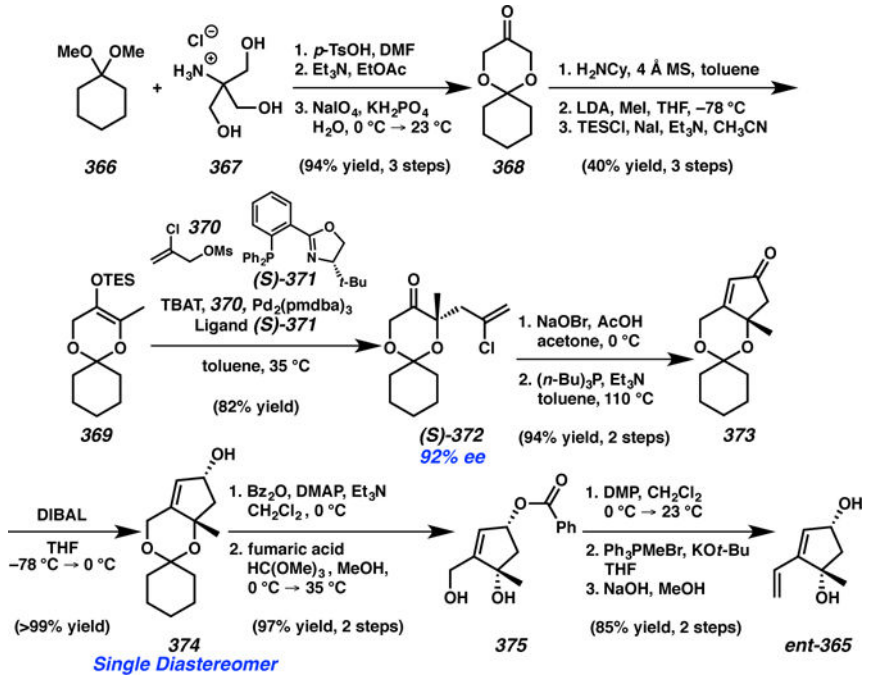

Scheme 85.

Enantioselective Synthesis of 1,3-*cis*-cyclopentenediol ***ent*-365** (Stoltz)

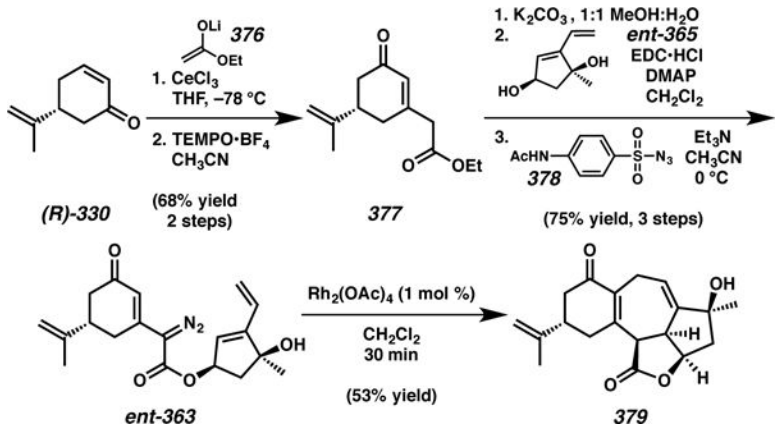

Scheme 86.

Convergent Assembly of the Tetracyclic Core of *ent*-Ineleganolide (***ent*-9**, Stoltz)

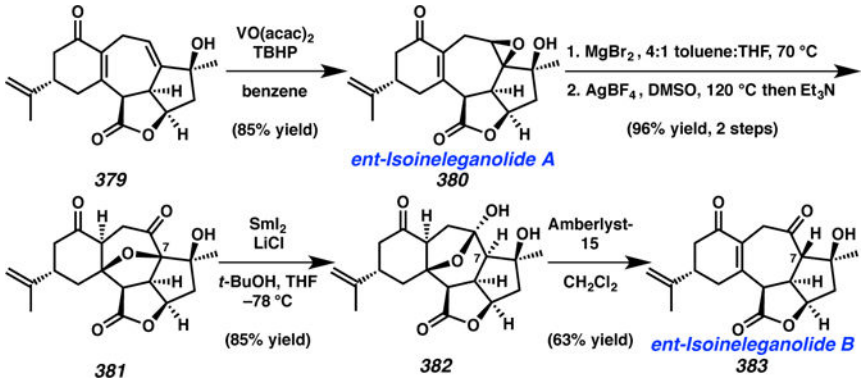

Scheme 87.

Advanced Synthetic Progression Toward *ent*-Ineleganolide (***ent*-9**, Stoltz)

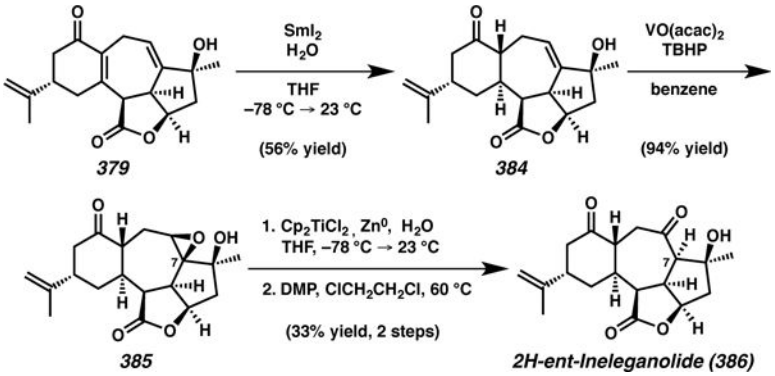

Scheme 88.

Alternative Synthetic Manipulation of the *ent*-Ineleganolide Tetracyclic Core (Stoltz)